Simulation of Adaptive Array Algorithms for 3G CDMA Systems

Danyan Chen

A Thesis

in

The Department

of

Electrical and Computer Engineering

Presented in Partial Fulfillment of the Requirements

for the Degree of Master of Applied Science at

Concordia University

Montréal, Québec, Canada

February 2002

Your file Votre référence
ISBN: 0-612-90368-0
Our file Notre référence
ISBN: 0-612-90368-0

ABSTRACT

Simulation of Adaptive Array Algorithms for 3G CDMA Systems

Danyan Chen

The increasing demand for mobile communication services without a corresponding increase in RF spectrum allocation motivates the need for new techniques to improve spectrum utilization. CDMA systems and adaptive antenna array are two approaches that show real promise for increasing spectrum efficiency. In this research, we investigate the performance of different adaptive array algorithms, blind and non-blind, in the CDMA systems. Three algorithms, least-squares despread respread multitarget constant modulus algorithm (LS-DRMTCMA), Wiener solution with pilot channel on reverse link of 3G CDMA and least-mean-square (LMS) algorithm with training sequence, are developed. A C++ simulation testbed is created to compare the performance of these algorithms. It is shown from the simulation results that system performance is greatly improved by using adaptive array. Wiener solution with pilot channel can outperform the other algorithms in all the test situations considered (e.g., AWGN channel, four types of fading channels). However the LMS algorithm with training sequence has less computational requirements than the other algorithms.

Dedicated to my dearest parents .....

ACKNOWLEDGEMENTS

I would like to thank my academic advisor, Dr. Ahmed K. Elhakeem, for the invaluable support, guidance and encouragement he has provided over the past year.

I would like to thank all my friend all my friends who have provided me all kinds of help in the last two years.

Most of all, I would like to thank my parents for their love and encouragement. I could not have completed my degree without their continuous and immeasurable support.

TABLE OF CONTENTS

LIST OF TABLES

LIST OF FIGURES

Chapter 1

INTRODUCTION

1.1 Antenna Array

The radio frequency spectrum is, and always will be, a finite and scarce resource, thus there is a fundamental limit on the number of radio channels that can be made available to mobile telephony. Hence, it is essential that cellular land mobile radio (LMR) networks utilize the radio spectrum allocated to this facility efficiently, so that the service can be offered to as large a subscriber community as possible. Indeed, networks which employ either omni-directional, or broad sector-beam, base-station antennas, will be beset with the problem of severe spectral congestion as the subscriber community continues to expand. The number of subscribers is growing at a phenomenal rate and will continue to do so, as illustrated in Figure 1.1.

A measure often used to assess the efficiency of spectrum utilization is the number of voice channels per megahertz of available bandwidth per square kilometer[1]. This defines the amount of traffic that can be carried and is directly related to the ultimate capacity of the network. Hence, as traffic demands increase, the spectral efficiency of the network must also increase, if the quality and availability of service is not to be degraded. In areas with a high traffic density, at present this is overcome by employing a technique known as *cell splitting.* However, the continuing growth

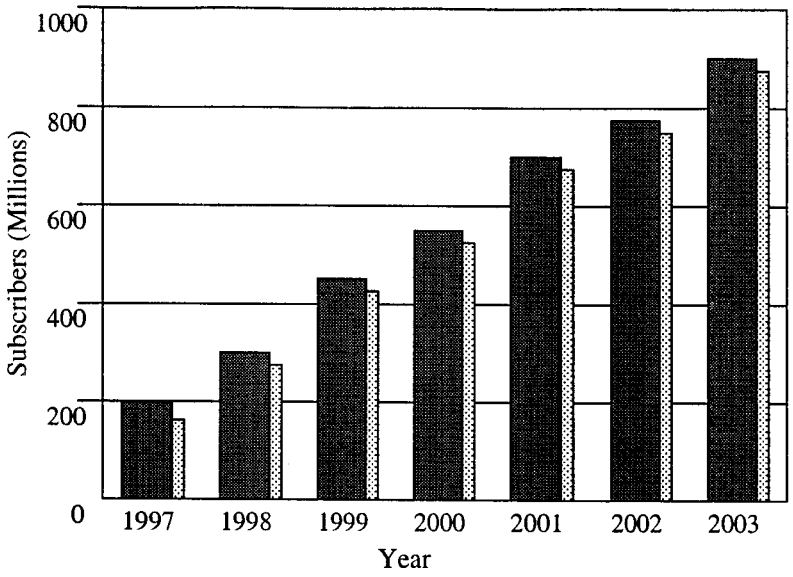

Figure 1.1: The growth rate of wireless subscribers is phenomenal[16].

in traffic demands has meant that cell sizes have had to be reduced to a practical minimum in many city centers in order to maintain the quality of service. This has resulted in increase in the infrastructure costs. Moreover, the number of subscribers able to access these systems simultaneously is still well below the long-term service forecasts due to the reduced *trucking efficiency* of the network. This places great emphasis on maximizing the spectral efficiency, or ultimate capacity, of future generation systems, and thereby fulfilling the earlier promises of performance. There have already been significant developments in terms of spectral efficient modulation schemes, e.g., the proposed US narrow-band digital linear system[2], [3], and the second generation Pan-European cellular network[4]. Also, in the area of antenna technology, the use of fixed coverage directional antennas has been considered[5]. In particular, the use of fixed phased array antennas, with carefully controlled amplitude tapers and side-lobe levels for the enhanced UK TACS network[6] are currently under evaluation. However, the application of *adaptive antenna arrays* in civil land mobile radio systems has hitherto received little attention, in spite of the significant advances made in this field for both military and satellite communications.

An adaptive antenna array may be defined as one that modifies its radiation pattern, frequency response, or other parameters, by means of internal feedback control or other known characteristic of channels or signals while the antenna system is operational. The basic operation is usually described in terms of a receiving system steering a *null*, that is, a reduction in sensitivity in a certain angular position, towards a source of interference. The first practical implementation of electronically steering a null in the direction of an unwanted signal, a jammer, was the Howells-Applebaum side-lobe canceler for radar. This work started in the late 1950's, and a fully developed system for suppressing five jammers was reported in open literature in 1976 by Applebaum. At about the same time Widrow[8] independently developed an approach for controlling an adaptive array using a recursive least squares minimization technique, now known as the LMS algorithm. Following the pioneering work of Howells, Applebaum, and Widrow, there has been a considerable amount of research activity in the field of adaptive antenna arrays, particularly for reducing the jamming vulnerability of military communication systems. However, to date, there has been little attention to the application of such techniques in the area of civil land mobile radio.

Adaptive antenna arrays cannot simply be integrated into any arbitrary communication system, since a control process has to be implemented which exploits some property of either the wanted, or interfering, signals. In general, adaptive antennas adjust their directional beam patterns so as to maximize the signal-to-noise ratio at the output of the receiver. Applications have included the development of receiving systems for acquiring desired signals in the presence of strong jamming, a technique known as *power inversion*[9]. Systems have also been developed for the reception of frequency hopping signals[10], [11], TDMA satellite channels[12] and spread spectrum signals[13]. Of particular interest for cellular schemes is the development of adaptive antenna arrays and signal processing techniques for the reception of multiple wanted signals[14].

The adaptive array consists of a number of antenna elements, not necessarily identical, coupled together via some form of amplitude control and phase shifting network to form a single output. The amplitude and phase control can be regarded as a set of *complex weights.* It can be shown[15] that an N element array has $N-1$ degrees of freedom giving up to $N-1$ independent pattern nulls. If the weights are controlled by a feedback loop which is designed to maximize the signal-to-noise ratio at the array output, the system can be regarded as an *adaptive spatial filter.*

The antenna elements can be arranged in various geometries, with uniform line, circular array geometry given particular interest here since beams can be steered through 2π , thus giving complete coverage from a central base-station. The elements are typically sited $\lambda/2$ apart, where λ is the wavelength of the received signal. Spacing of greater than $\lambda/2$ improves the spatial resolution of the array, however, the formation of grating lobes (secondary maxima) can also result. These are regarded as undesirable.

The main distinctive point in adaptive array considered here is the interest in adaptive beamforming algorithm. This thesis is thus centered around algebraic techniques for adaptive beamforming. We consider three classes of algorithms: those that are based on channel properties, and others based on signal properties.

1.2 Digital Beamforming

The early concepts underlying digital beamforming were first developed for applications in sonar and radar[17] systems[18]. Digital beamforming represents a quantum step in antenna performance and complexity. It is based on well-established theoretical concepts which are now becoming practically exploitable, largely as a result of recent major advances in areas such as *monolithic microwave integrated circuit* (MMIC) technology and *digital signal processing* (DSP) technology. Digital beamforming technology has reached a sufficient level of maturity that it can be applied

to communications for improving system performance. The application of digital beamforming to wireless communications is no longer only a theoretical possibility. It is fast becoming a reality. Furthermore, the demand for increased capacity is a major driving force for incorporating digital beamforming into future wireless communications systems.

Digital beamforming is a marriage between antenna technology and digital technology. A generic digital beamforming antenna system shown in Figure 1.2 consists of three major components: the antenna array, the digital transceivers, and the digital signal processor.

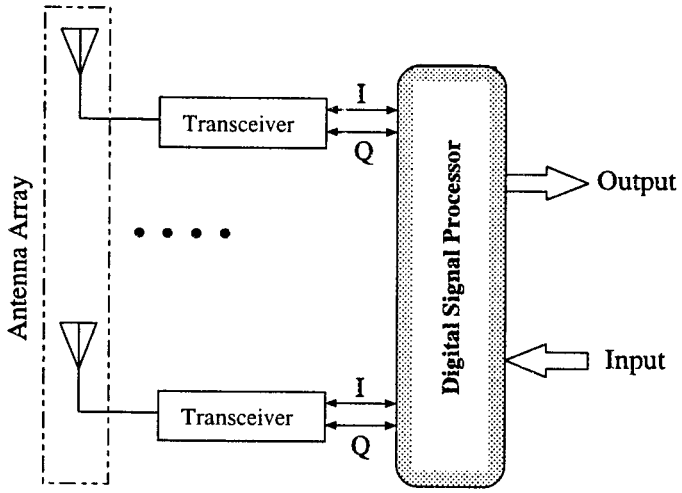

Figure 1.2: A generic digital beamforming antenna system.

In a digital beamforming antenna system, the received signals are detected and digitized at the element level. By capturing the RF information in the form of a digital stream, we open the door to a large domain of signal processing techniques and algorithms that can be used to extract information from the spatial domain data. Digital beamforming is based on capturing the radio frequency (RF) signals at each of the antenna elements and converting them into two streams of binary baseband

signals (i.e., in-phase (I) and quadrature-phase (Q) channels). Included within the digital baseband signals are the amplitudes and phases of signals received at each element of the array. The beamforming is carried out by weighting these digital signals, thereby adjusting their amplitudes and phases such that when added together they form the desired beam. This process can be carried out using a special-purpose digital signal processor. The key to this technology is the accurate translation of the analog signals into digital format. The receivers perform the following functions: frequency down-conversion, filtering, and amplification so that signal levels are commensurate with the input requirements of analog-to-digital converters (ADC). The main advantage to be gained from digital beamforming is greatly added flexibility without any additional degradation in signal-to-noise ratio (SNR).

Spatial processing receivers can be implemented in a number of different ways, using both analog and digital component, as shown in Figure 1.3. For base stations supporting multiple simultaneous uplink signals, the RF/IF spatial processing structure in Figure 1.3(a) is less attractive than the digital system in Figure 1.3(b), whereas a separate RF beamforming network is required for each independent beam when analog components are used. The digital system can form multiple simultaneous beams, one for each Signal Of Interest (SOI), whereas a separate RF beamformer network is required for each independent beam when analog components

Digital beamforming allows for a number of attractive features beyond the capabilities of conventional phased arrays:

1. A large number of independently steered high-gain beams can be formed without any resulting dan yan

2. All of the information arriving at the antenna array is accessible to the signal processors so that system performance can be optimized.

3. Beams can be assigned to individual users, thereby assuring that all links operate with maximum gain.

4. Adaptive beamforming can be easily implemented to improve the system capacity by suppressing cochannel interference. A ny algorithm that can be expressed in mathematical form can be implemented. As a byproduct, adaptive beamforming can be used to enhance the system immunity to multipath fading.

5. Digital Beamforming systems are capable of carrying out antenna system real-time calibration in the digital domain. Therefore, one can relax the requirements for a close match of amplitude and phase between transceivers, because variation in these parameters can be corrected in real time.

1.3 Objective and Outline of Thesis

The aim of this research is to develop adaptive algorithms for the antenna array used in a 3G CDMA system, and compare the performance of these algorithms with that of the algorithms presented in the literature.

This thesis is organized as follows.

Chapter 2 introduces the fundamentals of CDMA system, 3G CDMA system and fading channel model. Chapter 3 gives the introduction of the fundamentals of adaptive antenna array, the terminology, and the basic concepts related to the adaptive beamforming.

Chapter 4 provides a detailed survey of the adaptive beamforming algorithms. Both non-blind and blind algorithms are described. For the non-blind algorithms, the *least-mean-square* (LMS) with training sequence and LMS with pilot channel on reverse link of 3G CDMA are discussed. For the blind algorithms, the algorithms based on property-restoral techniques, such as the *multitarget least-squares -constant modulus algorithm* (MT-LSCMA), the *least-squares despread respread multitarget array* (LS-DRMTA), and *the least-squares despread respread multitarget constant modulus algorithm* (LS-DRMTCMA), are presented. Followed by the beam patterns of both single user and multi user system of different adaptive array algorithms.

Chapter 5 combines the concepts of CDMA and adaptive antenna to derive classic results of system capacity and performance using CDMA with and without adaptive antennas. Followed by the simulation results of system performance of different adaptive array algorithms.

Comparison of different adaptive algorithms is made in Chapter 6. And a brief summary and conclusions are provided in Chapter 7 along with some suggestions for future work.

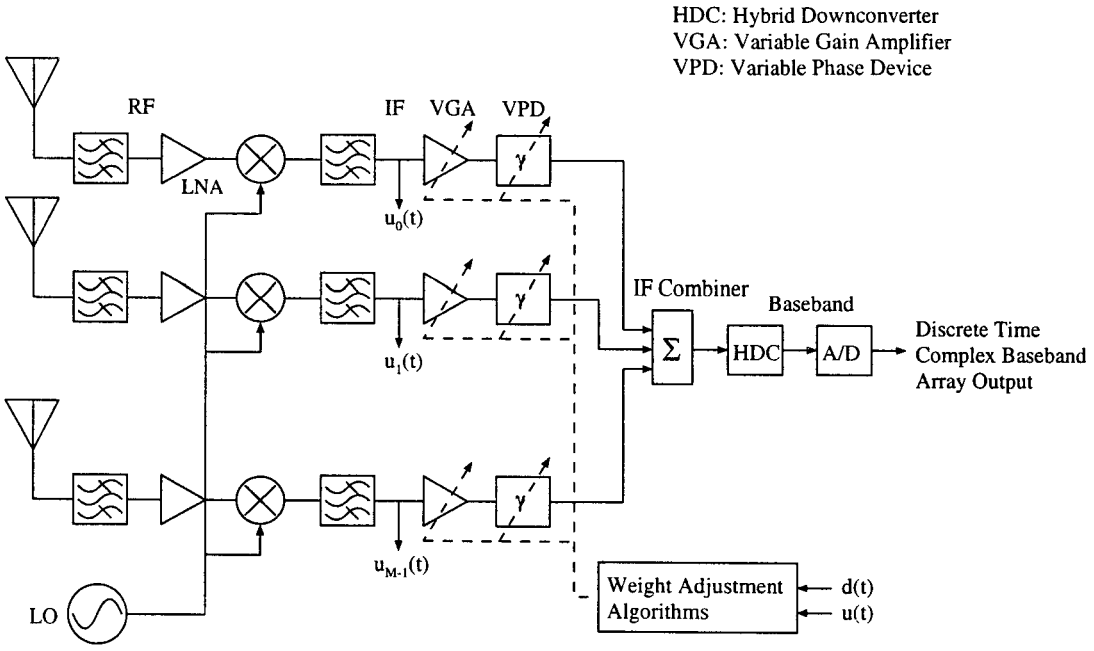

(a) Analog IF weighting and combining

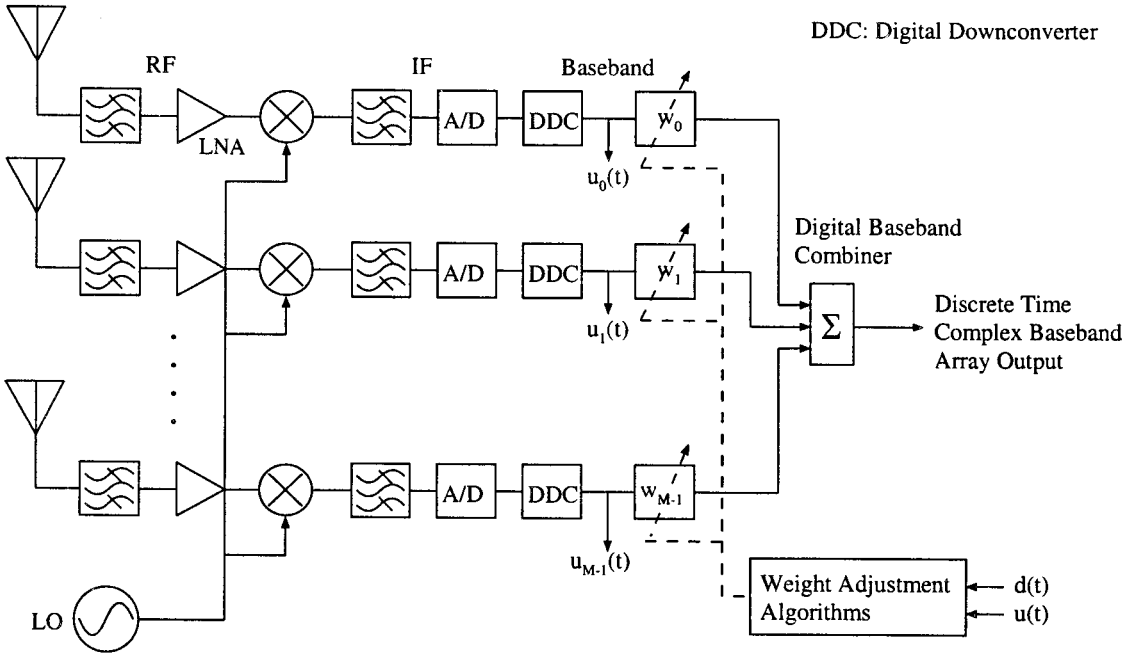

(b) Digital complex baseband weighting and combining

Figure 1.3: Array-based spatial processing can be performed at an RF or IF frequency, using analog components, or it can be performed digitally at baseband. Note that $d(t)$ is an estimate or replica of the desired signal at the array output.

Chapter 2

CDMA AND CHANNEL MODEL

2.1 Code Division Multiple Access (CDMA)

Traditionally, in radio communication systems, the carrier was modulated with user data using techniques that minimize the transmitted bandwidth to conserve spectrum resources. That was the case because radio systems were designed so that only a single channel occupied a given frequency band. If signals are transmitted in multiple non-overlapping frequency bands, they do not interfere with each other and the signals may each be recovered, provided that the power levels are high enough relative to the noise which is always present in the channel. In a CDMA system, rather than trying to minimize the bandwidth of the modulated signal, the goal is to create a modulated signal that uses a large amount of bandwidth.

2.1.1 Direct-Sequence Spread Spectrum

In CDMA systems, a narrowband signal, containing a message with bandwidth $B1$, is multiplied by a signal with a much larger bandwidth $B2$, which is called the spreading signal. Assuming $B2$ is much larger than $B1$, the transmitted signal will have a bandwidth which is essentially equal to the bandwidth of the spreading signal.

The spreading signal is comprised of symbols that are defined by a pseudo random sequence which is known to both the transmitter and receiver. Typically, the rate of chips in the spreading code, R_c, is much greater than the symbol rate, R_b, of the original date sequence. The pseudo random chip sequence is also called a *Pseudo Noise* (PN) sequence because the power spectral density of the PN-sequence looks approximately like white noise filtered to have the spectral envelope as a chip. The spreading factor, or processing gain, is defined as the ratio of the chip rate to the date symbol rate, or $N = R_c/R_b$.

Consider an information signal $b(t)$. This signal may be a voice or date signal. We will assume that $b(t)$ is a digital signal composed of a sequence of symbols, b_j, each of duration T_b. The data signal is given by

$$b(t) = \sum_{j=-\infty}^{\infty} b_j \Psi\left(\frac{t - jT_b}{T_b}\right) \tag{2.1}$$

where $\Psi\left(\frac{t}{T}\right)$ is the unit pulse function:

$$\Psi\left(\frac{t}{T}\right) = \begin{cases} 1 & 0 \leq t < T \\ 0 & otherwise \end{cases}$$

This signal is multiplied by a spreading sequence $c(t)$ which is composed of a sequence of chips:

$$c(t) = \sum_{j=-\infty}^{\infty} \sum_{i=0}^{M-1} c_i \Psi\left(\frac{t - (i + jM)T_c}{T_c}\right) \quad |c_i| = 1 \tag{2.2}$$

where T_c is the chip period, and M is the number of PN symbols in the sequence before the sequence repeats. It should be noted that the chips serve to spread and identify the signal, whereas the data symbols convey information.

The multiplied signal, $b(t)\,c(t)$, is up concerted to a carrier frequency f_c by multiplying $b(t)\,c(t)$ by the carrier,

$$s(t) = b(t)\, c(t) \cos(2\pi f_c t) \tag{2.3}$$

Let us assume, for the moment, that the channel does not distort the signal in any way, so the received signal, $r(t)$, consists of a weighted version of the transmitted signal with added white Gaussian noise, $n(t)$:

$$r(t) = As(t) + n(t) = Ab(t)\, c(t) \cos(2\pi f_c t) + n(t) \tag{2.4}$$

At the receiver, a local replica of the chip sequence, $c(t - \tau_0)$, is generated, where τ_0 is a random time offset between 0 and MT_c. To despread the signal at the receiver, the local chip sequence must be "delay locked" with the received signal. This means that the timing offset, τ_0, must be set to zero. For 3G CDMA systems, the coherent demodulation at the receiver on the reverse link can ensure τ_0 very small. Using this quantities, a decision statistic is formed by multiplying the received signal by the local PN sequence and the local oscillator and integrating the result over one data symbol:

$$z_j = \int_{jT_b}^{(j+1)T_b} r(t)\, c^*(t) \cos(2\pi f_c t)\, dt$$

$$= \int_{jT_b}^{(j+1)T_b} \left[Ab(t)\, c(t) \cos(2\pi f_c t) + n(t)\right] c^*(t) \cos(2\pi f_c t)\, dt \tag{2.5}$$

Let us assume that $c(t)\, c^*(t) = 1$, then

$$z_j = \int_{jT_b}^{(j+1)T_b} \left[Ab(t) \cos^2(2\pi f_c t) + n(t)\, c^*(t) \cos(2\pi f_c t)\right] dt$$

$$= \int_{jT_b}^{(j+1)T_b} \left[A\left(\sum_{i=-\infty}^{\infty} b_i \Psi\left(\frac{t - iT_b}{T_b}\right)\right) \cos^2(2\pi f_c t) + n(t)\, c^*(t) \cos(2\pi f_c t)\right] dt$$

$$= A \int_{jT_b}^{(j+1)T_b} \sum_{i=-\infty}^{\infty} b_i \Psi \left(\frac{t - iT_b}{T_b} \right) \cos^2 (2\pi f_c t)\, dt$$

$$+ \int_{jT_b}^{(j+1)T_b} n(t)\, c^*(t) \cos(2\pi f_c t)\, dt$$

$$= Ab_j \left(\frac{T_b}{2} + \frac{1}{2 \times 4\pi f_c} \left(\sin \left(4\pi f_c (j+1) T_b \right) - \sin \left(4\pi f_c j T_b \right) \right) \right) + \eta \qquad (2.6)$$

where η represents the influence of channel noise on the decision statistic. Assuming that the carrier frequency is large relative to the reciprocal of the bit period, then

$$z_j = \frac{Ab_j T_b}{2} + \eta \qquad (2.7)$$

Therefore, the decision statistic, z_j, is an estimate, $\widehat{b_j}$, of the transmitted data symbol b_j.

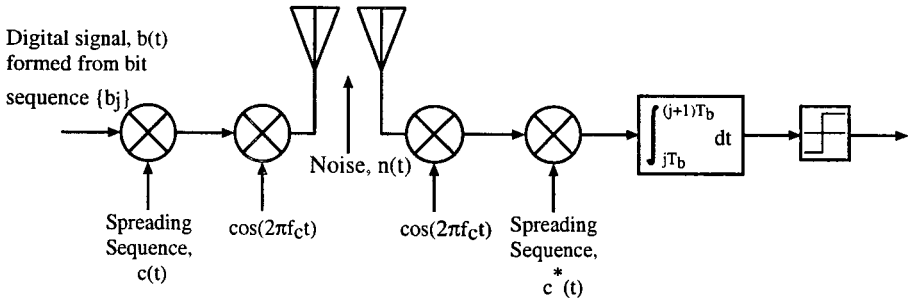

Figure 2.1: CDMA transmitter and receiver.

In mobile and portable radio channels, the fact that the CDMA signal is spread over a large bandwidth can significantly mitigate the effects of fading which can degrade the performance of narrowband systems. The coherence bandwidth of the channel quantifies the region of spectrum over which the amplitudes of all signal

components at the receiver undergo approximately the same fading level. Typical values for coherence bandwidth are 3 MHz in indoor channels and 0.1 MHz for outdoor channels. If the signal bandwidth is smaller than the coherence bandwidth of the channel and one part of the spectrum of the signal experiences a fade, then, in all likelihood, the entire signal spectrum experiences a fade and it is not possible to recover the lost data symbols except through error control coding. Using CDMA techniques, the signal can be made to cover a large enough bandwidth so that if one part of the signal spectrum is in a fade, other parts of the signal spectrum are not faded. One result of this is that the short-time variation of the total received power for a wide band CDMA signal is much less than that of the narrowband signal. Various techniques can be used to recover the signal as long as some portion of the received signal is not in a fade.

Finally, one property of the CDMA signal alluded to earlier is that many CDMA signals can be overlaid on top of each other in the same frequency band. Let us assume that there are two users in the system using the same frequency band at the same time. We assume that the PN sequence from user 0 is $c_0(t)$ and the PN sequence from user 1 is $c_1(t)$ where

$$c_k(t) = \sum_{j=-\infty}^{\infty} \sum_{i=0}^{M-1} c_{k,i} \Psi\left(\frac{t-(i+jM)T_c}{T_c}\right) \qquad |c_{k,i}| = 1 \tag{2.8}$$

The signals are said to be orthogonal over a bit period if

$$\int_{jT_b}^{(j+1)T_b} c_0(t)\, c_1^*(t)\, dt = 0 \tag{2.9}$$

Let us assume for the moment that the repetition rate of the PN-sequence is the same as the symbol period such that $MT_c = T_b$. When the length of the PN sequence, MT_c, is equal to the message symbol period, T_b, the system is called a $code - on - pulse$ system. If the sequences are chip aligned, and bit aligned, then the orthogonality over a symbol period may be expressed as

$$\sum_{i=0}^{M-1} c_{0,i} c_{1,i}^{*} = 0 \tag{2.10}$$

If each user has a different orthogonal underlying code sequence, then many users can share the same medium without interfering with each other.

The received signal at user 0's receiver consists of the desired signal, multiple assess interference from user 1, and noise

$$r_0(t) = A_0 b_0(t) c_0(t) \cos(2\pi f_c t) + A_1 b_1(t) c_1(t) \cos(2\pi f_c t + \vartheta_1) + n(t) \tag{2.11}$$

where

$$b_k(t) = \sum_{j=-\infty}^{\infty} b_{k,j} \Psi\left(\frac{t - jT_b}{T_b}\right)$$

The decision statistic for user 0 is obtained using equation (2.5). The component of the decision statistic due to the desired signal is $A_0 T_b b_{0,j}/2$, just as before. The component of the decision statistic due to the noise component is again a zero mean Gaussian random variable with variance $N_0 T_b/4$. In synchronous CDMA, the component due to the interference is

$$\int_{jT_b}^{(j+1)T_b} A_1 b_1(t) c_1(t) c_0^{*}(t) \cos(2\pi f_c t) \cos(2\pi f_c t + \vartheta_1)\, dt$$

$$= A_1 b_{1,j} \left(\sum_{i=0}^{M-1} c_{1,i} c_{0,i}^{*}\right) \int_{jT_b}^{(j+1)T_b} \cos(2\pi f_c t) \cos(2\pi f_c t + \vartheta_1)\, dt$$

$$= A_1 b_{1,j} \left(\sum_{i=0}^{M-1} c_{1,i} c_{0,i}^{*}\right) \frac{T_b}{2} \cos\vartheta_1 \tag{2.12}$$

3G CDMA systems use coherent demodulation on both forward link and reverse link. So in equation (2.12), $\vartheta_1 = 0$.

Thus if the spreading sequences of user 0 and user 1 are orthogonal, so that they satisfy equation (2.10), then the component of the decision statistic due to interference will be zero. In this case, the addition of the users in the same time and frequency slots will not affect the performance of other users. On the reverse link, since it is difficult to synchronize spatially separated mobile users on the bit and chip level, and since the signals travel different path lengths from the transmitter to the base station, it is not feasible to operate in a synchronous mode.

In the asynchronous case, where usually the sequence for user 1 is delayed by τ_1 seconds relative to the chip sequence for user 0, the expression describing the interaction between the signals from two users at the receiver for user 0 becomes considerable more complicated. We may express the delay as an integer number of chip periods γ_1 such that $\tau_1 = \gamma_1 T_c + \Delta_1$ where $0 \leq \Delta_1 \leq T_c$. We will further assume that for values of $i \geq M$ and $i < 0$ that $a_{1,i} = a_{1,i-mM}$, so that $0 \leq i - mM < M - 1$. Then the signals from user 0 and 1 will not interfere with each other if

$$\left(b_{1,j-1} \sum_{i=0}^{\gamma_1 - 1} c_{1,i-\gamma_1} c_{0,i}^* + b_{1,j} \sum_{i=\gamma_1}^{M-1} c_{1,i-\gamma_1} c_{o,i}^* \right) (T_c - \Delta_1)$$

$$+ \left(b_{1,j-1} \sum_{i=0}^{\gamma_1 - 1} c_{1,i-\gamma_1} c_{0,i+1}^* + b_{1,j} \sum_{i=\gamma_1}^{M-2} c_{1,i-\gamma_1} c_{o,i+1}^* \right) \Delta_1 = 0 \qquad (2.13)$$

It is not possible to select useful spreading codes which satisfy over equation (2.13) all possible values of $b_{i,j}$, $\Delta_1$and γ_1. Thus, in an asynchronous CDMA system, the signals from different users interfere with each other, resulting in higher bit error rates as compared with orthogonal CDMA. Therefore, in asynchronous CDMA systems, every user contributes interference, called Multiple Access Interference, to the decision statistic for other users.

For 3G CDMA, we use "gold code" for spreading code. Gold code has so excellent orthogonality that any two codes are still orthogonal even though they are asynchronous, having a phase shift. That is it can satisfy equation (2.13). Gold codes are families of codes with well-behaved cross-correlation properties which are constructed by a modulo-2 addition of specific relative phases of a preferred pair of m-sequences. The shift register configuration used to generate the Gold code in our simulation is illustrated in Figure 2.2.

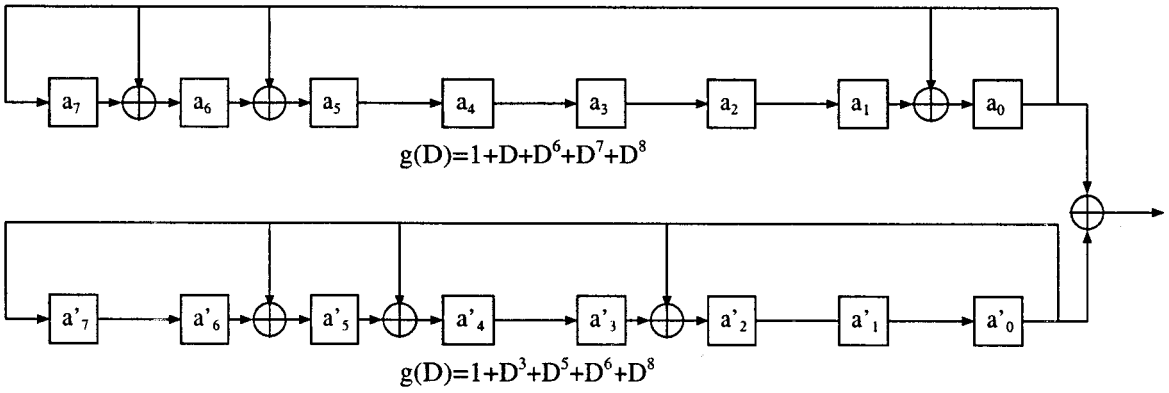

Figure 2.2: Gold code generator.

2.1.2 Multiple Access Interference in CDMA Systems

Consider a CDMA system in which K users occupy the same frequency band at the same time. These users may share the same cell, or some of the K users may communicate with other base stations.

The signal received at the base station from user k is given by[19]

$$s_k(t-\tau_k) = \sqrt{2P_k}b_k(t-\tau_k)\,c_k(t-\tau_k)\cos(2\pi f_c t + \phi_k) \tag{2.14}$$

where $b_k(t)$ is the data sequence for user k, $c_k(t)$ is the spreading (or chip) sequence for user k, τ_k is the delay of user k relative to a reference user 0, P_k is the

received power of user k, and ϕ_k is the phase offset of user k relative to a reference user 0. Since τ_k and ϕ_k are relative terms, we can define $\tau_0 = 0$ and $\phi_0 = 0$.

Let us assume that both $c_k(t)$ and $b_k(t)$ are binary sequences having values of -1 or +1.

The chip sequence $c_k(t)$ is of the form,

$$c_k(t) = \sum_{j=-\infty}^{\infty} \sum_{i=0}^{M-1} c_{k,i} \Psi \left(\frac{t - (i + jM) T_c}{T_c} \right) \quad c_{k,i} \in \{-1, 1\} \tag{2.15}$$

where M is the number of chips sent in a PN sequence period and T_c is the chip period. MT_c is the repetition period of the PN sequence.

For the data sequence, $b_k(t)$, T_b is the bit period. It is assumed that the bit period is an integer multiple of the chip period that $T_b = NT_c$. Note that M and N do not need to be the same. The binary data sequence $b_k(t)$ is given by

$$b_k(t) = \sum_{j=-\infty}^{\infty} b_{k,j} \Psi \left(\frac{t - jT_b}{T_b} \right) \quad b_{k,j} \in \{-1, 1\} \tag{2.16}$$

At the receiver, illustrated in Figure 2.3, the signal available at the input to the correlator is given by

$$r_0(t) = \sum_{k=0}^{K-1} s_k(t - \tau_k) + n(t) \tag{2.17}$$

where $n(t)$ is additive Gaussian noise with two-sided power spectral density $N_o/2$. It is assumed in equation (2.17) that there is no multipath in the channel with the possible exception of multipath that leads to flat fading such that the coherence time of the channel is considerably larger that a symbol period.

At the receiver, the received signal is mixed down to baseband, multiplied by the PN sequence of the desired user (user 0 for example) and integrated over one

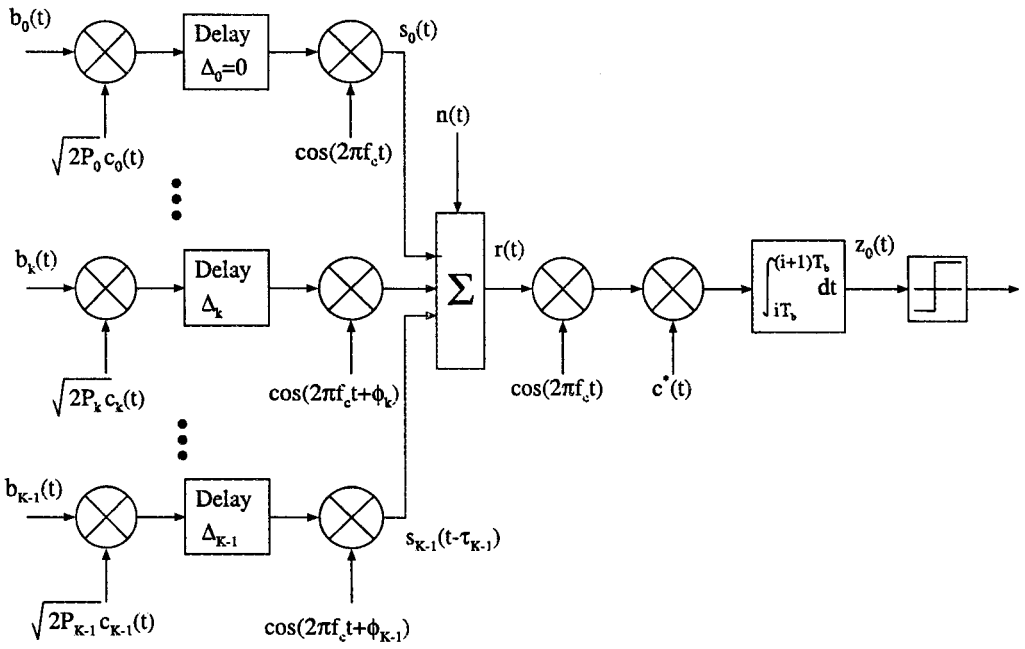

Figure 2.3: Model for CDMA multiple access interference[19]

bit period. Thus, assuming that the receiver is delay and phase synchronized with user 0, the decision statistic for user 0 is given by

$$z_0 = \int_{jT_b}^{(j+1)T_b} r_0(t)\, c_0^*(t) \cos(2\pi f_c t)\, dt \tag{2.18}$$

For convenience and simplicity of notation, the remainder of the analysis will be presented for the case of bit 0 (j=0 in equation (2.18)). Substituting equation (2.14) and (2.17) into equation (2.18),

$$z_0 = \int_0^{T_b} \left[\left(\sum_{k=0}^{K-1} \sqrt{2P_k} b_k(t-\tau_k)\, c_k(t-\tau_k) \cos(2\pi f_c t + \phi_k) \right) + n(t) \right] c_0^*(t) \cos(2\pi f_c t)\, dt \tag{2.19}$$

which may be expressed as

$$z_0 = I_0 + \eta + \zeta \tag{2.20}$$

where I_0 is the contribution to the decision statistic from the desired user ($k = 0$), ζ is the multiple access interference, and η is the noise contribution. The contribution from the desired user is given by

$$I_0 = \sqrt{2P} \int_0^{T_b} b_0(t) |c_0(t)|^2 \cos(2\pi f_c t)\, dt$$

$$= \sqrt{\frac{P}{2}} \int_0^{T_b} \left(\sum_{i=-\infty}^{\infty} b_{0,i} \Psi\left(\frac{t - iT_b}{T_b} \right) \right) (1 + \cos(2\pi f_c t))\, dt$$

$$= \sqrt{\frac{P}{2}} b_{0,0} \int_0^{T_b} (1 + \cos(2\pi f_c t))\, dt$$

$$= \sqrt{\frac{P}{2}} b_{0,0} T_b \tag{2.21}$$

The noise term, η is given by

$$\eta = \int_0^{T_b} n(t)\, c_0^*(t) \cos(2\pi f_c t)\, dt \tag{2.22}$$

where it is assumed that $n(t)$ is white Gaussian noise with two-sided power spectral density, $N_0/2$. The mean of η is

$$\mu_\eta = E[\eta] = \int_{t=0}^{T_b} E[n(t)]\, c_0^*(t) \cos(2\pi f_c t)\, dt = 0 \tag{2.23}$$

The third component in equation (2.20), ζ, represents the contribution of multiple access interference to the decision statistic. ζ is the summation of $K - 1$ terms, I_k ,

$$\zeta = \sum_{k=1}^{K-1} I_k \tag{2.24}$$

each of which is given by

$$I_k = \int_0^{T_b} \sqrt{2P} b_k (t - \tau_k) c_k (t - \tau_k) c_0^* (t) \cos(2\pi f_c t + \phi_k) \cos(2\pi f_c t) \, dt \tag{2.25}$$

Therefore, we get the received signal at the base station in detail.

2.2 Third Generation CDMA

2.2.1 Development Background of 3G

In 1980 the mobile cellular era started. Mobile communications have undergone significant changes and experienced enormous growth since then. First generation mobile systems using analog transmission for speech services were introduced in the 1980s. Several standards were developed: AMPS (Advanced Mobile Phone Service) in the United States, TACS (Total Access Communication System) in the United Kingdom, NTT (Nippon Telephone and Telegraph) in Japan, and so on.

Second generation systems using digital transmission were introduced in the late 1980s. They offer higher spectrum efficiency, better data services, and more advanced roaming than the first generation systems. GSM (Global System for Mobile Communications), PDC (Personal Digital Cellular), and IS-95 (US CDMA system) belong to the second generation systems. The services offered by these systems cover speech and low bit rate data.

The second generation systems will further evolve towards third generation systems and offer more advanced services such as bit rates of 100 to 200 Kbps for circuit and packet switch data. These evolved systems are commonly referred to as generation 2.5.

Recently, mobile communication services are penetrating. All of the current second-generation cellular communications systems (e.g., PDC, GSM and IS-95) have adopted digital technology. However, the major services they provide are limited to basic services, such as voice, facsimile, and low-bit-rate (far less than 64 Kbps) data. We are now in the 21st century, when demands for a variety of wideband services such as high-speed Internet access and video/high-quality image transmission, will continue to increase. The third-generation mobile communication system, called International Mobile Telecommunication-2000 (IMT-2000) in the International Telecommunication Union (ITU), must be designed to support wideband services at data rates as high as 2 Mbps, with the same quality as fixed networks. Table 2.1 shows the main differences between WCDMA and IS-95 air interfaces. Figure 2.4 shows the development of mobile cellular era.

	WCDMA	IS-95
Carrier Spacing	5 MHz	1.25 MHz
Chip Rate	3.84 $Mcps$	1.2288 $Mcps$
Power Control Frequency	1500 Hz *UL and DL*	800 Hz *UL; slow DL*
Base Station Sync	*No needed*	*Yes, typically via GPS*
Inter-frequency Handovers	*Yes, measurements with slotted mode*	*Possible; measurement method not specified*
Radio Resource Management	*Yes, provides QoS*	*No needed (speech only)*
Packet Data	*Load – based packet scheduling*	*Packet data transmitted as short circuit switched cells*
Downlink Transmit Diversity	*Supported*	*Not supported*

UL=uplink, DL=downlink, GPS=global positioning system.

Table 2.1: Main differences between WCDMA and IS-95 air interfaces.

The current Personal Communication Services (PCS) are based on narrowband technology optimized for basic services. To realize true IMT-2000 systems, a new wideband wireless access technology incorporating as many recent technology developments as possible is necessary. In IMT-2000 technology, there are North America's IS-95 method and Europe's GSM method. Currently, Europe is trying to commercialize WCDMA, a GSM method, to service IMT-2000. In future, it is

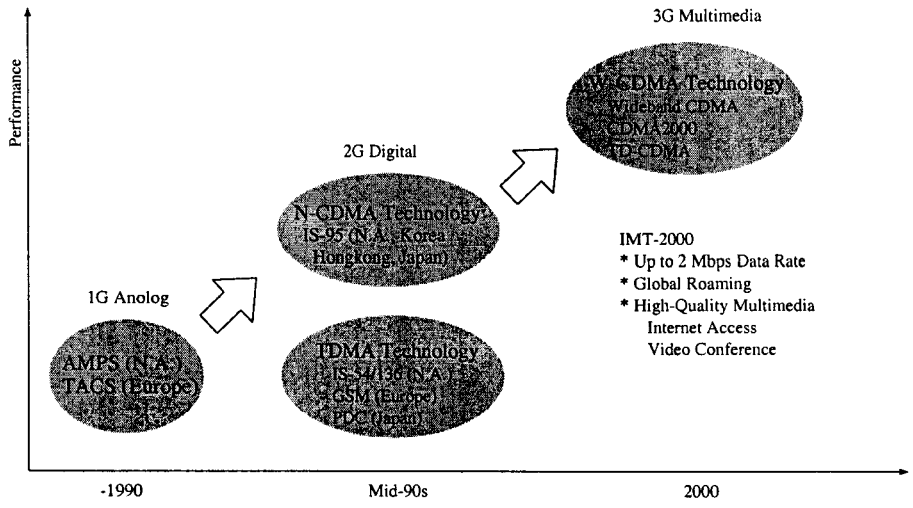

Figure 2.4: Development of mobile cellular era.

expected that the North America's CDMA2000 and Europe's WCDMA technologies will compete for the IMT-2000 market. Figure 2.5 and Figure 2.6 are the trends of two methods.

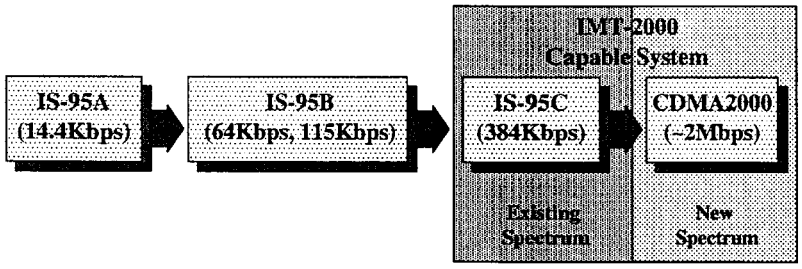

Figure 2.5: IMT-2000 trends in North America.

There are several differences between the two will-be-leading IMT-2000 technologies. Table 2.2 shows the differences between WCDMA and CDMA2000. If the two technologies are commercialized, the compatibility problem must be considered. Two users using different communication technologies must be possible to communicate anywhere and anytime.

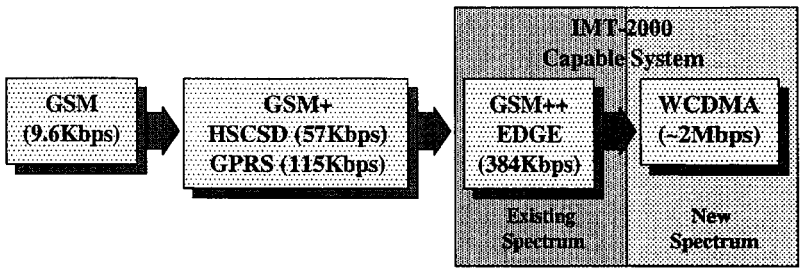

Figure 2.6: IMT-2000 trends in Europe.

	WCDMA	CDMA2000
Chip Rate	4.096 $Mcps$	3.6864 $Mcps$
Frame Duration	10 ms	10 ms
Base Station Sync	*Asynchronous*	*Synchronous*
Base Station Acq	3 *step paral code sync for base station slot/frame*	*Sync through time–shifted PN correlation*
Forward Link Pilot	*TDM dedicated pilot*	*CDM common pilot*
Antenna Beamforming	*TDM dedicated pilot*	*Auxiliary pilot*

Table 2.2: WCDMA Versus CDMA2000.

2.2.2 Key WCDMA Features

An air interface based on direct-sequence CDMA and operation at a wide bandwidth gives the opportunity to design a system with property fulfilling the third-generation requirements.

Performance Improvement

- Capacity Improvement – The wide bandwidth of WCDMA gives an inherent performance gain over previous cellular systems, since it reduces the fading of the radio signal. In addition, WCDMA uses coherent demodulation in the uplink, a feature that has not previously been implemented in cellular CDMA systems. Also, fast power control on the downlink will give improved performance. In total, for a speech service, these improvements are expected to increase the cell capacity of WCDMA by at least a factor of two(3dB).

- Coverage and Link Budget Improvements – The coverage of WCDMA is determined by the link performance through the link budget. Assumptions for the comparison are that the average mobile output power is equal in WCDMA and GSM. The results show that a WCDMA speech service will tolerate a few dB higher path loss than a GSM speech service. This means that WCDMA gives better speech coverage than GSM, reusing the same cell sites when being deployed in the same or a nearby frequency band.

Service Flexibility

- Support of a wide range of service with maximum bit rates about 2 Mbps and the possibility for multiple parallel services on one connection. This flexibility is supported in WCDMA with the use of orthogonal variable spreading factor (OVSF) codes for chanelization of different users.

Operator Flexibility

- Interfrequency Handover – The support of seamless through interfrequency handover through a downlink slotted mode is a key feature of WCDMA. Interfrequency handover is necessary for the support of hierarchical cell structure (HCS) with overlapping micro- and macrocells operation on different carrier frequencies. With HCS, a cellular system can provide very high system capacity through the microcell layer, at the same time offering full coverage and support high mobility by the macrolayer. Hot spot is a certain cell that serves a high traffic area uses additional carriers to those used by the neighboring cell. If the deployment of extra carriers is to be limited to the actual hot spot area, the possibility of interfrequency handover is essential.

- Support for Adaptive Antenna Arrays – WCDMA system supports full utilization of adaptive antenna through the use of dedicated pilot symbols on both uplink and downlink.

2.3 Channel Model

A CDMA system employing binary phase shift keying (BPSK) will be considered here. The voice coder used in the k^{th} mobile will generate a data sequence $b_k(t)$, with each symbol having a period of time T_b seconds. This is then modulated by the user's pseudo-noise (PN) sequence $c_k(t)$, which repeats with period T_b seconds. The PN sequence is composed of N binary "chips", each of period T_c. The transmitted RF signal, $s_k(t)$ is given by:

$$s_k(t) = \sqrt{2P_k} b_k(t) c_k(t) \cos(2\pi f_c t) \tag{2.26}$$

where f_c denotes the angular frequency of the carrier (with associated wavelength λ) and P denotes the signal power. In our simulation, for 3G CDMA system, the value of T_c will be 2.67×10^{-7} sec and processing gain will be 255, so that T_b=6.83×10^{-5}sec.

The received baseband signal for K active mobiles at a single antenna base station may be written as:

$$r(t) = \sum_{k=0}^{K-1} \sqrt{2P_k} \rho_k b_k (t - \tau_k) c_k (t - \tau_k) \exp\{j\phi_k\} + n(t) \tag{2.27}$$

where ρ_k, ϕ_k and τ_k denote the channel attenuation, phase shift and time delay for the k^{th} user. The complex scalar $n(t)$ is a white Gaussian noise process with single sided power spectral density N_0.

There are usually a large number of paths or multipaths, each with an associated time delay, by which $s_k(t)$ can reach the receiver. In a CDMA system, the base station receiver using a single antenna can resolve multipath components separated in time by at least T_c seconds. If significant multipath energy is received over the range of excess time delays [0,T_d], the receiver can resolve $Q = 1 + int(T_d/T_c)$ separate channel taps, $-int()$ denotes the integer part. The channel impulse response

for the k^{th} user may therefore be modeled as:

$$h_k(t) = \sum_{q=1}^{Q} \alpha_q^{(k)} \delta(t - \tau_q^{(k)}) \exp\{j\phi_q^{(k)}\} \tag{2.28}$$

where $\alpha_q^{(k)}$, $\tau_q^{(k)}$ and $\phi_q^{(k)}$ are the qth path gain, delay, and phase, respectively, for the kth user and Q is the number of paths. Further, for each q and k the path delay $\tau_q^{(k)}$ is assumed to be an independent random variable uniformly distributed over $[0, T]$ where T is the symbol interval duration. Likewise, the path gains $\alpha_q^{(k)}$ are assumed to be independent Rayleigh random variables with the average path power $E\left[\left(\alpha_q^{(k)}\right)^2\right] \equiv 2\rho$ for all k and q where ρ is some given constant. Then, the received signal is given by

$$y(t) = \sum_{k=1}^{K} \sum_{q=1}^{Q} \sqrt{2P_k}\alpha_q^{(k)} b_k\left(t - \tau_q^{(k)}\right) c\left(t - \tau_q^{(k)}\right) \cos\left(2\pi\left(f_c - f_d\right)t + \phi_q^{(k)}\right) + n(t) \tag{2.29}$$

where $\phi_q^{(k)}$ is an independent random variable uniformly distributed over $[0, 2\pi]$ representing the path phase of the received signal, and f_d is Doppler frequency shift.

The type of fading experienced by a signal propagating through a mobile radio channel depends on the nature of the transmitted signal with respect to the characteristics of the channel. The time dispersion and frequency dispersion mechanisms in a mobile radio channel lead to four possible distinct effects. While multipath delay spread leads to time dispersion and frequency selective fading, Doppler spread leads to frequency dispersion and time selective fading. The propagation mechanisms are independent of one another. So, we have four types of small-scale fading, flat slow fading, flat fast fading and frequency selective slow fading, frequency selective fast fading.

2.4 Flow Chart

Figure 2.7 is the flow chart of the simple CDMA system, including transmitter, channel and receiver.

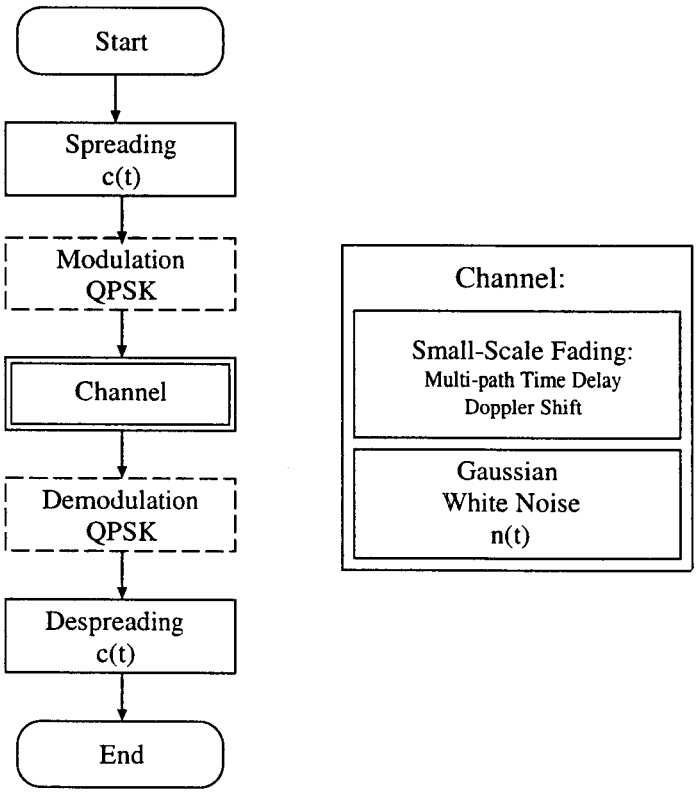

Figure 2.7: Flow chart of CDMA system and fading channel.

2.5 Simulation

As a starting point, we have computer simulated a simple model for the 3G CDMA transmitter and receiver and evaluated the P_b performance under AWGN and cochannel interference without any adaptive antenna.

2.5.1 Simulation Parameters

- Chip rate of 3G CDMA: $R_c = 3.75 \times 10^6 chips/sec.$

- Bit rate of 3G CDMA system: $R_b = 1.46 \times 10^4 bits/sec.$
- Processing gain of 3G: $N = 255.$
- Carrier frequency: $f_c = 1.9 \times 10^9 Hz.$
- Time shift between multipaths for flat fading: $\tau < 5 \times 10^{-8} second.$
- Time shift between multipaths for frequency selective fading: $\tau > 10^{-6} second.$
- The moving speed of subscriber for slow fading: $v_{SlowFading} = 2.7m/sec(10Km/h)$.
- The moving speed of subscriber for fast fading: $v_{FastFading} = 33.3m/sec(120Km/h)$ (Because the chip rate of 3G CDMA is very high. The fast fading here is comparatively fast, not the fast fading by definition, which requires $v_{FastFading} > 110Km/sec$).
- In the simulation, we assume both baseband modulation and demodulation processes are ideal.
- Channel model: the 2-ray resolvable channel where each user has two multipaths. (The reason for using the 2-ray resolvable channel is that the bandwidth of the transmitted signal, i.e., the direct sequence spread spectrum signal, is very high compared to the bandwidth of the wireless radio channel, therefore the multipaths are resolvable in time.)

2.5.2 Single User CDMA System

Figure 2.8 shows the probability of bit error of four types of small scale fading of single user CDMA system according to different bit SNR of Gaussian White Noise. From Figure 2.8, we see that the BER increases as the E_b/N_0 decreases. Also BER is more sensitive to frequency selective fading.

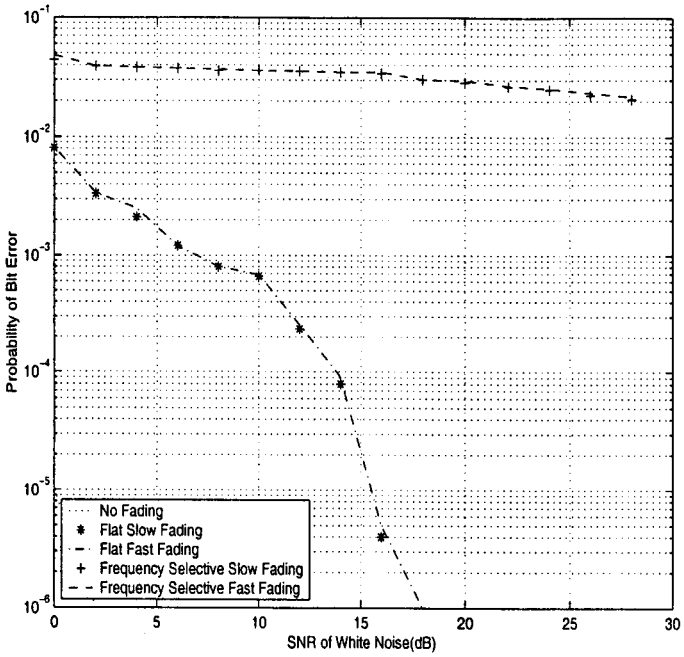

Figure 2.8: Probability of error of single user CDMA system (no interference).

2.5.3 Muti User CDMA System

Figure 2.9 shows the probability of bit error of four types of small scale fading of multi user CDMA system according to different number of users per cell.

From Figure 2.9, we see that the BER increases as the number of users per cell increases. The BER increase for higher E_b/N_0 case is more obvious than the lower E_b/N_0 case. This is because for a low E_b/N_0, in addition to the interference, the noise also play an important role in determining the BER. The BER increases are higher in fading channels in the order: frequency selective fast fading channel, frequency selective slow fading channel, flat fast channel, flat slow channel.

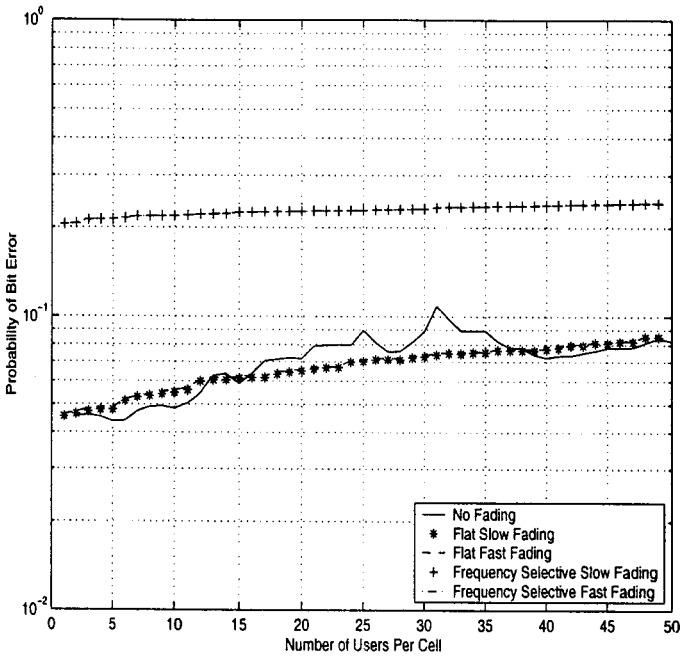

(a) $E_b/N_0 = 5$ dB

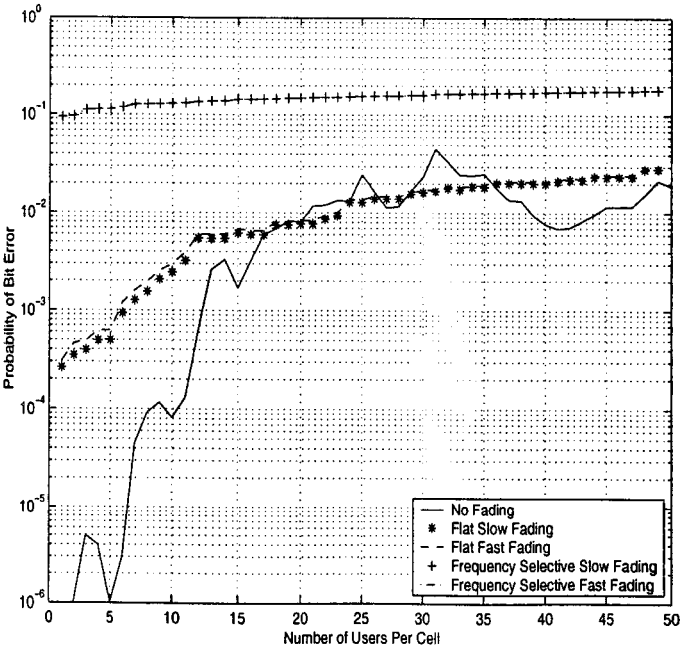

(b) $E_b/N_0 = 15$ dB

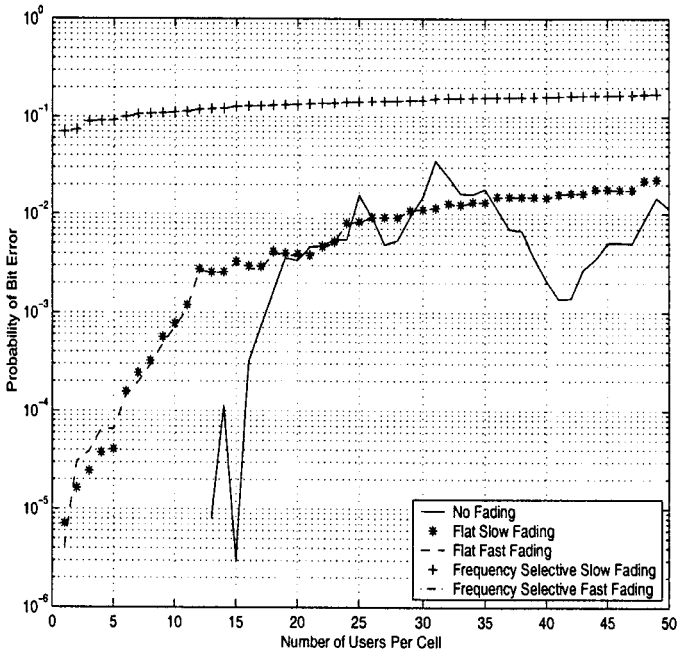

(c) $E_b/N_0 = 25$ dB.

Figure 2.9: Probability of error of multi-user CDMA system.

Chapter 3

FUNDAMENTALS OF ADAPTIVE ANTENNA ARRAYS

An antenna array consists of a set of antenna elements that are spatially distributed at known locations with reference to a common fixed point. By changing the phase and amplitude of the exciting currents in each of the antenna elements, it is possible to electronically scan the main bea m and/or place nulls in any direction.

The antenna elements can be arranged in various geometries, with linear, circular and planar arrays being very common. In the case of a linear array, the centers of the elements of the array are aligned along a straight line. If the spacing between the array elements is equal, it is called a uniformly spaced linear array.

The radiation pattern of an array is determined by the radiation pattern of the individual elements, their orientation and relative positions in space, and amplitude and phase of the feeding currents. If each element of the array is an isotropic point source, then the radiation pattern of the array will depend solely on the geometry and feeding current of the array, and the radiation pattern so obtained is called the array factor.

3.1 Uniformly Spaced Linear Array

Consider an M-element uniformly spaced linear array which is illustrated in Figure 3.1. In Figure 3.1, the array element are equally spaced by a distance d, and a plane wave arrives at the array from a direction θ off the array broadside. The angle θ is called the direction-of-arrival (DOA) of the received signal, and is measured clockwise from the broadside of the array. The received signal at the first element may be expressed as

$$\widetilde{x}_0(t) = u(t)\cos(2\pi f_c t + \gamma(t) + \varphi) \tag{3.1}$$

where f_c is the carrier frequency of the modulated signal, $\gamma(t)$ is the information carrying component, $u(t)$ is the amplitude of the signal, and φ is a random phase. It is convenient to use the complex envelope representation of $\widetilde{x}_0(t)$ which is given by

$$x_0(t) = u(t)\exp\{j(\gamma(t) + \varphi)\} \tag{3.2}$$

The received signal at the first element $\widetilde{x}_0(t)$ and its complex envelope $x_0(t)$ may be related by

$$\widetilde{x}_0(t) = Re[x_0(t)\exp\{j(2\pi f_c t)\}] \tag{3.3}$$

where $Re[\,]$ stands for the real part of $[\,]$. Now taking the firs t element in the array as the reference point, if the signals have originated far away from the array, and these plane waves advance through a non-dispersive medium that only introduces propagation delays, the output of any other array element can be represented by a time-advanced or time-delayed version of the signal at the first element. From Figure 3.1, we see that the plane wavefront at the first element

should propagate through a distance $d\sin\theta$ to arrive at the second element. The time delay due to this additional propagation distance is given by

$$\tau = \frac{d\sin\theta}{c} \tag{3.4}$$

where c is the velocity of light. Now, the received signal of the second element may be expressed as

$$\widetilde{x}_1(t) = \widetilde{x}_0(t-\tau) = u(t-\tau)\cos\left(2\pi f_c(t-\tau) + \gamma(t-\tau) + \varphi\right) \tag{3.5}$$

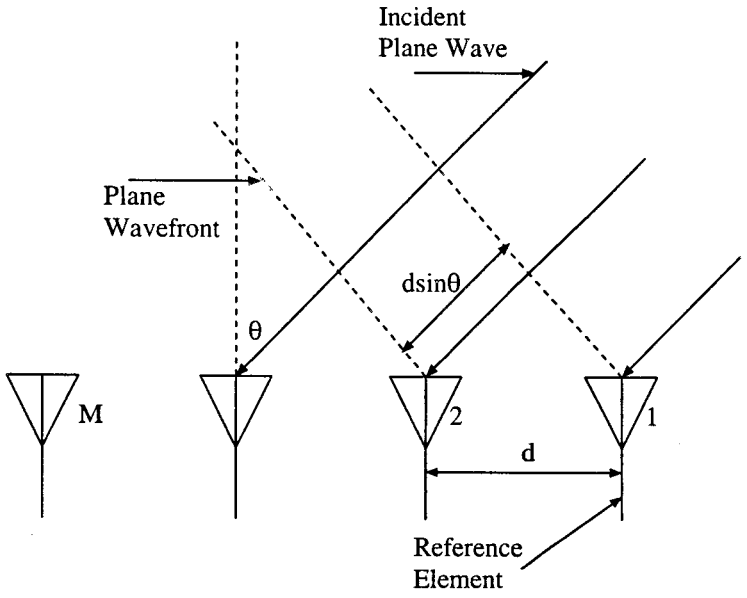

Figure 3.1: Illustration of a plane wave incident on a uniformly spaced linear array from direction θ.

If the carrier frequency f_c is large compared to the bandwidth of the impinging signal, then the modulation signal may be treated as quasi-static during time intervals of order τ and in that case equation (3.5) reduces to

$$\widetilde{x}_1(t) = u(t)\cos\left(2\pi f_c t - 2\pi f_c\tau + \gamma(t) + \varphi\right) \tag{3.6}$$

The complex envelope of $\widetilde{x}_1(t)$ is therefore given by

$$x_1(t) = u(t)\exp\{j(-2\pi f_c\tau + \gamma(t) + \varphi)\} \tag{3.7}$$

$$= x_0(t)\exp\{-j(2\pi f_c\tau)\}$$

From equation (3.7) we see that the effect of the time delay on the signal can now be represented by a phase shift term $\exp\{-j(2\pi f_c\tau)\}$. Substituting equation (3.4) to (3.7), we have

$$x_1(t) = x_0(t)\exp\left\{-j\left(2\pi f_c\frac{d\sin\theta}{c}\right)\right\} \tag{3.8}$$

$$= x_0(t)\exp\left\{-j\left(\frac{2\pi}{\lambda}d\sin\theta\right)\right\}$$

where λ is the wavelength of the carrier. In equation (3.8), we have used the relation between c and f_c , that is, $f_c = \frac{c}{\lambda}$. Similarly, for element m, the complex envelop of the received signal may be expressed as

$$x_m(t) = x_0(t)\exp\left\{-j\left(\frac{2\pi}{\lambda}md\sin\theta\right)\right\} \qquad m = 0, ..., M-1. \tag{3.9}$$

Let

$$\overrightarrow{x}(t) = \begin{bmatrix} x_0(t) \\ x_1(t) \\ \vdots \\ x_{M-1}(t) \end{bmatrix} \tag{3.10}$$

and

$$\overrightarrow{a}(\theta) = \begin{bmatrix} 1 \\ e^{-j\left(\frac{2\pi}{\lambda} d \sin\theta\right)} \\ \vdots \\ e^{-j\left(\frac{2\pi}{\lambda}(M-1) d \sin\theta\right)} \end{bmatrix} \tag{3.11}$$

then equation (3.9) may be expressed in vector form as

$$\overrightarrow{x}(t) = \overrightarrow{a}(\theta)\, x_0(t) \tag{3.12}$$

The vector $\overrightarrow{x}(t)$ is often referred to as the array *input data vector*, and $\overrightarrow{a}(\theta)$ is called the *steering vector.* The steering vector is also called *direction vector, array vector, array response vector, array manifold vector, DOA vector, or aperture vector.* In this case, the steering vector is only a function of the angle-of-arrival. In general, however, the steering vector is also a function of the individual element response, the array geometry, and signal frequency.

In the above discussion, the bandwidth of the impinging signal expressed in equation (3.9) is assumed to be much smaller than the reciprocal of the propagation time across the array. Any signal satisfying this condition is referred to as *narrowband*, otherwise it is referred to as *wideband.* In most of the discussion that follows, the signal is assumed to be narrowband unless specified otherwise.

We could extend the above simple case to a more general case. Suppose there are Q signals $s_1(t), ..., s_Q(t)$, all centered around a known frequency, say, f_c, impinging on the array with a DOA θ_q, $q = 1, 2, ..., Q$. These signals may be uncorrelated, as happens in multipath propagation, where each path is a scaled and time-delayed version of the original transmitted signal, or can be partially correlated due to the noise corruption. The received signal at the array is a superposition of all the impinging signals and noise. Therefore, the input data vector may be expressed as

$$\vec{x}(t) = \sum_{q=1}^{Q} \vec{a}(\theta_q)\, s_q(t) + \vec{n}(t) \tag{3.13}$$

where

$$\vec{a}(\theta_q) = \begin{bmatrix} 1 \\ e^{-j\left(\frac{2\pi}{\lambda} d \sin\theta_q\right)} \\ \vdots \\ e^{-j\left(\frac{2\pi}{\lambda}(M-1) d \sin\theta_q\right)} \end{bmatrix} \tag{3.14}$$

and $\vec{n}(t)$ denotes the $M \times 1$ vector of the noise at the array elements. In matrix notation, equation (3.13) becomes

$$\vec{x}(t) = A(\Theta)\, \vec{s}(t) + \vec{n}(t) \tag{3.15}$$

where $A(\Theta)$ is the $M \times Q$ matrix of the steering vectors

$$A(\Theta) = \begin{bmatrix} \vec{a}(\theta_1) & \vec{a}(\theta_2) & \cdots & \vec{a}(\theta_Q) \end{bmatrix} \tag{3.16}$$

and

$$\vec{s}(t) = \begin{bmatrix} s_1(t) \\ s_2(t) \\ \vdots \\ s_Q(t) \end{bmatrix} \tag{3.17}$$

Equation (3.15) represents the most commonly used *input data model.*

Now let us consider a special case. Assume that P users transmit signals from different locations, and each user's signal arrives at the array through multiple paths.

Let L_{Mi} denote the number of multipath components of the i^{th} user. We have

$$\sum_{i=1}^{P} L_{Mi} = Q.$$

Let us further assume that all of the multipath components for a particular user arrive within a time window which is much less than the channel symbol period for that user, then the input data vector could be expressed as

$$\vec{x}(t) = \sum_{i=1}^{P} \sum_{k=1}^{L_{Mi}} \alpha_{i,k} \vec{a}(\theta_{i,k}) s_i(t) + \vec{n}(t) \tag{3.18}$$

$$= \sum_{i=1}^{P} \vec{b}_i s_i(t) + \vec{n}(t)$$

where $\theta_{i,k}$ is the DOA of the k^{th} multipath component for the i^{th} user, $\vec{a}(\theta_{i,k})$ is the steering vector corresponding to $\theta_{i,k}$, $\alpha_{i,k}$ is the complex amplitude of the k^{th} multipath component for the i^{th} user, and $\vec{b}_i$ is the spatial signature for the i^{th} user and is given by

$$\vec{b}_p = \sum_{k=1}^{L_{Mi}} \alpha_{i,k} \vec{a}(\theta_{i,k}) \tag{3.19}$$

Similarly, equation (3.18) can be written in matrix form

$$\vec{x}(t) = B\vec{s}(t) + \vec{n}(t) \tag{3.20}$$

where

$$B = \left[\vec{b}_1 \quad \vec{b}_2 \quad \cdots \quad \vec{b}_P \right] \tag{3.21}$$

and

$$\vec{s}(t) = \begin{bmatrix} s_1(t) \\ s_2(t) \\ \vdots \\ s_P(t) \end{bmatrix}$$

The matrix B is called the *spatial signature matrix.*

In equation (3.15), if the data vector $\vec{x}(t)$ is sampled K times, at $t_1, ..., t_K$, the sampled data may be expressed as

$$X = A(\Theta) S + N \tag{3.22}$$

where X and N are the $M \times K$ matrices containing K snapshots of the input data vector and noise vector, respectively,

$$X = [\vec{x}(t_1), ..., \vec{x}(t_K)] \tag{3.23}$$

$$= [\vec{x}(1), ..., \vec{x}(K)]$$

$$N = [\vec{n}(t_1), ..., \vec{n}(t_K)] \tag{3.24}$$

$$= [\vec{x}(1), ..., \vec{x}(K)]$$

and S is the $Q \times K$ matrix containing K snapshots of the signals

$$S = [\vec{s}(t_1), ..., \vec{s}(t_K)] \tag{3.25}$$

$$= [\overrightarrow{s}(1), ..., \overrightarrow{s}(K)]$$

in equation (3.23), (3.24) and (3.25), we have replaced the time index t_k with $k = 1, ..., K$, for notational simplicity.

With the data model created above, most array processing problems may be categorized as follow. Given the sampled data X in a wireless system, determine:

1. the number of signals Q
2. the DOAs $\theta_1, ..., \theta_Q$
3. the signal waveform $\overrightarrow{s}(1), ..., \overrightarrow{s}(K)$.

We shall refer to (1) as the *detection* problem, to (2) as the *localization* problem, and to (3) as the *beamforming* problem, which is the focus of this research.

3.2 Beamforming and Spatial Filtering

Beamforming is one type of processing used to form beams to simultaneously receive a signal radiating from a specific location and attenuate signals from other locations[20]. Systems designed to receive spatially propagating signals often encounter the presence of interference signals. If the desired signal and interference occupy the same frequency band, unless the signals are uncorrelated, e.g., CDMA signals, then temporal filtering often cannot be used to separate signal from interference. However, the desired and interfering signals usually originate from different spatial locations. This spatial separation can be exploited to separate signal from interference using a spatial filter at the receiver. Implementing a temporal filter requires processing of data collected over a temporal aperture. Similarly, implementing a spatial filter requires processing of data collected over a spatial aperture.

A Beamformer is a processor used in conjunction with an array of sensors (i.e., antenna elements in an adaptive array) to provide a versatile form of spatial filtering.

The sensor array collects spatial samples of propagating wave fields, which are processed by the beamformer. Typically a beamformer linearly compiles the spatially sampled time series from each sensor to obtain a scalar output time series in the same manner that an FIR filter linearly combines temporally sampled data. There are two types of beamformers, narrowband beamformer, and wideband beamformer.

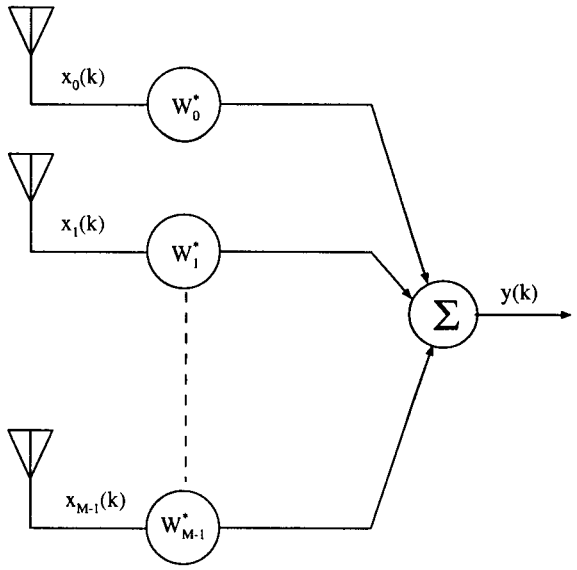

Figure 3.2: A narrowband beamformer forms a linear combination of the sensor outputs.

A narrowband beamformer is shown in Figure 3.2. In Figure 3.2, the output at time k, $y(k)$, is given by a linear combination of the data at the M sensors at time k,

$$y(k) = \sum_{m=0}^{M-1} w_m^* x_m(k) \tag{3.26}$$

where * denotes complex conjugate. Since we are now using the complex envelope representation of the received signal, both $x_m(k)$ and w_m are complex. The weight w_i is called the complex weight. The beamformer shown in Figure 3.2 is typically used for processing narrowband signals. In the following following

discussion, each sensor is assumed to have all necessary receiver electronics and A/D converters if beamforming is performed digitally.

Substituting equation (3.2) and (3.9) into (3.26), we have

$$y(k) = \sum_{m=0}^{M-1} w_m^* x_m(k) = u(t) \sum_{m=0}^{M-1} w_m^* e^{-j\beta md\sin\theta} = u(t) f(\theta) \tag{3.27}$$

where $\beta = 2\pi/\lambda$ is the phase propagation factor.

The term $f(\theta)$ is called the array factor. The array factor determines the ratio of the received fsignal available at the array output, $y(t)$, to the signal, $u(t)$, measured at the reference element, as a function of DOA. By adjusting the set of weights, $\{w_m\}$, it is possible to direct the maximum of the main beam of the array factor in any desired direction θ_0. That is to say, the array factor determines the beam patterns of adaptive arrays..

To show how the weight, $\{w_m\}$, can be used to change the antenna pattern of the array, let the m^{th} weight be given by

$$w_m = e^{j\beta md\sin\theta_0} \tag{3.28}$$

Then the array factor is

$$f(\theta) = \sum_{m=0}^{M-1} e^{-j\beta md(\sin\theta - \sin\theta_0)} \tag{3.29}$$

$$= \frac{\sin\left(\frac{\beta Md}{2}(\sin\theta - \sin\theta_0)\right)}{\sin\left(\frac{\beta d}{2}(\sin\theta - \sin\theta_0)\right)} e^{-j\frac{\beta d}{2}(\sin\theta - \sin\theta_0)}$$

From equation (3.29), we will know the antenna gain in any direction, θ.

Equation (3.26) may also be written in vector form as

$$y(k) = \overrightarrow{w}^H x(k) \tag{3.30}$$

where

$$\overrightarrow{w} = \begin{bmatrix} w_0 \\ w_1 \\ \vdots \\ w_{M-1} \end{bmatrix} \tag{3.31}$$

and H denotes the Hermitian (complex conjugate) transpose. The vector $\overrightarrow{w}$ is called the complex weight vector.

Different from a narrowband beamformer, a wideband beamformer samples the propagating wave field in both space and time and is often used when signals of significant frequency extent (broadband) are of interest[20]. A wideband beamformer is show in Figure 3.3.

The output in this case may be expressed as

$$y(k) = \sum_{m=0}^{M-1} \sum_{l=0}^{K-1} w_{m,l}^* x_m(k-l) \tag{3.32}$$

where $K-1$ is the number of delays in each of the M sensor channels. Let

$$\overrightarrow{w} = [w_{0,0}, ..., w_{0,K-1}, ..., w_{M-1,0}, ..., w_{M-1,K-1}]^T \tag{3.33}$$

and

$$\overrightarrow{x}(k) = [x_0(k), ..., x_0(k-K+1), ..., x_{M-1}(k), ..., x_{M-1}(k-K+1)]^T \tag{3.34}$$

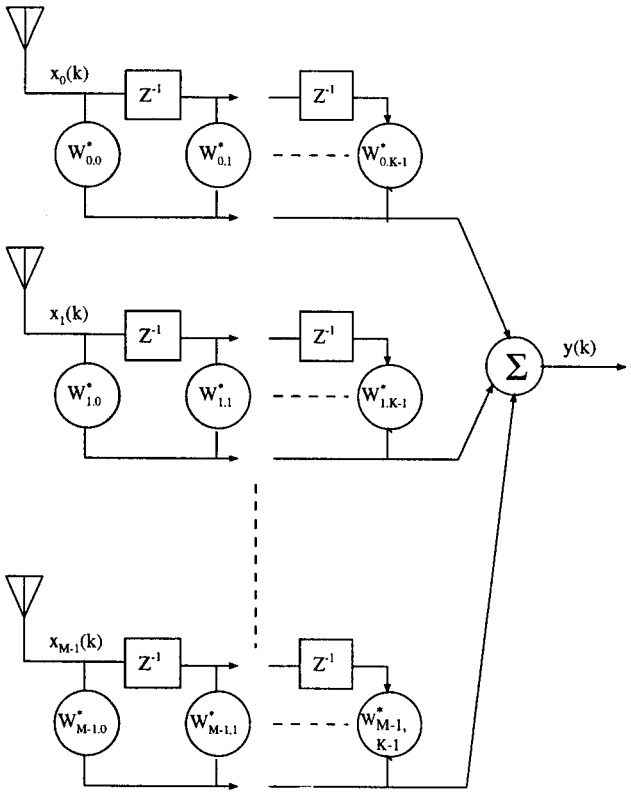

Figure 3.3: A wideband beamformer samples the signal in both space and time.

where T denotes the conventional transpose, equation (3.32) may also be expressed in vector for as in equation (3.30). In this case, both $\vec{w}$ and $\vec{x}(k)$ are $MK \times 1$ column vectors.

Comparing Figure 3.2 with Figure 3.3, we see that a wideband beamformer is more complex than a narrowband beamformer. Since both types of beamformers may share the same data model, we concentrate on the narrowband beamformer in the following discussion.

3.3 Adaptive Arrays

In a mobile communication system, the mobile is generally moving, therefore the DOAs of the received signals in the base station are time-varying. Also, due to the

time-varying wireless channel between the mobile and the base station, and the existence of the cochannel interference, multipath, and noise, the parameters of reach impinging signal are varied with time. For a beamformer with constant weight, the resulting beam pattern cannot track these time-varying factors. However, an adaptive array may change its patterns automatically in response to the signal environment. An adaptive array is a antenna system that can modify its beam pattern or other parameters, by means of internal feedback control while the antenna system is operating. Adaptive arrays are also known as adaptive beamformers, or adaptive antennas. A simple narrowband adaptive array is show in Figure 3.4. And Figure 3.5 is a general flow chart of a CDMA system with antenna array. The following flow charts in this chapter is only the "antenna array" part in this figure.

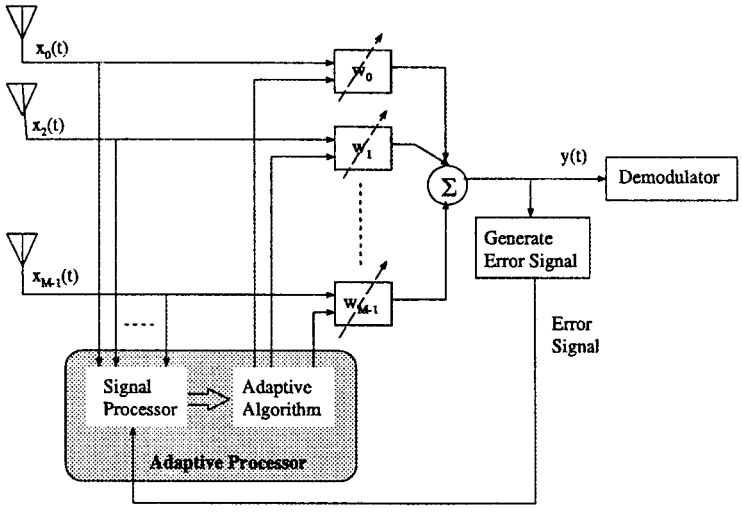

Figure 3.4: A simple narrowband adaptive array.

In Figure 3.4, the complex weight $w_1, ..., w_M$ are adjusted by the adaptive control processor. The method used by the adaptive control processor to change the weights is called the adaptive algorithm. Most adaptive algorithms are derived by first creating a performance criterion, and then generating a set of iterative equations to adjust the weights such that the performance criterion is met. Some of the most frequently used performance criteria include minimum mean squared error (MSE),

maximum signal-to-interference-and-noise ratio (SINR), maximum likelihood (ML), minimum noise variance, minimum output power, maximum gain, etc[21]. These criteria are often expressed as cost functions which are typically inversely associated with the quality of the signal at the array output. As the weights are iteratively adjusted, the cost function becomes smaller and smaller. When the cost function is minimized, the performance criterion is met and the algorithm is said to have converged.

3.4 Summary

In this chapter we introduced terminology and basic concepts related to antenna array and adaptive beamforming. The correspondence between a narrowband beamformer and a FIR filter is also introduced. In Chapter 4, a survey of adaptive beamforming algorithms is presented.

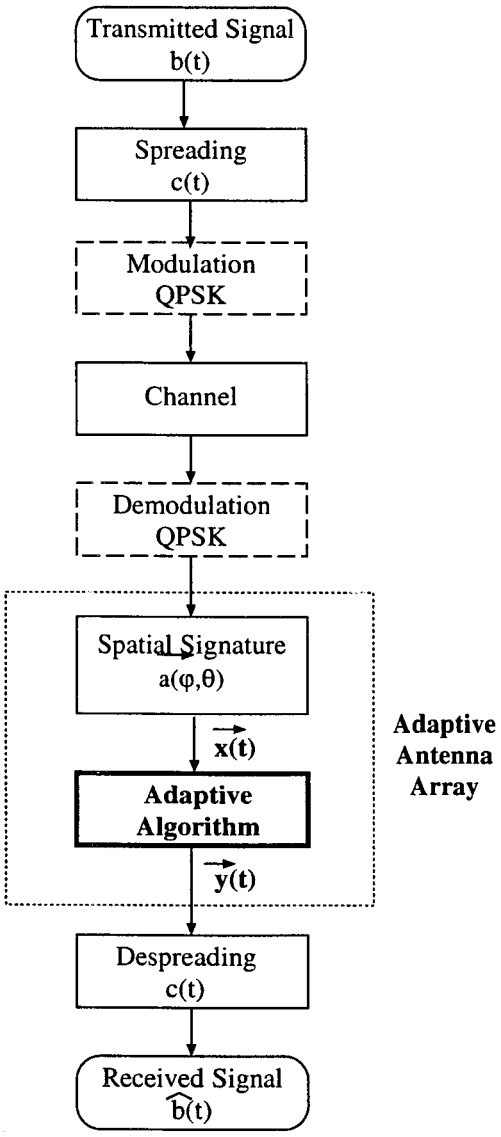

Figure 3.5: Flow chart of CDMA system with adaptive antenna array.

Chapter 4

ADAPTIVE BEAMFORMING ALGORITHMS

4.1 Introduction

In CDMA mobile communication system, multiple users occupy the same frequency band. The beamformer in the base station attempts to form a beam directed to each user, so that for one desired user, the interference from other directions is reduced. For a system with P users, the beamformer will generate P complex weight vectors.

Figure 4.1 shows the structure of a multitarget adaptive beamformer with M antenna elements and Q output ports. In Figure 4.1, $y_1(k), ..., y_Q(k)$ are the outputs of ports $1, ..., Q$, respectively, and $\overrightarrow{w}_1, ..., \overrightarrow{w}_Q$ are the weight vectors of port $1, ..., Q$, respectively. From Figure 4.1, the multitarget beamformer can be viewed as a multi-input multi-output system.

This chapter provides a thorough survey of adaptive beamforming algorithms. Most of these algorithms may be categorized two classes according to whether a reference signal is used or not. One class of these algorithms is the non-blind adaptive algorithm in which a reference signal is used to adjust the array weight vector. Another technique is to use a blind adaptive algorithm which does not require a

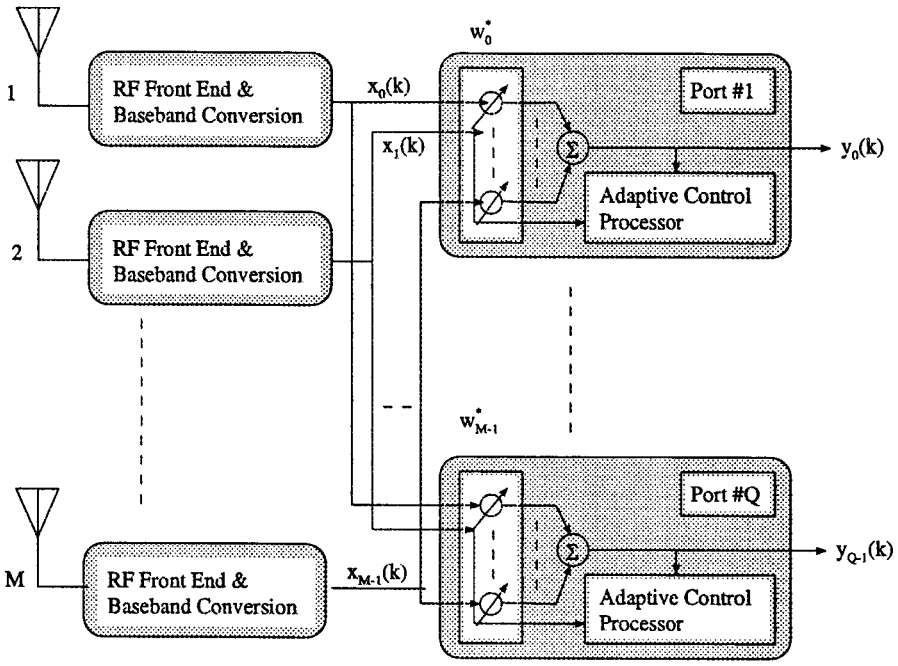

Figure 4.1: A multitarget adaptive beamformer with M antenna elements and Q output ports.

reference signal.

Since the non-blind algorithms use a reference signal, data cannot be sent over the radio channels all the time. This reduces the spectral efficiency of the system. Therefore , the blind algorithm are of more research interest. The research here focuses primarily on blind beamforming algorithms.

4.2 Non-blind Adaptive Beamforming Algorithm

In a non-blind adaptive algorithm, a reference signal, $d(t)$, which is known to both the transmitter and receiver, is sent from the transmitter to the receiver. The beamformer in the receiver uses the information of the training signal to compute the optimal weight vector, $\vec{w}_{opt}$.

4.2.1 Adaptive Beamforming with Pilot Channel on Reverse Link of 3G CDMA System

4.2.1.1 Wiener Solution

Most of the non-blind algorithms try to minimize the mean-squared error between the desired signal $d(t)$ and the array output $y(t)$. Let $y(k)$ and $d(k)$ denote the sampled signal of $y(t)$ and $d(t)$ at time instant t_k, respectively. Then the error signal is given by [23]

$$e(k) = d(k) - y(k) \tag{4.1}$$

and the mean-square error is defined by

$$J = E\left[|e(k)|^2\right] \tag{4.2}$$

where $E[\,]$ denotes the ensemble expectation operator. Substituting equation (4.1) and (3.30) into equation (4.2), we have

$$J = E\left[|d(k) - y(k)|^2\right] \tag{4.3}$$

$$= E\left[\{d(k) - y(k)\}\{d(k) - y(k)\}^*\right]$$

$$= E\left[\left\{d(k) - \vec{w}^H \vec{x}(k)\right\}\left\{d(k) - \vec{w}^H \vec{x}(k)\right\}^*\right]$$

$$= E\left[|d(k)|^2 - d(k)\,\vec{x}^H(k)\,\vec{w} - \vec{w}^H \vec{x}(k)\,d^*(k) + \vec{w}^H \vec{x}(k)\,\vec{x}^H(k)\,\vec{w}\right]$$

$$= E\left[|d(k)|^2\right] - P^H \vec{w} - \vec{w}^H P + \vec{w}^H R \vec{w}$$

where

$$R = E\left[\vec{x}\,\vec{x}^H\right] \tag{4.4}$$

and

$$P = E\left[\vec{x} d^*(k)\right] \tag{4.5}$$

In equation (4.3), R is the $M \times M$ *correlation matrix* of the input data vector $x(k)$, and P is the $M \times 1$ *cross-correlation vector* between the input data vector and the desired signal $d(k)$.

The gradient vector of J, $\nabla(J)$, is defined by

$$\nabla(J) = 2\frac{\partial J}{\partial \vec{w}^*} \tag{4.6}$$

where $\frac{\partial}{\partial \vec{w}^*}$ denotes the conjugate derivative with respect to the complex vector $\vec{w}$. When the mean-squared error J is minimized, the gradient vector will be equal to a $M \times 1$ null vector.

$$\nabla(J)\big|_{\vec{w}_{opt}} = 0 \tag{4.7}$$

Substituting equation (4.3) into equation (4.7), we have

$$-2P + 2R\vec{w}_{opt} = 0 \tag{4.8}$$

or equivalently

$$R\vec{w}_{opt} = P \tag{4.9}$$

Equation (4.9) is called the *Wiener-Hopf equation*[23]. Multiplying both sides of equation (4.9) by R^{-1}, the inverse of correlation matrix, we obtain

$$\vec{w}_{opt} = R^{-1}P \tag{4.10}$$

The optimum weight vector $\vec{w}_{opt}$ in equation (4.10) is called the *Wiener solution*. From equation (4.10), we see that computation of the optimum weight vector $\vec{w}_{opt}$ requires knowledge of two quantities:

1. the correlation matrix R of the input data vector $\vec{x}(k)$,
2. the cross-correlation vector P between the input data vector $\vec{x}(k)$ and the desired signal $d(k)$.

4.2.1.2 Adaptive Beamforming for 3G CDMA System

Coherent data detection of phase-modulation signals requires a reference signal that can be sent by the data source or reconstructed from the received data. In practice, it is often difficult to reconstruct the reference signal, especially in wireless communications that are subjected to fading effects.

As we know, different from current CDMA system, the third generation (3G) CDMA has pilot channel on both downlink and uplink. Figure 4.2 and Figure 4.3 are the uplink channel modulator of IS-95 and cdma2000, respectively. The pilot channel in uplink is very helpful in synchronization, cell searching, coherent demodulation, and so on. It is transmitted either continuously or is multiplexed into the data stream, as illustrated in Figure 4.4. These approaches provide different benefits: The continuous pilot is immune to fast fading, while the multiplexed pilot is better

at minimizing self-interference. In either case, the effectiveness of the pilot is based on the transmitted power level.

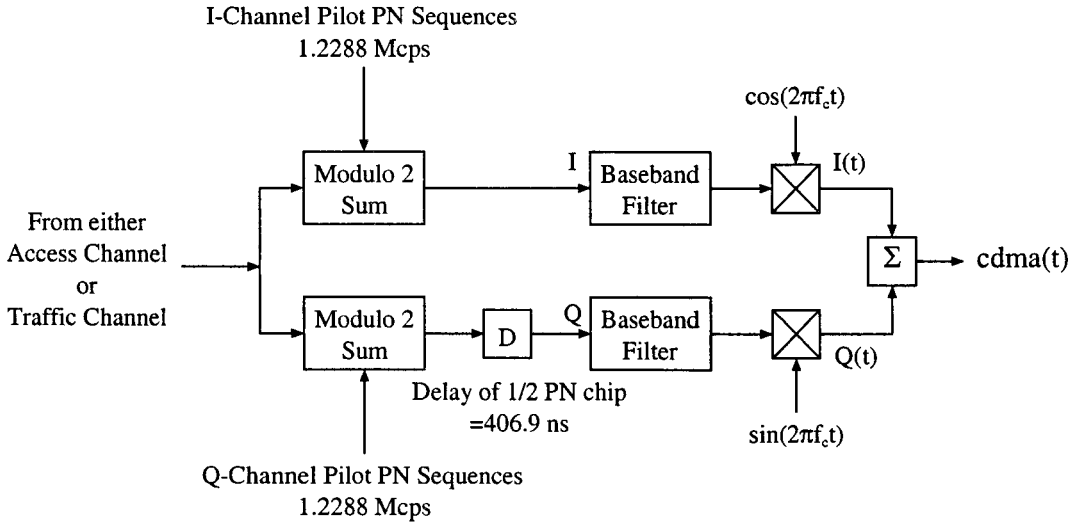

Figure 4.2: Uplink CDMA modulator.

So for 3G CDMA system, the pilot signal on uplink can also be used as reference signal for adaptive beamforming. In this thesis, we adopt continuously transmitted pilot signal.

For this case, we use Wiener solution, equation (4.10) to get the optimum weight, because the pilot signal is transmitted continuously and transmitted through the same fading channel as data.

4.2.2 Adaptive Beamforming with Training Sequences

For this case, training sequences and information datas are transmitted. Training sequences are transmitted during the training period. The optimal weight vectors are generated. After the training period, data is sent and the beamformer uses the weight vectors generated in the previous training period to process the received signal. If the radio channel and the interference characteristics remain constant from one training period until the next, the weight vector $\vec{w}_{opt}$ will contain the

Bandwidth (MHz)	PN Rate (Mcps)
5.0	4.096
10.0	8.196
15.0	12.288

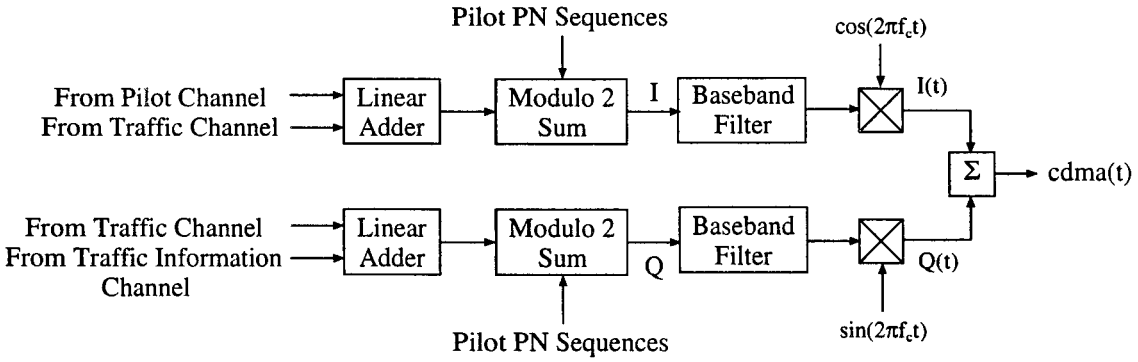

Figure 4.3: Uplink CDMA2000 modulator.

information of the channel and the interference, and their effect on the received signal will be compensated in the output of the array.

4.2.2.1 Method of Steepest-Descent

Although the Wiener-Hopf equation may be solved directly by calculating the product of the inverse of the correlation matrix R and the cross-correlation vector P, nevertheless, this procedure presents serious computational difficulties since calculation the inverse of the correlation matrix results in the high computational complexity. An alternative procedure is the use the method of steepest-descent [23]. To find the optimum weight vector $\overrightarrow{w}_{opt}$ by the steepest-descent method we proceed as follows:

1. Begining with an initial value $\overrightarrow{w}(0)$ for the weight vector, which is chosen arbitrarily. Typically, $\overrightarrow{w}(0)$ is set equal to a column vector of an $M \times M$ identity matrix.

2. Using this initial or present guess, compute the gradient vector $\nabla(J(k))$ at time k (i.e., the k^{th} iteration).

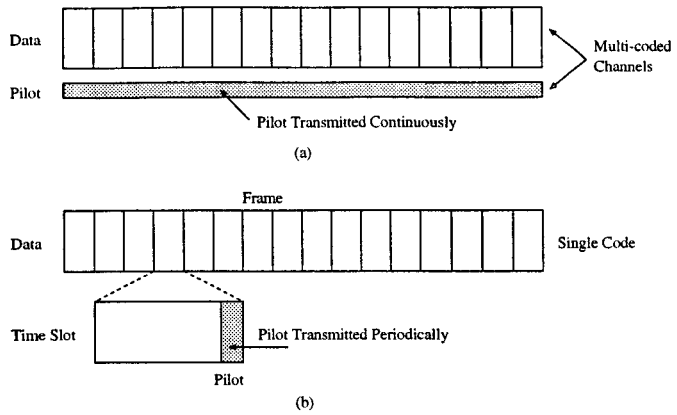

Figure 4.4: Pilot signal concepts: (a) continuous and (b) multiplexed.

3. Compute the next guess at the weight vector by making a change in the initial or present guess in a direction opposite to that of the gradient vector.

4. Go back to step 2 and repeat the process.

It is intuitively reasonable that successive corrections to the weight vector in the direction of the negative of the gradient vector should eventually lead to the minimum mean-squared error J_{min}, at which the weight vector assumes its optimum value $\vec{w}_{opt}$.

Let $\vec{w}(k)$ denote the value of the weight vector at time k. According to the method of steepest-descent, the update value of the weight vector at time $k+1$ is computed by using the simplest recursive relation

$$\vec{w}(k+1) = \vec{w}(k) + \frac{1}{2}\mu[-\nabla(J(K))] \tag{4.11}$$

where μ is a positive real-valued constant. The factor $\frac{1}{2}$ is used merely for convenience. From equation (4.8) we have

$$\nabla(J(k)) = -2P + 2R\vec{w}(k) \tag{4.12}$$

Substituting equation (4.12) into (4.11), we obtain

$$\vec{w}(k+1) = \vec{w}(k) + \mu[P - R\vec{w}(k)], \qquad k = 0, 1, 2, ... \tag{4.13}$$

Using equation (4.4), (4.5), (4.1) and (3.30), the gradient vector in equation (4.12) may be written in another form

$$\nabla(J(k)) = -2E\left[\vec{x}(k)\, d^*(k) - \vec{x}(k)\, \vec{x}^H(k)\, \vec{w}(k)\right] \tag{4.14}$$

$$= -2E\left[\vec{x}(k)\left\{d(k) - y(k)\right\}^*\right]$$

$$= -2E\left[\vec{x}(k)\, e^*(k)\right]$$

Also, equation (4.11) can be expressed as

$$\vec{w}(k+1) = \vec{w}(k) + \mu E\left[\vec{x}(k)\, e^*(k)\right] \tag{4.15}$$

We observe that the parameter μ controls the size of the incremental correction applied to the weight vector as we proceed from one iteration cycle to the next. We therefore refer to μ as the step-size parameter of weight constant. Equation (4.13) and (4.15) describe the mathematical formulation of the steepest-descent method.

4.2.2.2 Least-Mean-Squares Algorithm

If it were possible to make exact measurements of the gradient vector $\nabla(J(k))$ at each iteration, and if the step-size parameter μ is suitably chosen, then the weight vector computed would indeed converge to the optimum Wiener solution. In reality,

however, exact measurements of the gradient vector are not possible since this would require prior knowledge of both the correlation matrix R of the input data vector and the cross-correlation vector P between the input data vector and the desired signal. Consequently, the gradient vector must be estimated from the available data. In other words, the weight vector is updated in accordance with an algorithm that adapts to the incoming data. One such algorithm is the least-mean-squares (LMS) algorithm [22][23]. A significant feature of the LMS algorithm is its simplicity; it does not require measurements of the pertinent correlation functions, nor does it require matrix inversion.

To develop an estimate of the gradient vector $\nabla (J(k))$, the most obvious strategy is to substitute the expected value in equation (4.14) with the instantaneous estimate,

$$\widehat{\nabla} (J(k)) = -2 \overrightarrow{x} (k) e^{*} (k) \tag{4.16}$$

Substituting this instantaneous estimate of the gradient vector in equation (4.11), we have

$$\overrightarrow{w} (k+1) = \overrightarrow{w} (k) + \mu \overrightarrow{x} (k) e^{*} (k) \tag{4.17}$$

Now, we can describe the LMS algorithm by the following three equations

$$y(k) = \overrightarrow{w}^{H} (k) \overrightarrow{x} (k) \tag{4.18}$$

$$e(k) = d(k) - y(k) \tag{4.19}$$

$$\overrightarrow{w} (k+1) = \overrightarrow{w} (k) + \mu \overrightarrow{x} (k) e^{*} (k) \tag{4.20}$$

For the case of beamforming with training sequence, during training period, we use equation (4.18), (4.19), (4.20) to get adaptive weights. In equation (4.18) and (4.20), $\vec{x}(k)$ is the training bits. During the data period, we do not use adaptive algorithm to adjust weight.

4.2.3 Flow Chart

Figure 4.5 Flow chart for non-blind adaptive beamforming algorithms.

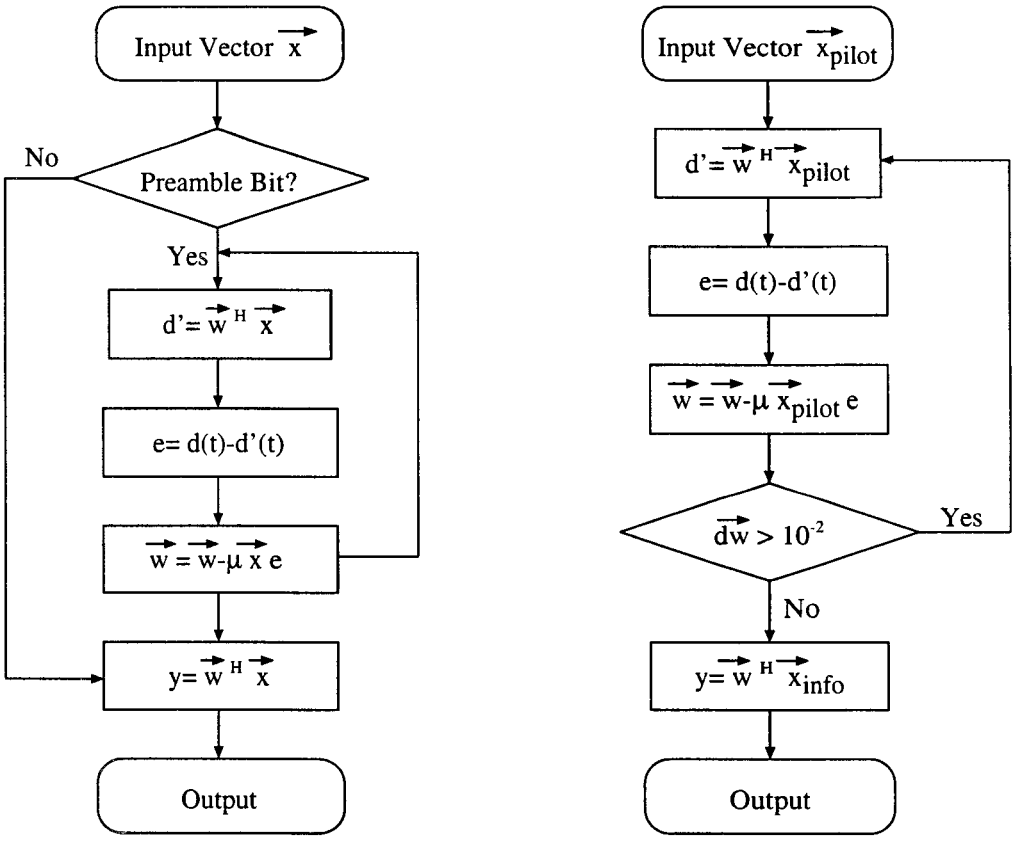

(a) Adaptive Beamforming with Preamble

(b) Adaptive beamforming with pilot channel on reverse link

Figure 4.5: Flow chart for non-blind adaptive beamforming algorithms.

4.3 Blind Adaptive Beamforming Algorithm

Blind adaptive algorithms are the techniques have been developed which do not require any reference signal. They adapt by attempting to restore some known property to the received signal.

In our simulation, Least Squares De-spread Re-spread Multitarget Constant Modulus Algorithm (LS-DRMTCMA) are chose.

4.3.1 Derivation of MT-LSCMA

Generally, most digital communication signals possess some kinds of properties such as the constant modulus property. Due to the interference, noise, and the time-varying channel in a communication system, these properties may be corrupted when the signal is received at the receiver. The adaptive array in the receiver tries to restore these properties using a property-restoral-based algorithm, and hopes that by restoring these properties, the output of the array is a reconstructed version of the transmitted signal.

Figure 4.6 shows structure of a LS-CMA adaptive array.

4.3.1.1 Constant Modulus Algorithms

Some communication signals such as phase-shift keying (PSK), frequency-shift keying (FSK), and analog FM signals have a constant envelope. This constant envelope may be distorted when the signal is transmitted through the channel. The constant modulus algorithm (CMA) adjusts the weight vector of the adaptive array to minimize the variation of the envelope at the output of the array. After the algorithm converges, the array can steer a beam in the direction of the signal of interest (SOI), and nulls in the directions of the interference.

The CMA tries to minimize the cost function

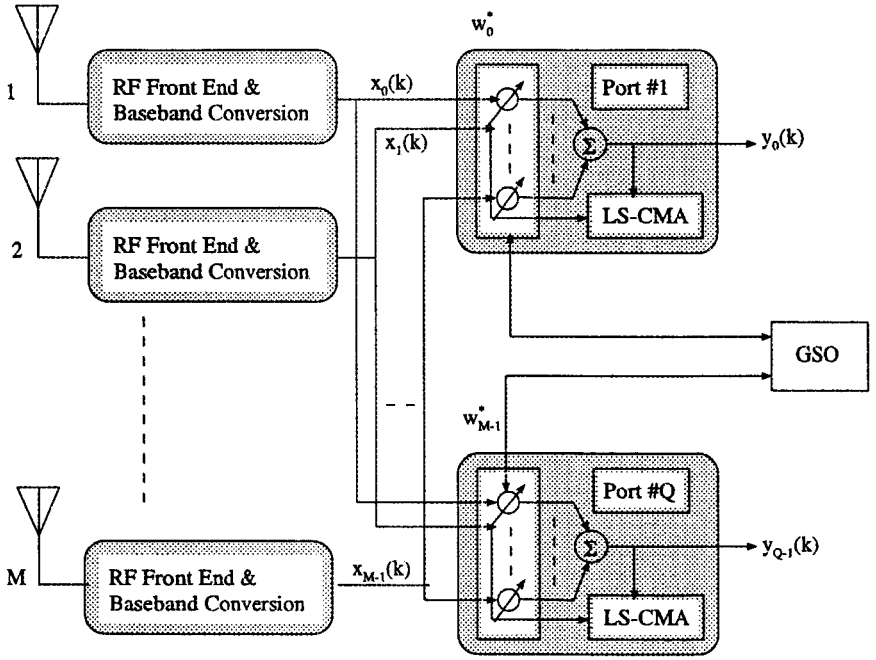

Figure 4.6: Structure of a beamformer using LS-CMA.

$$J(k) = E\left[\left||y(k)|^p - 1\right|^q\right] \tag{4.21}$$

The convergence of the algorithm depends on the coefficients p and q in equation (4.21). Usually, the cost function J with $p = 1$, $q = 2$ or $p = 2$, $q = 2$ is used. Here we use J with $p = 1$, $q = 2$. With the cost function of the 1-2 form, the CMA minimizes the function

$$J(k) = E\left[\left||y(k)| - 1\right|^2\right] \tag{4.22}$$

The gradient vector is given by

$$\begin{aligned}\nabla(J(k)) &= 2\frac{\partial J(k)}{\partial \vec{w}^*(k)} \\ &= 2 \times 2E\left[\left(|y(k) - 1|\frac{\partial |y(k)|}{\partial \vec{w}^*(k)}\right)\right] \\ &= 2 \times 2E\left[\left(|y(k) - 1|\right)\frac{\partial \{y(k)y^*(k)\}^{\frac{1}{2}}}{\partial \vec{w}^*(k)}\right]\end{aligned}$$

$$
\begin{aligned}
&= 2 \times 2E\left[\left(|y(k)-1|\right)\frac{\partial\left\{\overrightarrow{w}^{H}(k)\overrightarrow{x}(k)\overrightarrow{x}^{H}(k)\overrightarrow{w}(k)\right\}^{\frac{1}{2}}}{\partial\overrightarrow{w}^{*}(k)}\right] \\
&= 2E\left[\left(|y(k)-1|\right)\left\{\overrightarrow{w}^{H}(k)\overrightarrow{x}(k)\overrightarrow{x}^{H}(k)\overrightarrow{w}(k)\right\}^{-\frac{1}{2}}\frac{\partial\left\{\overrightarrow{w}^{H}(k)\overrightarrow{x}(k)\overrightarrow{x}^{H}(k)\overrightarrow{w}(k)\right\}}{\partial\overrightarrow{w}^{*}(k)}\right] \\
&= 2E\left[\left(|y(k)-1|\right)\frac{1}{|y(k)|}\overrightarrow{x}(k)\overrightarrow{x}^{H}(k)\overrightarrow{w}(k)\right] \\
&= 2E\left[\left(1-\frac{1}{|y(k)|}\right)\overrightarrow{x}(k)y^{*}(k)\right] \\
&= 2E\left[\overrightarrow{x}(k)\left(y(k)-\frac{y(k)}{|y(k)|}\right)^{*}\right]
\end{aligned}
\tag{4.23}
$$

Ignoring the expectation operation in equation (4.23), the instantaneous estimate of the gradient vector can be written as

$$
\widehat{\nabla}\left(J(k)\right) = \overrightarrow{x}(k)\left(y(k)-\frac{y(k)}{|y(k)|}\right)^{*} \tag{4 24}
$$

Using the method of steepest-descent, and replacing the gradient vector with its instantaneous estimate, we can update the weight vector by

$$
\overrightarrow{w}(k+1) = \overrightarrow{w}(k) - \mu\widehat{\nabla}\left(J(k)\right)
$$

$$
= \overrightarrow{w}(k) - \mu\overrightarrow{x}(k)\left(y(k)-\frac{y(k)}{|y(k)|}\right)^{*} \tag{4.25}
$$

where μ is the step-size parameter. Now, we can describe the steepest-descent CMA (SD-CMA) by the following three equations

$$
y(k) = \overrightarrow{w}^{H}(k)\overrightarrow{x}(k) \tag{4.26}
$$

$$
e(k) = y(k) - \frac{y(k)}{|y(k)|} \tag{4.27}
$$

$$\overrightarrow{w}(k+1) = \overrightarrow{w}(k) - \mu \overrightarrow{x}(k) e^*(k) \tag{4.28}$$

From equation (4.27) we see that when the output of the array has a unity magnitude, i.e., $|y(k)| = 1$, the error signal becomes zero. Comparing the above three equations with equation (4.18), (4.19) and (4.20), we see that the CMA is very similar to the LMS algorithm, and the term $\frac{y(k)}{|y(k)|}$ in CMA plays the same role as the desired signal $d(t)$ in the LMS algorithm. However, the reference signal $d(t)$ must be sent from the transmitter to the receiver and must be known for both the transmitter and receiver if the LMS algorithm is used. The CMA algorithm does not require a reference signal to generate the error signal at the receiver.

4.3.1.2 Least-Squares CMA

The constant modulus algorithm was first used by Gooch [38] in the beamforming problem. After that, many CMA-type algorithms have been proposed for use in adaptive arrays. In [39], B. G. Agee developed the least-squares constant modulus algorithm (LS-CMA) by using the extension of the method of nonlinear least-squares (Gauss's method) [40]. The extension of Gauss's method states that if a cost function can be expressed in the form

$$F(\overrightarrow{w}) = \sum_{k=1}^{K} |g_k(\overrightarrow{w})|^2 \tag{4.29}$$

$$= \|\overrightarrow{g}(\overrightarrow{w})\|_2^2$$

where

$$\overrightarrow{g}(\overrightarrow{w}) = [g_1(\overrightarrow{w}), g_2(\overrightarrow{w}), ..., g_K(\overrightarrow{w})] \tag{4.30}$$

Then the cost function has a partial Taylor-series expansion with the sum-of-sequence form:

$$F\left(\vec{w}+\Delta\right) \approx \left\| g\left(\vec{w}\right) + D^{H}\left(\vec{w}\right)\Delta \right\|_{2}^{2} \tag{4.31}$$

where Δ is an offset vector, and

$$D\left(\vec{w}\right) = \left[\ \nabla\left(g_{1}\left(\vec{w}\right)\right),\ \ \nabla\left(g_{2}\left(\vec{w}\right)\right),\ \ \cdots\ \ \nabla\left(g_{K}\left(\vec{w}\right)\right)\ \right] \tag{4.32}$$

The gradient vector of $F\left(w+\Delta\right)$ with respect to Δ is given by

$$\nabla_{\Delta}\left(F\left(\vec{w}+\Delta\right)\right) = 2\frac{\partial F\left(\vec{w}+\Delta\right)}{\partial \Delta^{*}} \tag{4.33}$$

$$= 2\frac{\partial\left\{\left(g\left(\vec{w}\right)+D^{H}\left(\vec{w}\right)\Delta\right)^{H}\left(g\left(\vec{w}\right)+D^{H}\left(\vec{w}\right)\Delta\right)\right\}}{\partial\Delta^{*}}$$

$$= 2\frac{\partial\left\{\left\|g\left(\vec{w}\right)\right\|_{2}^{2}+g^{H}\left(\vec{w}\right)D^{H}\left(\vec{w}\right)\Delta+\Delta^{H}D\left(\vec{w}\right)g\left(\vec{w}\right)+\Delta^{H}D\left(\vec{w}\right)D^{H}\left(\vec{w}\right)\Delta\right\}}{\partial\Delta^{*}}$$

$$= 2\left\{D\left(\vec{w}\right)g\left(\vec{w}\right)+D\left(\vec{w}\right)D^{H}\left(\vec{w}\right)\Delta\right\}$$

Setting $\nabla_{\Delta}\left(F\left(\vec{w_{i}}+\Delta\right)\right)$ equal to zero, we will find the offset that minimizes the cost function $F\left(\vec{w_{i}}+\Delta\right)$

$$\Delta = -\left[D\left(\vec{w}_{i}\right)\ D^{H}\left(\vec{w}_{i}\right)\right]^{-1} D\left(\vec{w}_{i}\right)\ g\left(\vec{w}_{i}\right) \tag{4.34}$$

Therefore, the weight vector can be updated by

$$\vec{w_i}(l+1) = \vec{w_i}(l) + \Delta \tag{4.35}$$

$$= \vec{w_i}(l) - \left[D(\vec{w}_i) D^H(\vec{w}_i)\right]^{-1} D(\vec{w}_i) g(\vec{w}_i)$$

where l denotes the iteration number. The LS-CMA is derived by applying equation (4.35) to the constant modulus cost function,

$$F(\vec{w}) = \sum_{k=1}^{K} ||y(k)| - 1|^2 \tag{4.36}$$

$$= \sum_{k=1}^{K} \left|\left|\vec{w}^H \vec{x}(k)\right| - 1\right|^2$$

Comparing equation (4.36) with (4.29), we see that in this case,

$$g_k(\vec{w}) = |y(k)| - 1 \tag{4.37}$$

$$= \left|\vec{w}^H \vec{x}(k)\right| - 1$$

Substituting equation (4.37) into (4.30), we obtain

$$g(\vec{w}) = \begin{bmatrix} |y(1)| - 1 \\ |y(2)| - 1 \\ \vdots \\ |y(K)| - 1 \end{bmatrix} \tag{4.38}$$

The gradient vector of $g_k(\vec{w})$ is given by

$$\nabla(g_k(\vec{w})) = 2\frac{\partial g_k(\vec{w})}{\partial \vec{w}^*} \tag{4.39}$$

$$= x(k)\frac{y^*(k)}{|y(k)|}$$

Substituting (4.39) into (4.32), $D(\vec{w})$ can be written as

$$D(\vec{w}) = \left[\nabla(g_1(\vec{w})) \quad \nabla(g_2(\vec{w})) \quad \cdots \quad \nabla(g_K(\vec{w})) \right] \tag{4.40}$$

$$= \left[\vec{x}(1)\frac{y^*(1)}{|y(1)|} \quad \vec{x}(2)\frac{y^*(2)}{|y(2)|} \quad \cdots \quad \vec{x}(K)\frac{y^*(K)}{|y(K)|} \right]$$

$$= XY_{cm}$$

where

$$X = \left[\vec{x}(1) \quad \vec{x}(2) \quad \cdots \quad \vec{x}(K) \right]$$

and

$$Y_{cm} = \begin{bmatrix} \frac{y^*(1)}{|y(1)|} & 0 & \cdots & 0 \\ 0 & \frac{y^*(1)}{|y(1)|} & & \vdots \\ \vdots & & \ddots & 0 \\ 0 & \cdots & 0 & \frac{y^*(1)}{|y(1)|} \end{bmatrix}$$

Using equation (4.40) and (4.38), we have

$$D(\overrightarrow{w})\,D^H(\overrightarrow{w}) = XY_{cm}Y_{cm}^H X^H = XX^H \tag{4.41}$$

and

$$D(\overrightarrow{w})\,g(\overrightarrow{w}) = XY_{cm}\begin{bmatrix} |y(1)|-1 \\ |y(2)|-1 \\ \vdots \\ |y(K)|-1 \end{bmatrix} \tag{4.42}$$

$$= X\begin{bmatrix} y^*(1) - \frac{y^*(1)}{|y(1)|} \\ y^*(2) - \frac{y^*(2)}{|y(2)|} \\ \vdots \\ y^*(K) - \frac{y^*(K)}{|y(K)|} \end{bmatrix}$$

$$= X(\overrightarrow{y} - \overrightarrow{r})^*$$

where

$$\overrightarrow{y} = \begin{bmatrix} y(1) & y(2) & \cdots & y(K) \end{bmatrix}^T$$

$$\overrightarrow{r} = \begin{bmatrix} \frac{y(1)}{|y(1)|} & \frac{y(2)}{|y(2)|} & \cdots & \frac{y(K)}{|y(K)|} \end{bmatrix}^T \tag{4.43}$$

The vector $\overrightarrow{y}$ and $\overrightarrow{r}$ are called the output data vector and complex-limited output data vector, respectively. Substituting equation (4.41) and (4.42) into equation (4.35),

$$\vec{w}(l+1) = \vec{w}(l) - \left[XX^H\right]^{-1} X\left(\vec{y}(l) - \vec{r}(l)\right)^* \tag{4.44}$$

$$= \vec{w}(l) - \left[XX^H\right]^{-1} XX^H \vec{w}(l) + \left[XX^H\right]^{-1} X\vec{r}^*(l)$$

$$= \left[XX^H\right]^{-1} X\vec{r}^*(l)$$

where $\vec{y_i}$, $\vec{r_i}$ are the output data vector and estimate of signal waveform of user i over one bit period corresponding to the weight vector $\vec{w}(l)$ in the l-th iteration, respectively.

The LS-CMA can be implemented either statically or dynamically. The static LS-CMA repeatedly uses one data block X, which contains K snapshots of the input data vectors, in the updating of the weight vector $\vec{w}$. In the static LS-CMA, after a new weight vector $\vec{w}(l+1)$ is calculated using equation (4.44), this new weight vector is used with the input data block X, which was also used in the last iteration, to generate the new output data vector $\vec{y}(l+1)$ and the complex-limited output data vector $\vec{r}(l+1)$. The new complex-limited output data vector is then substituted into equation (4.44) to generate a new weight vector. In dynamic LS-CMA, however, different input data blocks are used during the updating of the weight vector. Let $X(l)$ denote the input data block used in the l^{th} iteration. $X(l)$ can be expressed as

$$X(l) = \left[\vec{x}(1+lK),\ \vec{x}(2+lK),\ ....,\ \vec{x}(K+lK)\right] \qquad l = 1, 2, ..., L \tag{4.45}$$

where L is the number of iterations required for the algorithm to converge. Using $X(l)$, we can describe the dynamic LS-CMA by the following equations

$$\vec{y}(l) = \left[\vec{w}^{H}(l)\, X(l)\right]^{T}$$

$$= [y(1+lK),\ y(2+lK),\ ....,\ y(K+lK),\ ]^{T} \tag{4.46}$$

$$\vec{r}(l) = \left[\frac{y(1+lK)}{|y(1+lK)|},\ \frac{y(2+lK)}{|y(2+lK)|},\ ...,\ \frac{y(K+lK)}{|y(K+lK)|}\right] \tag{4.47}$$

$$\vec{w}(l) = \left[X(l)\, X^{H}(l)\right]^{-1} X(l)\, r^{*}(l) \tag{4.48}$$

If we define

$$\widehat{R}_{xx}(l) = \frac{1}{K} X(l)\, X^{H}(l) \tag{4.49}$$

$$\widehat{P}_{xx}(l) = \frac{1}{K} X(l)\, r^{*}(l) \tag{4.50}$$

equation (4.48) can also be written as

$$\vec{w}(l+1) = \widehat{R}_{xx}^{-1}(l)\, \widehat{P}_{xx}(l) \tag{4.51}$$

Some may find that equation (4.51) is very similar to (4.10), however, in equation (4.51), $\widehat{R}_{xx}(l)$ is an estimate of the correlation matrix of the input data vector, computed over the l^{th} data block containing K snapshots of the input data vector, and $\widehat{P}_{xx}(l)$ is an estimate of the cross-correlation between the input data vector and the complex-limited output signal.

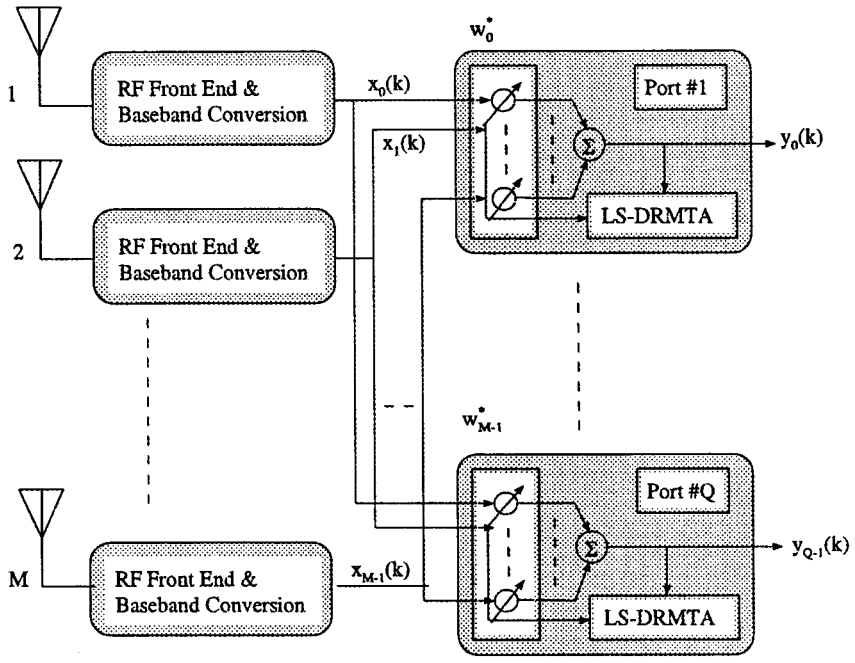

Figure 4.7: Structure of a beamforming using LS-DRMTA.

4.3.2 Derivation of LS-DRMTA

The LS-CMA discussed earlier does not utilize any information of the spreading signal of each user in the CDMA system. However, in the base station of a CDMA system, the spreading signals of all the users are previously known. It is these spreading signals that distinguish different users occupying the same frequency band. Therefore, it will be very useful if the information of these spreading signals can be utilized in the multitarget adaptive algorithm.

In the conventional receiver, to detect the i^{th} user's data bits, the received signal is correlated with the time delayed spreading signal of the i^{th} user, $c_i\left(t-\tau_i\right)$, and the correlation output is sent to the detector, which makes a decision based on the correlation output. There exist many techniques to estimate the time delay, τ_i, for the i^{th} user, and we are not going to cover this topic in this research. So from now on, we assume that the time delay for each user is detected perfectly unless specified otherwise.

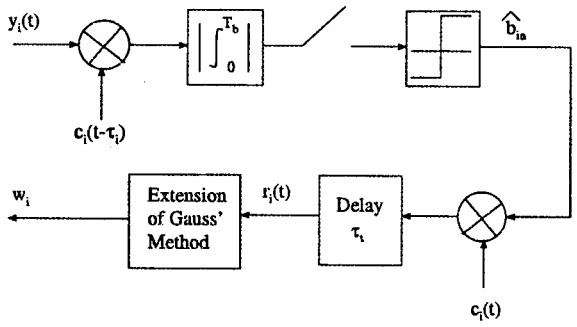

Figure 4.8: LS-DRMTA block diagram for user i.

If the n^{th} data bit of the i^{th} user is detected correctly by the detector, i.e., $\widehat{b}_{in} = b_{in}$, where $\widehat{b}_{in}$ is the detector output, then the waveform of the i^{th} user's transmitted signal during time period $[(n-1)T_b, \quad nT_b)$ can be obtained by re-spreading the detected data bit $\widehat{b}_{in}$ with the PN sequence of the i^{th} user, $c_i(t)$. This re-spread signal can then be used in the beamformer to adapt the weight vector for user i. The adaptive algorithm that uses this de-spread-and-re-spread technique is referred to as Least Square De-spread Re-spread Multitarget Algorithm (LS-DRMTA). Figure 4.7 shows the structure of a beamformer using the LS-DRMTA and Figure 4.8 shows the block diagram of the LS-DRMTA for user i.

In Figure 4.8, $r_i(t)$ is a time-delayed version of the re-spread signal for user i and is given by

$$r_i(t) = \widehat{b}_{in} c_i(t - \tau_i), \qquad (n-1)T_b \leq t < nT_b \tag{4.52}$$

In a CDMA system, the PN sequence is repeated every bit period; therefore, both $c_i(t)$ and $r_i(t)$ have a time period T_b. Let $y_i(k)$ and $r_i(k)$ denote the k^{th} sample of $y_i(t)$ and $r_i(t)$, respectively, in a digital system; the LS-DRMTA adapts the weight vector $\overrightarrow{w}_i$ to minimize the cost function, in equation (4.53)

$$F(\overrightarrow{w_i}) = \sum_{k=1}^{K} |y_i(k) - r_i(k)|^2 \tag{4.53}$$

$$= \sum_{k=1}^{K} \left| \overrightarrow{w}_i^H \overrightarrow{x}(k) - r_i(k) \right|^2$$

where K is the data block size and is set to be equal to the number of samples in one bit period in LS-DRMTA. So if the signal is sampled with a sampling rate $R_s = N_s R_c$, where R_c is the chip rate of the CDMA signal, and N_s is an integer greater than two, the block size K will be equal to $N_s N_c$, where N_c is the processing gain.

Using the extension of Gauss' method described in section 4.3.1.2, and comparing equation (4.53) and (4.29), we have

$$g_k(\overrightarrow{w}) = |y_i(k) - r_i(k)| \tag{4.54}$$

$$= \left| \overrightarrow{w_i}^H x(k) - r_i(k) \right|$$

Substituting equation (4.54) into (5.33), we have

$$g(\overrightarrow{w}_i) = \begin{bmatrix} |y_i(1) - r_i(1)| \\ |y_i(2) - r_i(2)| \\ \vdots \\ |y_i(K) - r_i(K)| \end{bmatrix} \tag{4.55}$$

The gradient vector of $g_k(\overrightarrow{w}_i)$ is given by

$$\nabla\left(g_k(\overrightarrow{w}_i)\right) = 2\frac{\partial g_k(\overrightarrow{w}_i)}{\partial \overrightarrow{w}_i^*} \tag{4.56}$$

$$= x(k) \frac{[y_i(k) - r_i(k)]^*}{|y_i(k) - r_i(k)|}$$

Let

$$v_i(k) = y_i(k) - r_i(k)$$

Then, equation (4.56) can be expressed as

$$\nabla\left(g_k\left(\vec{w}_i\right)\right) = x(k)\,\frac{v_i^*(k)}{|v_i(k)|} \tag{4.57}$$

From equation (4.35), the weight update can be written as

$$\vec{w}(l+1) = \vec{w_i}(l) - \left[D\left(\vec{w}_i\right)\,D\left(\vec{w}_i\right)^H\right]^{-1} D\left(\vec{w}_i\right)\,g\left(\vec{w}_i\right) \tag{4.58}$$

where

$$D\left(\vec{w}\right) = \left[\begin{array}{cccc} \nabla\left(g_1\left(\vec{w}\right)\right) & \nabla\left(g_2\left(\vec{w}\right)\right) & \cdots & \nabla\left(g_K\left(\vec{w}\right)\right) \end{array}\right] \tag{4.59}$$

Substituting equation (4.57) into (4.59), $D\left(\vec{w}\right)$ can be expressed as

$$D\left(\vec{w}_i\right) = \left[\begin{array}{cccc} \nabla\left(g_1\left(\vec{w}_i\right)\right) & \nabla\left(g_2\left(\vec{w}_i\right)\right) & \cdots & \nabla\left(g_K\left(\vec{w}_i\right)\right) \end{array}\right] \tag{4.60}$$

$$= \left[\begin{array}{cccc} x(1)\,\frac{v_i^*(1)}{|v_i(1)|} & x(2)\,\frac{v_i^*(2)}{|v_i(2)|} & \cdots & x(K)\,\frac{v_i^*(K)}{|v_i(K)|} \end{array}\right]$$

$$= XV_{iCM}$$

where

$$X = \left[\begin{array}{cccc} x(1) & x(2) & \cdots & x(K) \end{array}\right]$$

and

$$V_{iCM} = \begin{bmatrix} \frac{v_i^*(1)}{|v_i(1)|} & 0 & \cdots & 0 \\ 0 & \frac{v_i^*(2)}{|v_i(2)|} & & \vdots \\ \vdots & & \ddots & 0 \\ 0 & \cdots & 0 & \frac{v_i^*(K)}{|v_i(K)|} \end{bmatrix}$$

Using equation (4.60) and (4.55), we have

$$D(\vec{w}_i)\, D(\vec{w}_i)^H = X\, V_{iCM}\, V_{iCM}^H\, X^H \tag{4.61}$$

$$= X\, X^H$$

and

$$D(\vec{w}_i)\, g(\vec{w}_i) = X\, V_{iCM} \begin{bmatrix} |v_i(1)| \\ |v_i(2)| \\ \vdots \\ |v_i(K)| \end{bmatrix} \tag{4.62}$$

$$= \begin{bmatrix} v_i^*(1) \\ v_i^*(2) \\ \vdots \\ v_i^*(K) \end{bmatrix}$$

$$= X\, \vec{v}_i^*$$

$$D(\vec{w}_i)\, g(\vec{w}_i) = X(\vec{y}_i - \vec{r}_i)^* \tag{4.63}$$

where

$$\vec{v}_i = \begin{bmatrix} v_i(1) & v_i(2) & \cdots & v_i(K) \end{bmatrix}^T$$

$$\vec{y}_i = \begin{bmatrix} y_i(1) & y_i(2) & \cdots & y_i(K) \end{bmatrix}^T$$

$$\vec{r}_i = \begin{bmatrix} r_i(1) & r_i(2) & \cdots & r_i(K) \end{bmatrix}^T$$

The vector $\vec{y}_i$ is the output data vector for user i and $\vec{r}_i$ is the estimate of the signal waveform of user i over one bit period. Substituting equation (4.61) and (4.63) into equation (4.58).

$$\vec{w}(l+1) = \vec{w}(l) - \left[XX^H\right]^{-1} X(\vec{y}(l) - \vec{r}(l))^* \tag{4.64}$$

$$= \vec{w}(l) - \left[XX^H\right]^{-1} XX^H \vec{w}(l) + \left[XX^H\right]^{-1} X\vec{r}^*(l)$$

$$= \left[XX^H\right]^{-1} X\vec{r}^*(l)$$

where $\vec{y}(l)$ and $\vec{r_i}(l)$ are the output data vector and estimate of signal waveform of user i over one bit period corresponding to the weight vector $\vec{w_i}$ in the l^{th} iteration, respectively. Similar to the dynamic LS-CMA, LS-DRMTA can adapt the weight vectors using different input data blocks in each iteration. Let

$$X(l) = [\overrightarrow{x}(1+lK),\ \overrightarrow{x}(2+lK),\ ....,\ \overrightarrow{x}(K+lK)], \qquad l = 0, 1, ..., L \quad (4.65)$$

where L is the number of iterations required for the algorithm to converge, and K is the number of data samples per bit ($N_c N_s$) if the data samples over one bit period are all used for the adaptation. In Figure 4.7, the LS-DRMTA for the i^{th} user can be described by the following equations

$$\overrightarrow{y_i}(l) = \left[\overrightarrow{w_i}^H(l)\, X(l)\right]^T$$

$$= [y_i(1+lK),\ y_i(2+lK),\ ...,\ y_i(K+lK)]^T \quad (4.66)$$

$$\widehat{b}_{il} = sgn\left\{ Re\left(\sum_{k=1+lK}^{(K+lK)} y_i(k)\, c_i(k-k_{\tau_i}) \right) \right\} \quad (4.67)$$

$$\overrightarrow{r_i} = \widehat{b}_{il}\left[c_i(1+lK-k_{\tau_i}),\ c_i(2+lK-k_{\tau_i}), ...,\ c_i(K+lK-k_{\tau_i})\right] \quad (4.68)$$

$$\overrightarrow{w_i}(l+1) = \left[X(l)\, X^H(l)\right]^{-1} X(l)\, \overrightarrow{r_i}^*(l) \quad (4.69)$$

where $c_i(k)$ is the k^{th} sample of the spreading signal of user i, k_{τ_i} is the number of samples corresponding to τ_i, the delay of user i, and $\widehat{b}_{il}$ is the estimate of l^{th} bit for user i. The accumulated sum in equation (4.67) is equivalent to integration in the continuous time domain.

In equation (4.68), when $l = 0$, there may be some time indices less than zero, but since the PN sequence has a time period of T_b, or equivalently, a period of K in the discrete time domain, the index k, where $k < 0$, can be replaced by the index $k + K$.

4.3.3 Derivation of LS-DRMTCMA

In LS-DRMTA, we utilize the spreading signal of each user in a CDMA system to adapt the weight vectors of the beamformer. In LS-CMA, on the other hand, we utilize the constant modulus property of the transmitted signal to update the weight vectors. The approach is to combine the spreading signal and the constant modulus property of the transmitted signal to adapt the weight vector. The algorithm using this kind of combination in the adaptation of the weight vector is referred as Least Squares De-spread Re-spread Multitarget Constant Modulus Algorithm (LS-DRMTCMA) in this research. Figure 4.9 shows the structure of a beamformer using the LS-DRMTCMA and Figure 4.10 shows the block diagram of the LS-DRMTCMA for user i.

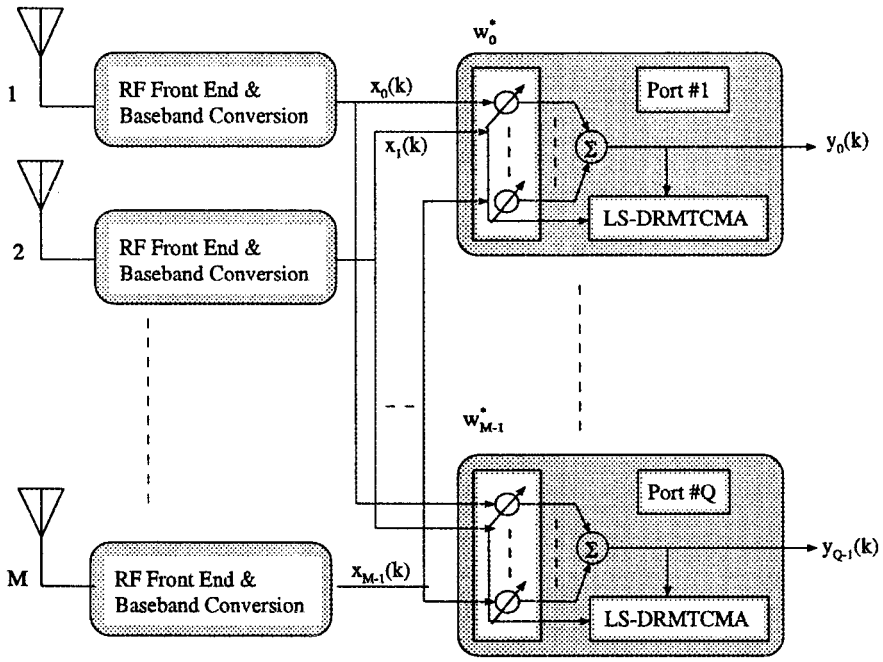

Figure 4.9: Structure of a beamformer using LS-DRMTCMA.

The derivation of the LS-DRMTCMA is very similar to that of the LS-DRMTA. In LS-DRMTA, the cost function that the algorithm wants to minimize is given in equation (4.70) and is repeated here for convenience

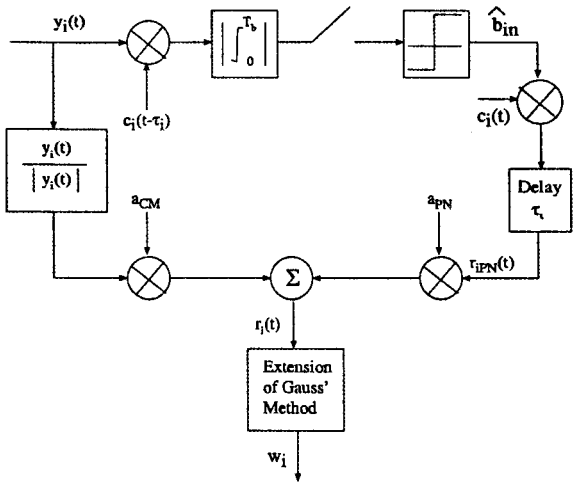

Figure 4.10: LS-DRMTCMA block diagram for user i.

$$F\left(\overrightarrow{w}_i\right) = \sum_{k=1}^{K} \left|y_i\left(k\right) - r_i\left(k\right)\right|^2 \tag{4.70}$$

$$= \sum_{k=1}^{K} \left|\overrightarrow{w}_i^H \overrightarrow{x}\left(k\right) - r_i\left(k\right)\right|^2$$

where

$$r_i\left(k\right) = \widehat{b}_{in} c_i\left(k - k_{\tau_i}\right), \quad \left(n-1\right)K \leq k < nK \tag{4.71}$$

In LS-DRMTCMA, the cost function that the algorithm wants to minimize has the same form as that shown in equation (4.70). However, as illustrated in Figure 4.10, $r_i\left(k\right)$ now becomes the sum of the weighted respread signal and the weighted complex-limited output,

$$r_i\left(k\right) = a_{PN} r_{iPN}\left(k\right) + a_{CM} r_{iCM}\left(k\right) \tag{4.72}$$

where $r_{iPN}\left(k\right)$ is the re-spread signal of user i and is given in equation (4.71), r_{iCM} is the complex-limited output of user i and can be expressed as

$$r_{iCM} = \frac{y_i(k)}{|y_i(k)|} \tag{4.73}$$

The terms, a_{PN} and a_{CM} , are the real positive weight coefficients for the re-spread signal and the complex-limited output of user i, respectively. The coefficients a_{PN} and a_{CM} should satisfy the condition

$$a_{PN} + a_{CM} = 1 \qquad a_{PN},\, a_{CM} > 0 \tag{4.74}$$

So, we can obtain the following equations for LS-DRMTCMA:

$$\vec{y}_i(l) = \left[\vec{w_i}(l)^H X(l)\right]^T \tag{4.75}$$

$$= \left[\begin{array}{cccc} y_i(1+lK) & y_i(2+lK) & \cdots & y_i((1+l)K) \end{array}\right]$$

$$\widehat{b}_{il} = sgn\left\{ Re\left(\sum_{k=1+lK}^{(l+1)K} y_i(k)\, c_i(k-k_{\tau_i}) \right) \right\} \tag{4.76}$$

$$\vec{r}_{iPN} = \widehat{b}_{il}\left[\begin{array}{cccc} c_i(1+lK-k_{\tau_i}) & c_i(2+lK-k_{\tau_i}) & \cdots & c_i((l+1)K-k_{\tau_i}) \end{array}\right]^T \tag{4.77}$$

$$\vec{r}_{iCM} = \left[\begin{array}{cccc} \frac{y(1+lK)}{|y(1+lK)|} & \frac{y(2+lK)}{|y(2+lK)|} & \cdots & \frac{y(1+l)K}{|y(1+l)K|} \end{array}\right]^T \tag{4.78}$$

$$\vec{r}_i(k) = a_{PN}\vec{r}_{iPN}(k) + a_{CM}\vec{r}_{iCM}(k) \tag{4.79}$$

$$\overrightarrow{w}(l+1) = \left[X(l)\,X(l)^H\right]^{-1} X(l)\,\overrightarrow{r_i}^*(l) \tag{4.80}$$

From the above equations we see that if a_{CM} is set to zero, the LS-DRMTCMA becomes the LS-DRMTA, therefore the LS-DRMTA can be viewed as a special case of the LS-DRMTCMA. Also we see that if a_{PN} is set to zero, the algorithms becomes LS-LSCMA. The choice of a_{PN} and a_{CM} can affect the resulting beam pattern and thus the performance of the system.

4.3.4 Flow Chart

Figure 4.11 shows the flow chart of LS-DRMTCMA.

4.4 Simulation

In the previous part of this chapter, we presented three adaptive beamformer algorithms for the base station in a CDMA system. In this section, we will compare the beam patterns got by equation (3.29) of these three algorithms under different conditions.

The system we consider in the simulation is a 3G direct sequence CDMA system with a processing gain, N, of 255. The CDMA signals were generated at the transmitter as in equation (2.26). And the CDMA signals with like users interference as well as both AWGN and different types of fading were generated as in equation (2.29). The modulation scheme used in the system is the binary phase-shift keying (BPSK). The signals were then passed through the every antenna element and the adaptive antenna array algorithms as in the equation performed above.

4.4.1 Description of System Parameters

- Antenna array: 10-element uniformly spaced linear array.

- Element spacing: $d = \frac{\lambda}{2}$.
- DOAs of interfering users are uniformly distributed in $(0, \pi)$. But once selected, they remain constant for the duration of calls.
- Channel model: the 2-ray resolvable channel where each user has two multipaths with indoor model. The power ratio between the multipaths is $15dB$.
- The sampling rate is 2 times the chip rate, in other words, there are 2 data samples per chip. So for the blind algorithm, the data block size is equal to 510, which is the number of samples per bit.

4.4.2 Beam Pattern Formed by Blind Adaptive Algorithm

Evolution of Beam Pattern with Desired User Moving

Figure 4.12 Beam patterns formed by blind adaptive algorithm with desired user moving (with 50 interfering users, flat slow fading, E_b/N_0 =15 dB).

Evolution of Beam Pattern while Increasing Interfering Users

Figure 4.13 Beam patterns formed by blind adaptive algorithm with the number of interfering users increasing. The location of desired user is fixed (DOA of desired user =1 rad, with flat slow fading, E_b/N_0 = 15 dB).

Evolution of Beam Pattern with Adaptive Algorithm Iterations

Figure 4.14 Beam patterns formed by blind adaptive algorithm iterations (with 50 interfering users, DOA of desired user = 1 rad, with flat slow fading, E_b/N_0 =15).

4.4.3 Beam Pattern Formed by LMS Algorithm with Training Sequences

Evolution of Beam Pattern with Desired User Moving

Figure 4.15 Beam patterns formed by LMS algorithm with training sequences (with 50 interfering users, flat slow fading, E_b/N_0=15 dB).

Evolution of Beam Pattern while Increasing Interfering Users

Figure 4.16 Beam patterns formed by LMS algorithm with training sequence with the number of interfering users increasing. The location of desired user is fixed (DOA of desired user = 2 rads, E_b/N_0 =15 dB, with flat slow fading).

4.4.4 Beam Patterns Formed by Wiener Solution with Pilot Channel on Reverse Link

Evolution of Beam Pattern with Desired User Moving

Figure 4.17, Beam patterns formed by Wiener Solution with pilot channel on reverse link with desired user moving (with 50 interfering users, E_b/N_0= 15 dB, flat slow fading).

Evolution of Beam Pattern while Increasing Interfering Users

Figure 4.18 Beam patterns by Wiener Solution with pilot channel on reverse link with the number of interfering users increasing. The location of desired user is fixed (DOA of desired user = 2 rads, E_b/N_0= 15 dB, with flat slow fading).

4.5 Results and Conclusion

In this chapter we present an overview of the adaptive beamforming algorithms. Both the non-blind and blind algorithms were described.

The beam patterns formed by different algorithms were presented in Section 4.4. From these simulation results, we can say the beam patterns with different algorithms are very similar. All of them can adjust the main beam towards the desired user, and put nulls or as small as possible gain in the directions of interfering users.

From Figure 4.13(a), Figure 4.16(a) and Figure 4.18(a) we see that most of the signals can be extracted by nulling out all the other interference when the number of interfering users is no more than the number of antenna elements.

From Figure 4.13(b, c, d), Figure 4.16(b, c, d) and Figure 4.18(b, c, d) we see that the beam patterns will change slightly in order to get as much as possible Signal-to-Interference-and-Noise-Ratio (SINR) while the number of interfering users increasing and more than the number of antenna elements. In such a case, although the interference is not rejected completely, most of the interference coming from other directions is rejected, thus the overall interference level is reduce. For the case of beamforming by LMS algorithm with Training Sequences shown in Figure 4.16, the beam patterns are not as sharp as the other two algorithms. But they still put very small gain in the direction of interfering users to increase SINR.

We also note that the beamwidth of the beam near the endfire is wider than that of the beam steered to the other direction.

In Chapter 5, we will give a detailed description of the benefits of system capacity and BER performance we can get by using adaptive antenna.

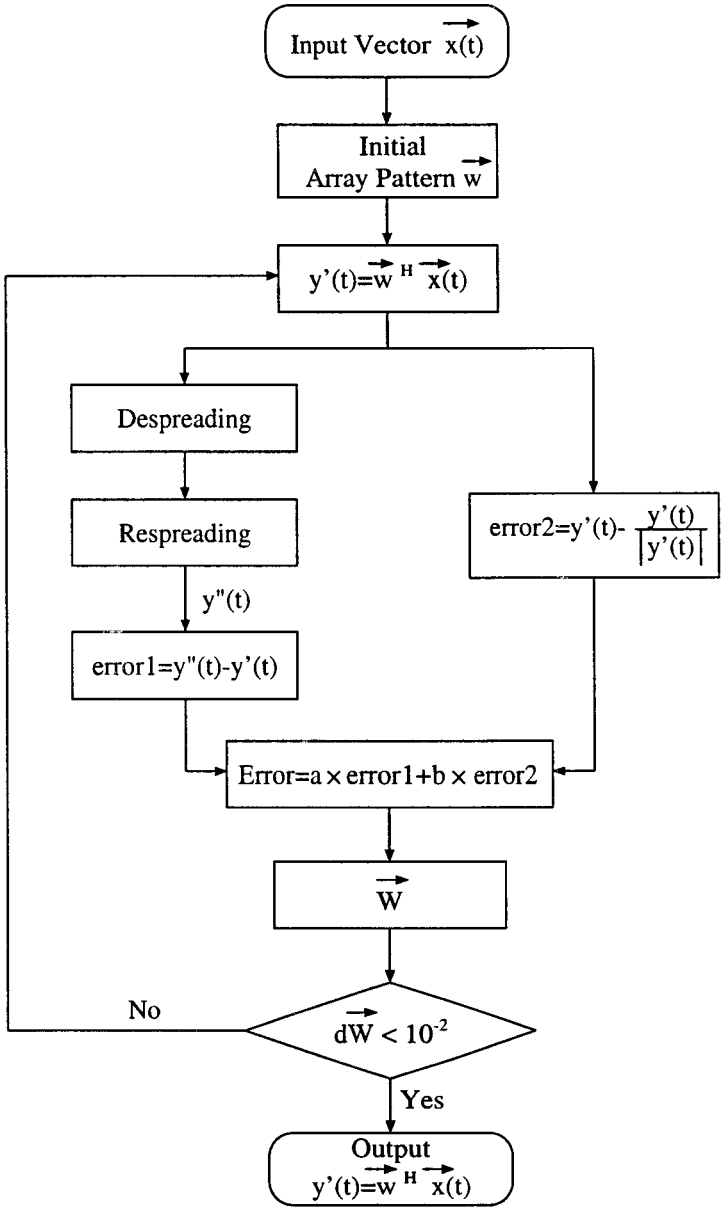

Figure 4.11: Flow chart of LS-DRMTCMA.

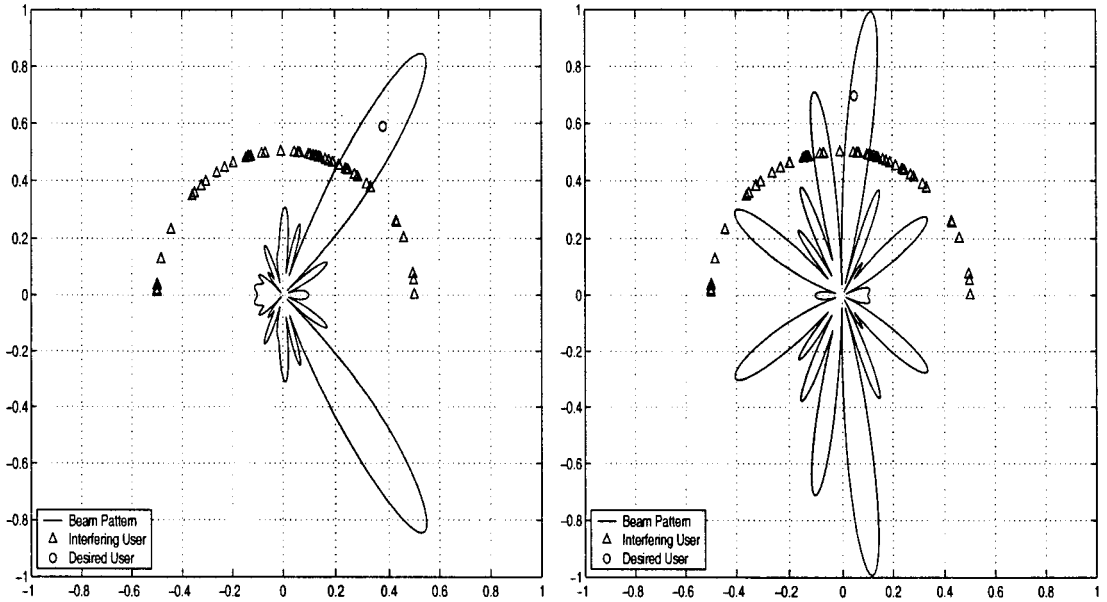

(a) DOA of desired user=1 rad (b) DOA of desired user= 1.5 rads

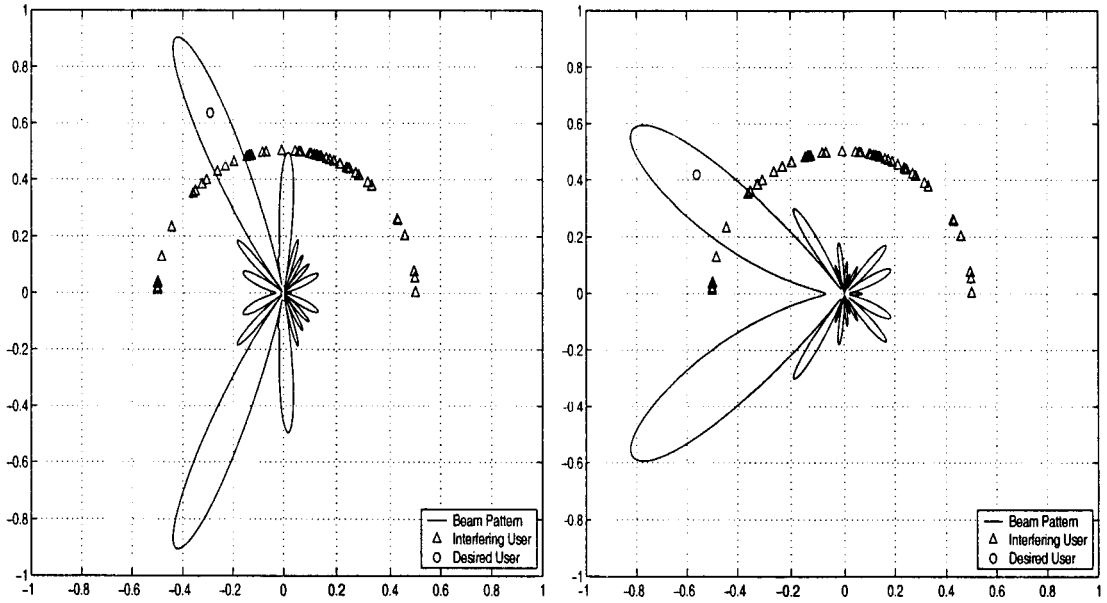

(c) DOA of desired user=2 rads (d) DOA of desired user=2.5 rads

Figure 4.12: Beam patterns with blind adaptive algorithm with the desired user moving (with 50 interfering users, $E_b/N_0 = 15$ dB, with flat slow fading). The ratio of the coefficients a_{PN}/a_{CM} used in the LS-DRMTCMA is set to 2.

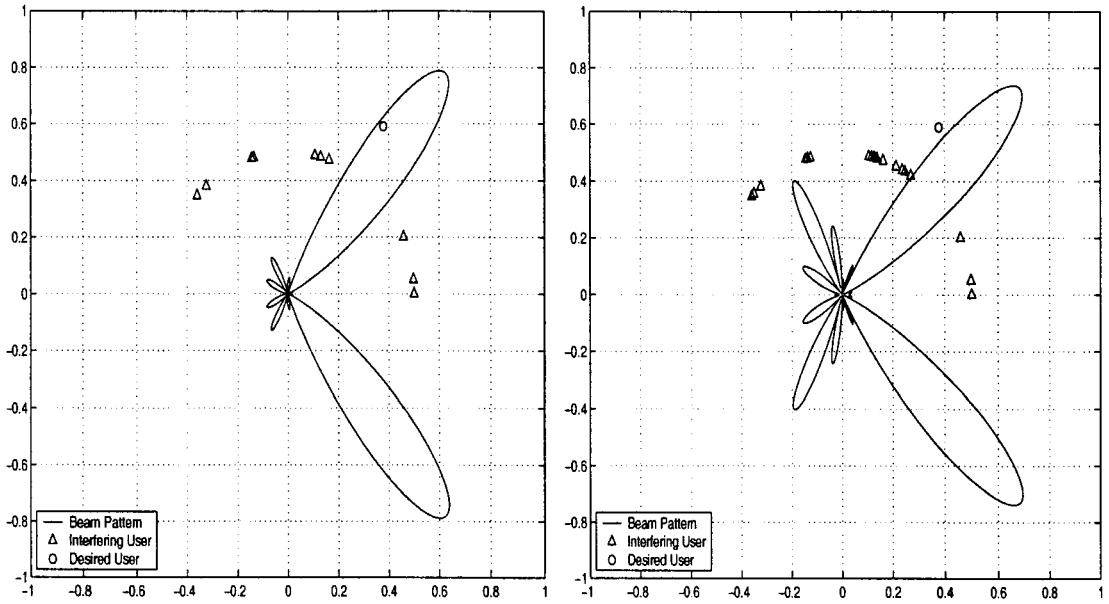

(a) 10 interfering users (b) 20 interfering users

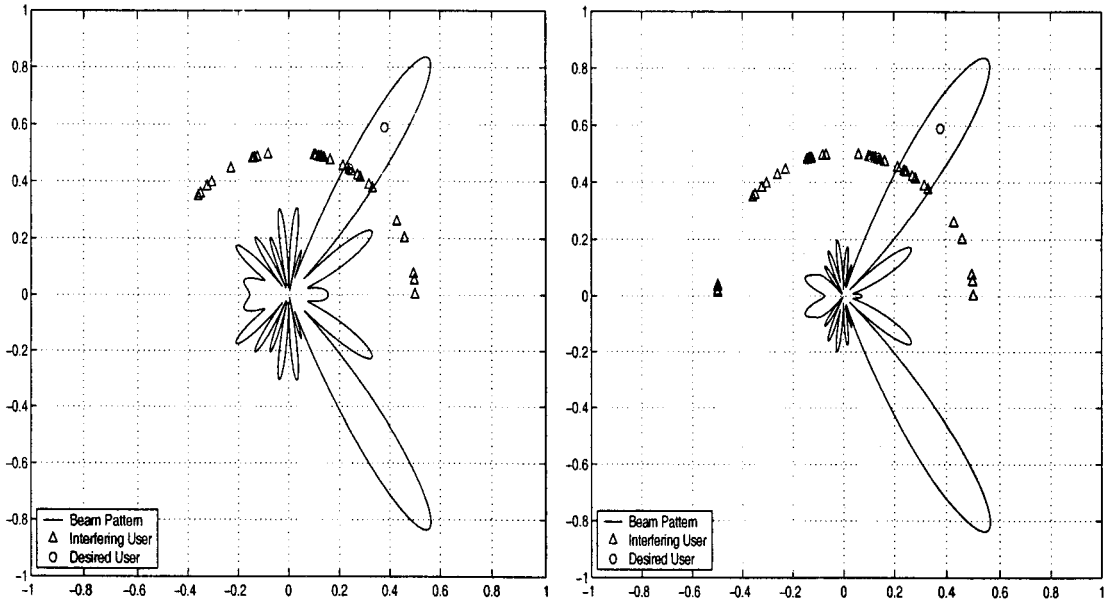

(a) 10 interfering users (b) 20 interfering users

Figure 4.13: Beam patterns with blind adaptive algorithm with the number of interfering users increasing (DOA of desired user = 1 rad, E_b/N_0 =15 dB, with flat slow fading).The ratio of the coefficients a_{PN}/a_{CM} used in the LS-DRMTCMA is set to 2.

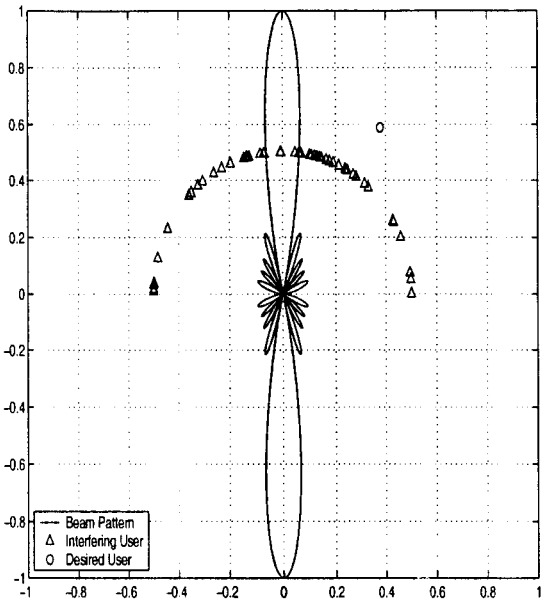

(a) Initial pattern

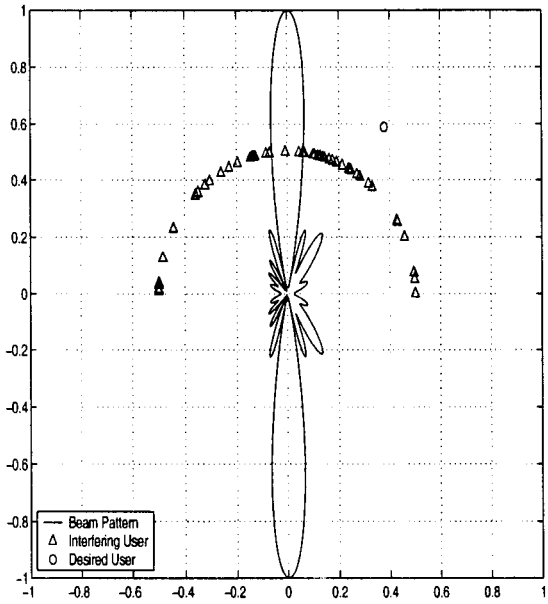

(b) After 200 iterations

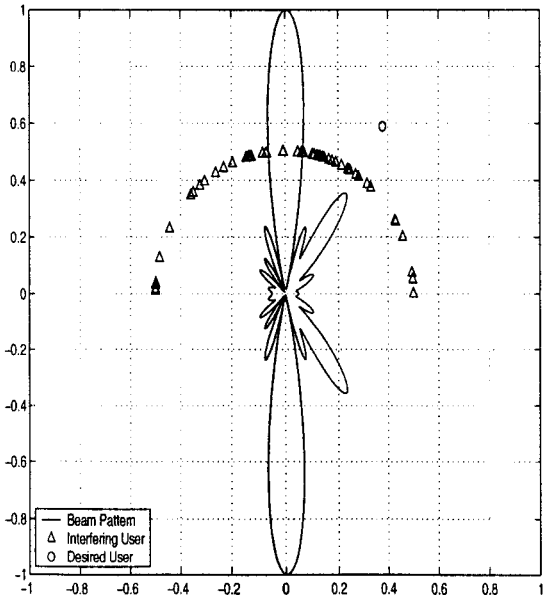

(c) After 300 iterations

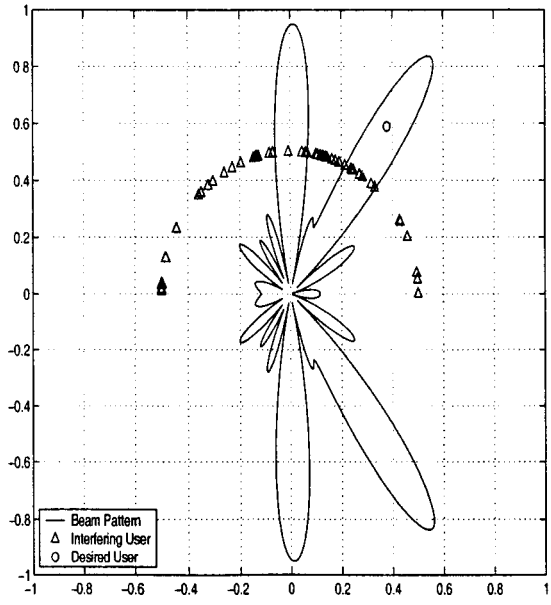

(d) After 500 iterations

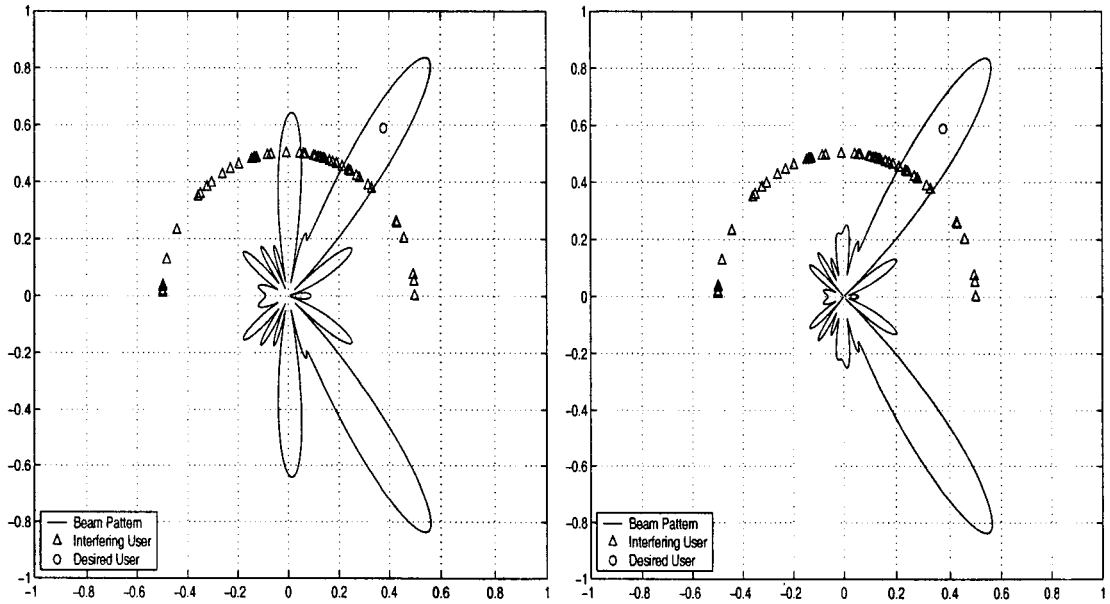

(e) After 600 iterations

(f) After 800 iterations

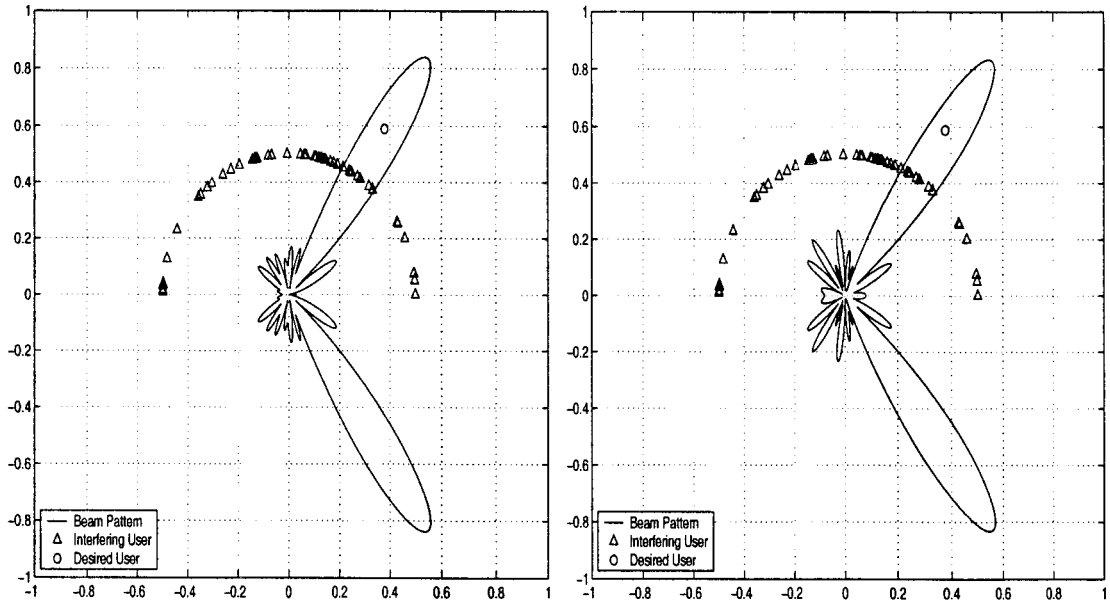

(g) After 1000 iterations

(f) Convergence pattern
(After 1364 iterations)

Figure 4.14: Beam patterns with blind adaptive algorithm iterations (with 50 interfering users, DOA of desired user = 1 rad, $E_b/N_0 = 15$ dB, with flat slow fading).The ratio of the coefficients a_{PN}/a_{CM} used in the LS-DRMTCMA is set to 2.

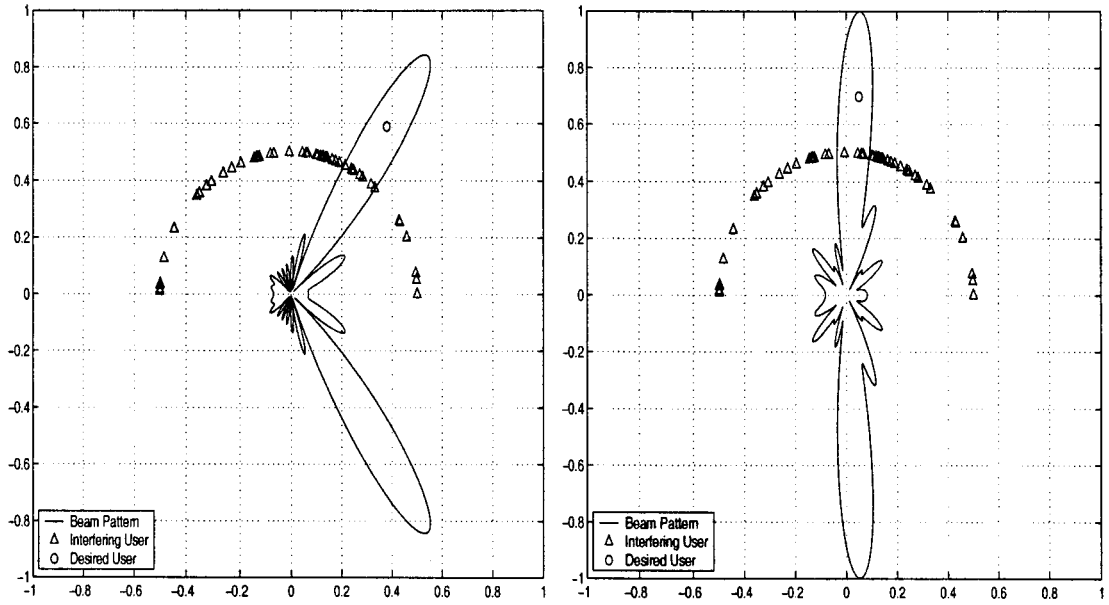

(a) DOA of desired user=1 rads (d) DOA of desired user=1.5 rads

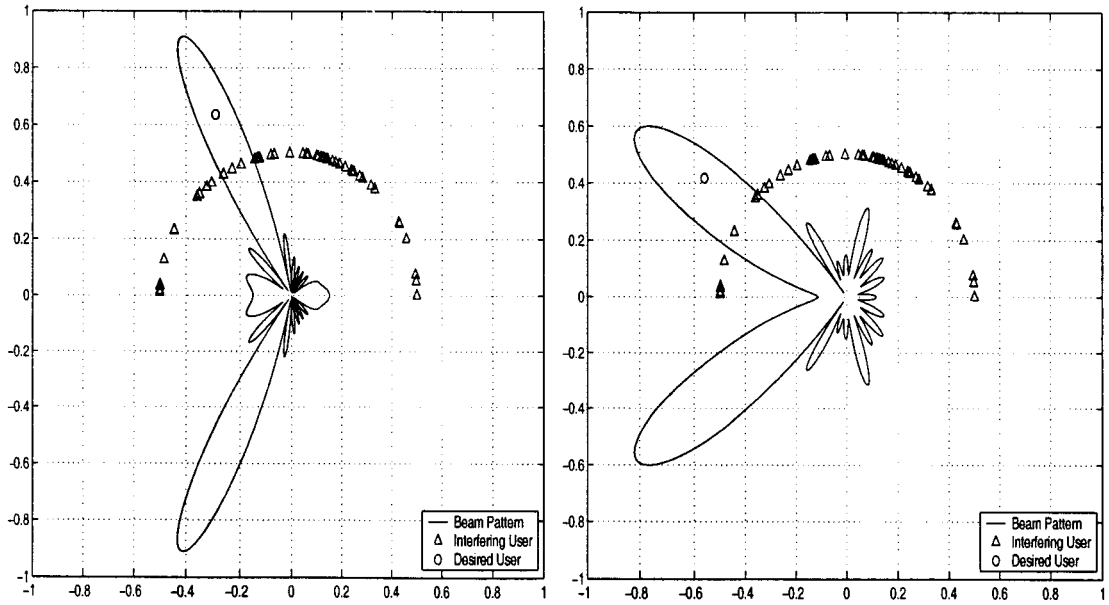

(c) DOA of desired user=2 rads (d) DOA of desired user=2.5 rads

Figure 4.15: Beam patterns with training sequences with desired user moving (with 50 interfering users, E_b/N_0 =15 dB, with flat slow fading).

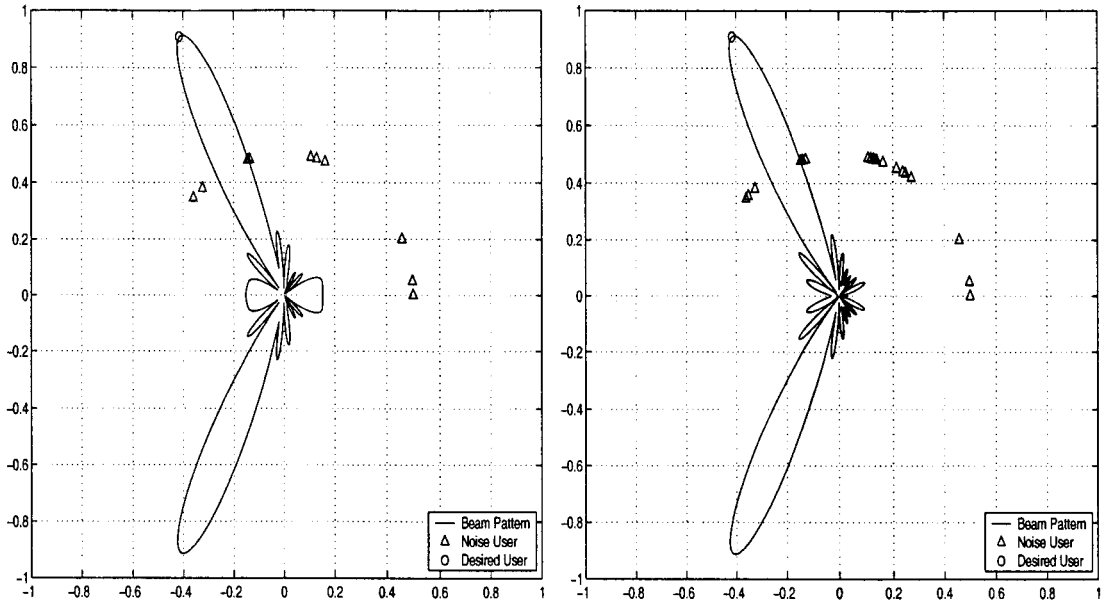

(a) 10 interfering users

(b) 20 interfering users

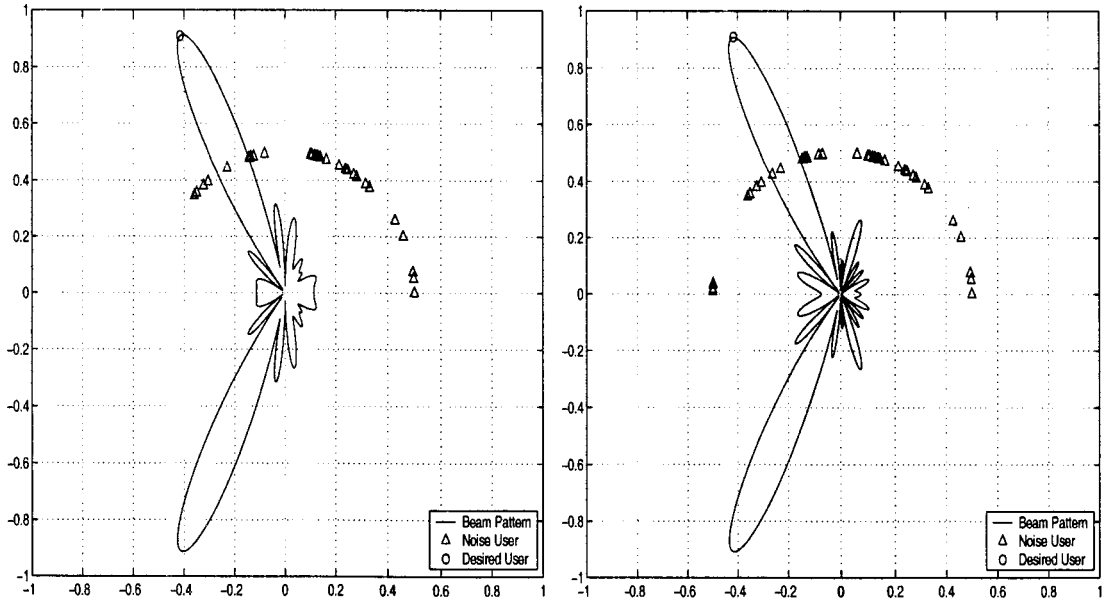

(c) 30 interfering users

(d) 40 interfering users

Figure 4.16: Beam patterns with training sequence with the number of interfering users increasing (DOA of desired user = 2 rads, E_b/N_0= 15 dB, with flat slow fading).

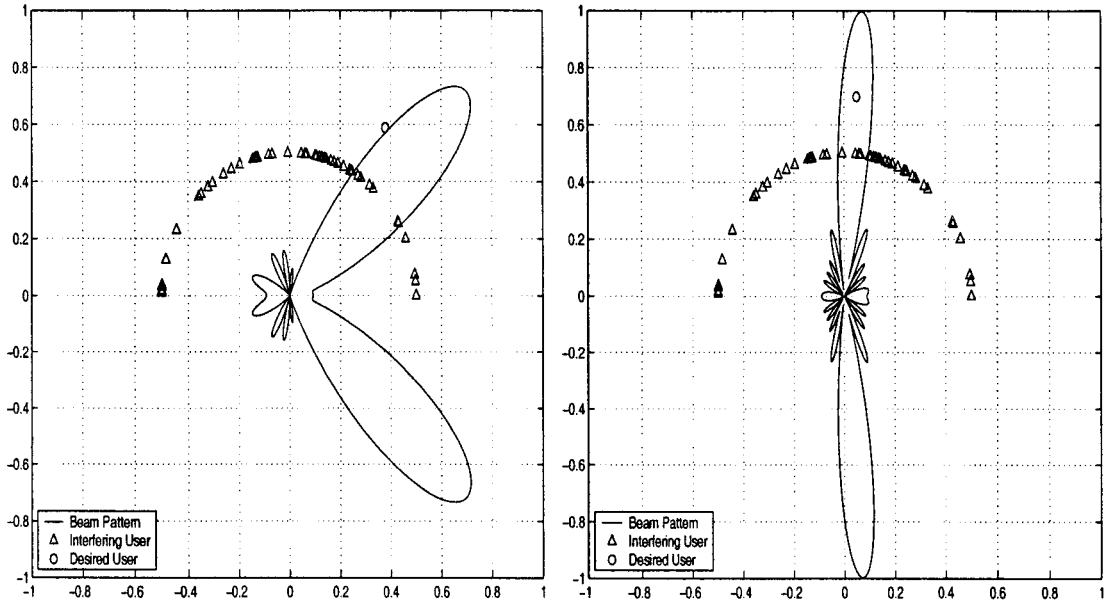

(a) DOA of desired user=1 rads (d) DOA of desired user=1.5 rads

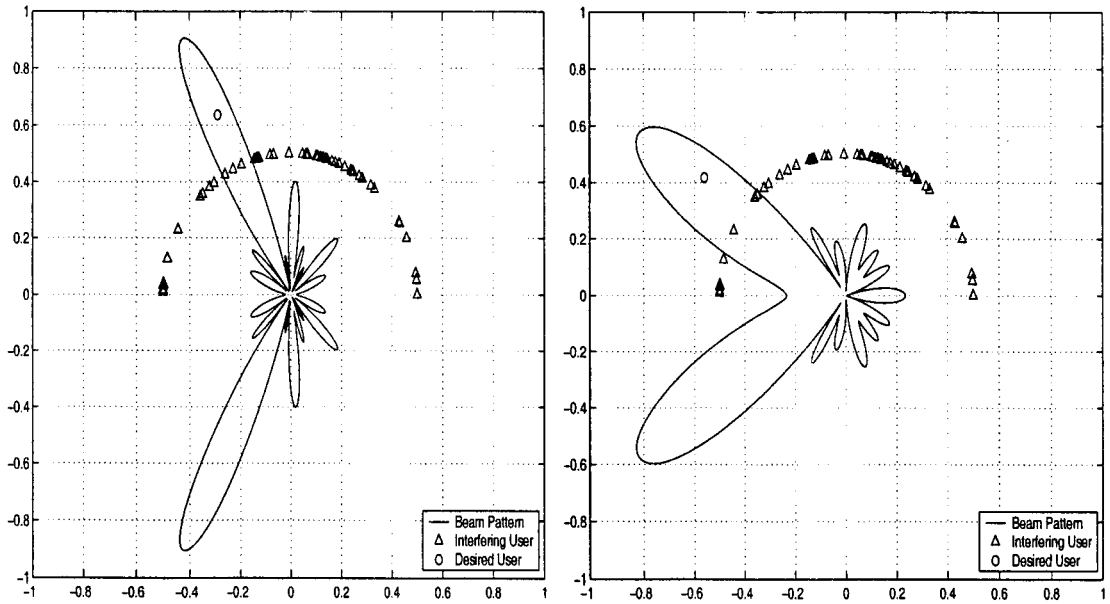

(c) DOA of desired user=2 rads (d) DOA of desired user=2.5 rads

Figure 4.17: Beam patterns with pilot channel on reverse link with desired user moving (with 50 interfering users, E_b/N_0= 15 dB, with flat slow fading).

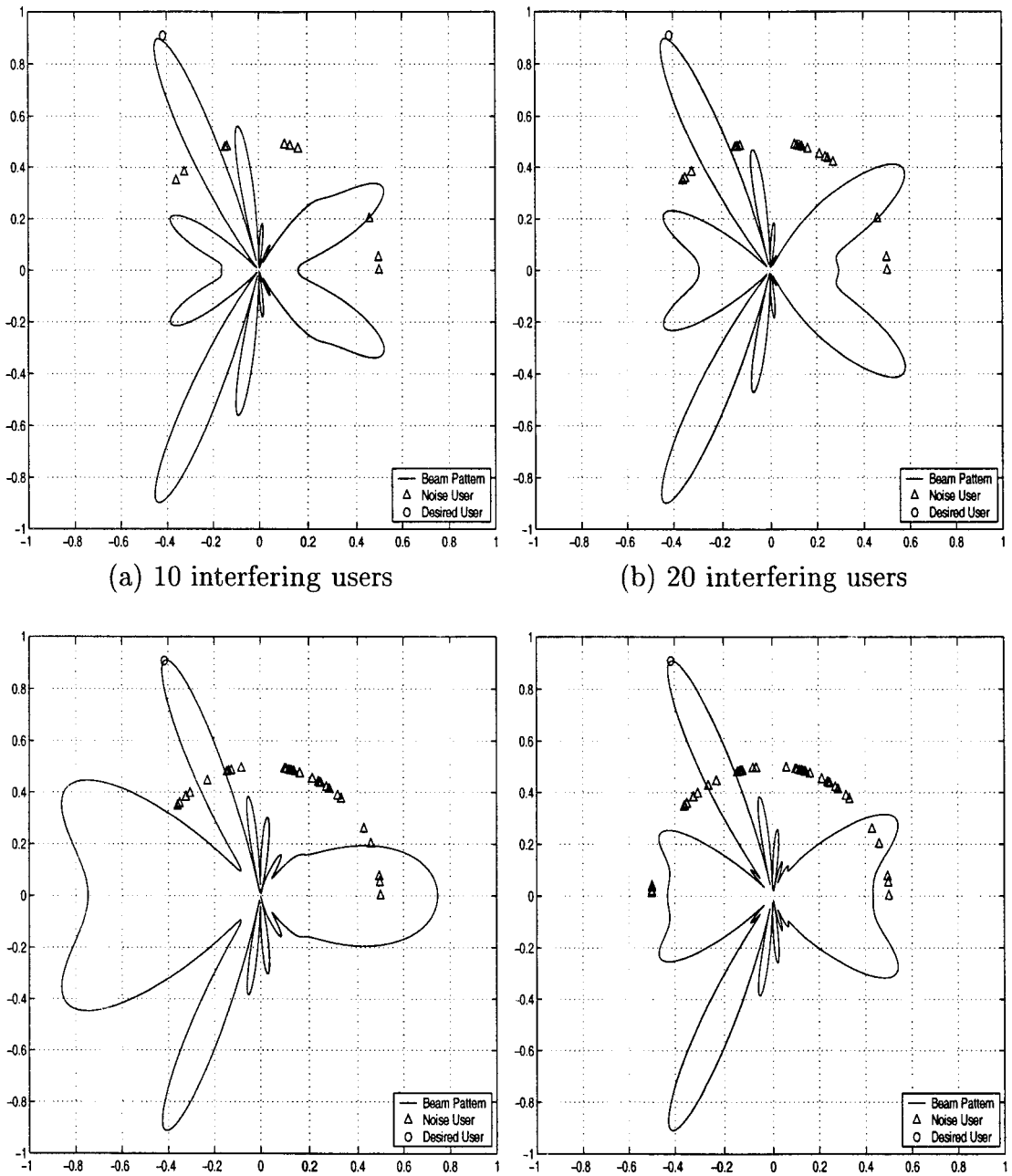

(a) 10 interfering users

(b) 20 interfering users

(c) 30 interfering users

(d) 40 interfering users

Figure 4.18: Beam patterns with pilot channel on reverse link with the number of interfering users increasing (DOA of desired user = 2 rads, E_b/N_0= 15 dB, with flat slow fading).

Chapter 5

OVERALL SIGNAL TO NOISE RATIO IMPROVEMENT OF ADAPTIVE ANTENNAS

5.1 Introduction

The investigation into the use of adaptive arrays in communications began more than two decades ago[12]. The objective then was to develop receiving systems for acquiring desired signals in the presence of strong jamming, especially in military communications. Adaptive array systems have been developed for receiving TDMA satellite communications signals[12] and spread-spectrum communications signals[13][25].

We have mentioned in Chapter 1 some general advantages of using digital beamforming. Here, we will discuss the specific benefits of using adaptive antennas in mobile communication. With the adaptive antenna technology, many of the system parameters that are considered constraints in a single-antenna system become parameters that a system designer has at his disposal to further optimize system performance. It is this aspect of adaptive antenna technology which is perhaps most

attractive with regard to its inclusion in the next generation of PCS system may benefit from the use of adaptive antenna technology in the following aspects.

Coverage

Adaptive beamforming can increase the cell coverage range substantially through antenna gain and interference rejection. In particular, the coverage range can be improved by a factor of $M^{1/n}$ for noise-limited environments, where M denotes the number of antenna elements and n denotes the propagation loss exponent. For example, if $n = 4$ and $M = 16$, the range is approximately doubled with respect to the omni-directional antenna case.

Generally, there will be fewer sites required with adaptive antennas employed at base stations. A larger coverage area can be achieved with base station antennas at a greater height above average terrain. However, this system trade-off between antenna height and coverage area can be eased by using the number of antenna elements as a design parameter. This leads to substantially eased siting requirements in many situations.

Capacity

Adaptive antenna technology provides the flexibility that, in conjunction with centralized dynamic channel assignment strategy, allows a reuse factor of unity; that is, a single frequency can be used in all cells. Reuse planning therefore becomes a dynamic programming problem that is solving the problem of maximizing the number and quality of mobile links. With respect to CDMA systems, the reuse is code reuse rather than frequency reuse, but the fundamental concept is the same.

In general, adaptive beamforming can increase the number of available voice channels through directional communication links[28]-[34]. The increase factor depends on the propagation environment, the number of antenna elements, and the

amount of DOA allowed by the system. The point is that it is possible to have multiple mobiles on the same RF channel but different spatial channels at a particular cell site. Furthermore, frequency-reuse patterns can be substantially improved or reduced though intelligent use of adaptive antennas.

Transmission bit rate can be increased due to the improved SIR at the output of the adaptive beamformer. The minimum rate improvement would be that attainable with $10 \log M$ dB SIR improvement in noise-limited environments and depends on the modulation format. Adaptive antennas allow RF channels to be adjusted through link power control to meet the requirements of user-selectable data transfer rates. Low-rate users can use lower power links; high-rate users require higher power links.

Reference [35] and [36] evaluate the capacity enhancement achieved by a base-station array antenna with adaptive beam forming, and we will analyzes the impact of base-station adaptive antennas on the capacity enhancement of a CDMA mobile communication system in the following section.

Signal Quality

In noise-limited environments, minimum receiver thresholds are reduced by $10 \log M$ dB on average. In interference-limited environments, the additional improvement in tolerable SIR at a single element results from interference rejection afforded against interferer directional interferer. The level of improvement depends on the distribution of cochannel users in neighboring cells. With centralized DOA, it is possible to improve system performance even further by providing optimization on a "global" system-wide basis.

Adaptive antennas can be considered as spatial equalizers and can provide substantial signal quality improvements through spatial signal processing. In fact, some implementations of adaptive antennas provide a spatial rake receiver capability to combine uplink multipath arrivals for improved output SIR. There is virtually

no limit to the amount of delay spread tolerable on the uplink, since the signals are with probability>95% spatially distinguishable.

Power Control

Power control requirements of the various modulation methods are somewhat eased through the inclusion of adaptive antenna technology; however, there are robustness benefits to be attained through coarse mobile unit and base station power control. The dynamic link budget control in normally a difficult process, but it can be made substantially easier through the use of angular information about the user signals provided by adaptive antennas.

Power control can be enforced to ensure maximum use of dynamic range. The objective is to keep all the users at a power level as low as possible under the constraint that the range of power levels seen at the base stations is within 10 to 20 dB.

Handover

In many cases, adaptive antenna technology provides mobile unit location information that can be used by the system to substantially improve handovers in both the low and high tiers. With sufficiently accurate position estimates, prediction of velocities is possible which allows further improvements in handover strategies.

Handover is performed by passing mobile unit tracking information from the base stations to the control center for resource allocation optimization. Deciding which cell to hand a mobile to is a much easier task when one knows where the unit is and how fast it is moving. Coupled with the good engineering practice of designing overlapping coverage areas, the result is "smart" handover, which is neither "soft" nor "hard".

Base Station Transmit Power

Using adaptive beamforming, the maximum peak Effective Isotropic Radiation Power (EIRP) required per user on a particular channel is $10 \log M$ dB less than without adaptive beamforming. The average EIRP is similarly reduced. On a per element basis, $10 \log M$ dB less power is transmitted while the antenna array is still able to maintain the same power level at the mobile unit as in the case without the use of an adaptive antenna.

Portable Terminal Transmit Power

If an adaptive antenna is implemented in a system without changing other parameters (e.g., cell size), the transmission power levels required for portable terminals can be reduced on average by at least $10 \log M$ dB. The reduction in transmission power levels, which results from the increase in antenna gain at the base station, relaxes the requirements on batteries. Other relevant issues include increased fade margin for improved signal quality (e.g., higher data rates, increased coverage area per cell to decrease deployment costs). With appropriate link management in the system, the power budgets for each of the radio links can be optimized for each particular link dynamically, a process made substantially easier through the use of mobile position estimates provided by adaptive antennas. The key point is that with adaptive antennas at cells, the transmit power levels from and to the mobile can be kept minimum to provide the requested service. The power levels will not exceed those that would otherwise be transmitted from an omni or hard-sectored site.

5.2 CDMA System Capacity Improvement

5.2.1 Single Cell System

5.2.1.1 Single Cell System with Isotropic Antenna

For interference limited asynchronous, BPSK-CDMA over an Additive White Gaussian Noise (AWGN) channel, operating with perfect power control and with omnidirectional antennas used at the base station, the bit error rate (BER), P_b, on the reverse link is approximated by [19]

$$p_b = Q\left(\sqrt{\frac{3N}{K-1}}\right) \tag{5.1}$$

where K is the number of users in a cell and N is the spreading factor. Equation (5.1) assumes that the signature sequences are random.

In CDMA system, a critical parameter to measure link performance is the Signal-to-Interference-and-Noise-Ratio (SINR) available for each subscriber. The SINR for each subscriber is measured after despreading.

We define the SINR after despreading, as the ratio of the desired signal to the sum of interference and noise.

$$SINR = \frac{P_0}{\frac{1}{N}\sum_{k=1}^{K} P_k + \sigma_n^2} \tag{5.2}$$

In equation (5.2), P_0 is the power of the desired signal at the input to the despreader at the base station, and P_k is the power from every other user for $k = 1, ...K-1$. The spreading factor is given by N, which was defined as

$$N = \frac{Chip\ Rate}{Information\ Symbol\ Rate} \tag{5.3}$$

Equation (5.2) reflects the fact that spreading reduces the impact of multiple access interference, P_k. The noise variance, σ_n^2, represents the noise contribution to the decision variable after despreading.

Multiplying the numerator and denominator of equation (5.2) by the bit duration, T_b, we have

$$SINR = \frac{P_0 T_b}{\frac{1}{N}\sum_{k=1}^{K-1} P_k T_b + \sigma_n^2 T_b} \tag{5.4}$$

The term $P_0 T_b$ is the energy per bit for the desired subscriber signal. After despreading, the noise bandwidth is approximately $\frac{1}{T_b}$. If the thermal noise has a power spectral density of N_n, then we can write the SINR as

$$SINR = \frac{E_b}{\frac{1}{N}\sum_{k=1}^{K-1} P_k T_b + N_n} = \frac{E_b}{\frac{I_0 T_b}{N} + N_n} \tag{5.5}$$

$$= \frac{E_b}{N_i + N_n} = \frac{E_b}{N_0}$$

The term N_i represents the power spectral density of the total multiple access interference after despreading.

It is also important to account for the fact that CDMA systems take advantage of voice inactivity. Because the vocoder reduces its output rate when the speaker is silent, the user subscribers unit does not transmit continuously, but is gated on the off with a duty cycle as low as $\frac{1}{8}$ during silent periods. This is captured in the voice activity factor, v. Typically, the voice activity factor reduces the average Multiple Access Interference level seen by the base station receiver by 50-60% (v=0.4 to 0.5) relative to the case where all user are transmitting continuously.

We can modify equation (5.5) to take in account the SINR improvement due to the voice activity factor:

$$SINR = \frac{E_b}{\frac{v}{N}\sum_{k=1}^{K-1} P_k T_b + N_n} = \frac{E_b}{v\frac{I_0 T_b}{N} + N_n} = \frac{E_b}{N_0} \tag{5.6}$$

where I_0 is the average total interference power, seen by the base station receiver for the desired user, measured at the output of the receiving array.

If perfect power control is applied so that the power incident at the base station antenna from each user is the same, P_c,

$$SINR = \frac{E_b}{\frac{v}{N}(K-1)P_c T_b + N_n} \tag{5.7}$$

5.2.1.2 Single Cell System with Smart Antenna

To illustrate how directional base station antennas can improve the reverse link in a single cell CDMA system, we consider the case in which each portable unit has an omni-directional antenna and the base station tracks each user in the cell, using a directive beam. It is assumed that a beam pattern, $F(\theta, \phi)$, is formed at the base station so that the pattern has a steer-able maximum in the direction of the desired user.

We will assume that the pattern is separable in the θ (elevation) and ϕ (azimuth) dimensions, so that we can express the pattern as

$$F(\theta, \phi) = F_e(\theta) F_a(\phi) \tag{5.8}$$

The elevation pattern, $F_e(\theta)$, is fixed with a maximum value on the horizon, at $\theta = \frac{\pi}{2}$. For simplicity, we will assume that

$$\max_{\phi}[F_a(\phi)] = 1 \qquad \max_{\theta}[F_e(\theta)] = 1 \tag{5.9}$$

We assume that K users in the single cell CDMA system are uniformly distributed throughout a two-dimensional cell (in the horizontal plane, $\theta = \frac{\pi}{2}$). On the reverse link, the received power from the desired mobile is $P_{r,0}$. The powers of the signals incident at the base station antenna from the $K-1$ interfering users are given by $G_m F_a(\phi_k) P_{r,k}$, where G_m is the maximum gain of the overall pattern, ϕ_k is the direction of the k^{th} user in the horizontal plane, measured from the x-axis. Then the average total interference power, I_0, seen by the base station receiver for user 0, measured at the output of the receiving array, is given by

$$I_0 = G_m E \left\{ \sum_{k=1}^{K-1} F_a(\phi_k) P_{r,k} \right\} \tag{5.10}$$

If perfect power control is applied so that the power incident at the base station antenna from each user is the same, then $P_{r,i} = P_c$ for each of the K users, and the average interference power seen by user 0 is given by

$$I_0 = G_m P_c E \left\{ \sum_{k=1}^{K-1} F_a(\phi_k) \right\} \tag{5.11}$$

Substituting equation (5.11) into (5.7) we have

$$SINR_{AAA} = \frac{G_m P_c T_b F_a(\phi_0)}{\frac{v}{N} T_b G_m P_c E \left\{ \sum_{k=1}^{K-1} F_a(\phi_k) \right\} + N_n} \tag{5.12}$$

From $F_a(\phi_0) \geq F_a(\phi_i)$, $i = 1, 2, ...K-1$, which is because the main beam is in the direction of the desired user, We can obtain,

$$(K-1) F_a(\phi_0) \geq E\left\{\sum_{k=1}^{K-1} F_a(\phi_k)\right\} \tag{5.13}$$

Assume $G_m F_a(\phi_0) = 1$. Substituting equation (5.13) into (5.12), we have

$$SINR_{AAA} \geq \frac{G_m P_c F_a(\phi_0) T_b}{\frac{v}{N} T_b G_m (K-1) F_a(\phi_0) P_c + N_n} \tag{5.14}$$

Then

$$SINR_{AAA} \geq \frac{P_c T_b}{\frac{v}{N} T_b (K-1) P_c + N_n} \tag{5.15}$$

The right hand side of equation (5.15) which is the same as equation (5.7), SINR of the system using isotropic antennas. Note that equation (5.15) holds for a single cell CDMA system, with perfect power control applied to all subscribers, when the base station antenna pattern may be steered toward the desired subscriber.

5.2.2 Reverse Channel Performance of Multi-cell Systems with Spatial Filtering at the Base Station

In this section, we investigate how smart antennas are used on the reverse link to improve CDMA system capacity in multi-cell systems. Note that equation (5.15) is valid only when a single cell is considered. To find the effects of spatial filtering on the reverse link when CDMA users are simultaneously active in several adjacent cells, we must first define the geometry of the of the cell region. For simplicity, we consider the geometry with a single tier of surrounding cells.

5.2.2.1 The Interference Power Received from Users in Adjacent Cells

Let user 0 is the desired user, and it is in desired cell 0,

$P_{0,0}$ is the power received at the base station of cell 0 from the users in cell 0,

$P_{0,j}$ is the power received at the base station of cell 0 from the users in cell j,

$P_{k,j}$ is the power received at the base station of cell k from the users in cell j.

Since users in adjacent cell j are power controlled by their base station, the interference power from them received at the base station in cell 0, $P_{0,j}$ is not $P_{0,0}$.

Assume that base station j applies perfect power control to all users in cell j, so that power $P_{j,j}$ is received at base station j, for each of the users in cell j. We also assume that for each cell, $P_{j,j}$ is same, that is to say

$P_{j,j} = P_c, \qquad j = 0, 1,...K\text{-}1$

Assume the channels have Rayleigh fading and log-normal shadowing effect[37],

$$\frac{P_{0,j}\left(\left|\alpha_{0,j}^{j}\right|\right)^2}{P_{j,j}\left(\left|\alpha_{0,j}^{0}\right|\right)^2} = \frac{\left(d_j^j\right)^n}{\left(d_j^0\right)^n} \tag{5.16}$$

where n is the path loss exponent,

d_j^j is the distance from the user in cell j to base station j,

d_j^0 is the distance from the user in cell j to base station 0,

$\alpha_{0,j}^{j}$ and $\alpha_{0,j}^{0}$ have a Rayleigh distribution

$E\left[\left|\alpha_{0,j}^{j}\right|^2\right]$ and $E\left[\left|\alpha_{0,j}^{0}\right|^2\right]$ is log- normal,

$P_{j,j} = P_c$.

From equation (5.16), we can get

$$P_{0,j} = P_c\left(\frac{d_j^j}{d_j^0}\right)^n \frac{\left(\left|\alpha_{0,j}^{j}\right|\right)^2}{\left(\left|\alpha_{0,j}^{0}\right|\right)^2} = P_c\beta_{0,j}^2 \tag{5.17}$$

where

$$\beta_{0,j} = \left(\frac{d_j^j}{d_j^0}\right)^{\frac{n}{2}} \frac{\alpha_{0,j}^j}{\alpha_{0,j}^0}, \qquad \beta_{0,j}^2 \leq 1$$

5.2.2.2 System Performance

The way of getting SINR for multi-cell system is similar to the way we use in the previous part, i.e. single-cell system.

For the system using isotropic antenna,

$$SINR = \frac{P_c}{P_{in} + P_{out} + \sigma_n^2} \tag{5.18}$$

$$= \frac{P_c}{\sum_{k=1}^{K-1} P_{0,0,k} + \sum_{j=1}^{J} \sum_{k=0}^{K-1} P_{0,j,k} + \sigma_n^2}$$

where P_{in} is the interference power from the users in the desired cell,

P_{out} is the interference power from the users in adjacent cells,

K is the maximum number of users per cell,

J is the number of adjacent cells we consider,

$P_{0,0,k}$ is the interference power from the k^{th} user in the desired cell,

$P_{0,j,k}$ is the interference power from the k^{th} user in cell j.

Since prefect power control is applied,

$$SINR = \frac{P_c}{(K-1)P_c + P_c \sum_{j=1}^{J} \sum_{k=0}^{K-1} \beta_{0,j,k}^2 + \sigma_n^2} \tag{5.19}$$

For the system using smart antenna,

$$P_{in} = G_m E\left\{\sum_{k=1}^{K-1} P_{0,k} F_a\left(\phi_{0,k}\right)\right\} \tag{5.20}$$

$$P_{out} = G_m E \left\{ \sum_{j=1}^{J} \sum_{k=0}^{K-1} P_{j,j,k} \beta_{0,j,k}^2 \bullet F_a \left(\phi_{j,k} \right) \right\} \tag{5.21}$$

Substituting equation (5.21) and (5.20) into equation (5.19), we have

$SINR_{AAA} =$

$$\frac{G_m F_a \left(\phi_0 \right) P_c}{G_m E \left\{ \sum_{k=1}^{K-1} P_{0,0,k} F_a \left(\phi_{0,k} \right) \right\} + G_m E \left\{ \sum_{j=1}^{J} \sum_{k=0}^{K-1} P_{j,j,k} \beta_{0,j,k}^2 F_a \left(\phi_{j,k} \right) \right\} + \sigma_n^2} \tag{5.22}$$

Assume $G_m F_a \left(\phi_0 \right) = 1$, and perfect power control is applied,

$SINR_{AAA} =$

$$\frac{P_c}{G_m P_c E \left\{ \sum_{k=1}^{K-1} F_a \left(\phi_{0,k} \right) \right\} + G_m P_c E \left\{ \sum_{j=1}^{J} \sum_{k=0}^{K-1} \beta_{j,j,k}^2 \bullet F_a \left(\phi_{j,k} \right) \right\} + \sigma_n^2} \tag{5.23}$$

Since

$$F_a \left(\phi_0 \right) \geq F_a \left(\phi_{j,k} \right), \qquad when\ j = 0,\ k = 1, 2, ...K - 1$$

$$when\ j = 1, 2, ...J,\ k = 0, 1, ...K - 1$$

So

$$G_m P_c E\left\{\sum_{k=1}^{K-1} F_a\left(\phi_{0,k}\right)\right\} \leq G_m P_c\left(K-1\right) F_a\left(\phi_0\right) = P_c\left(K-1\right) \tag{5.24}$$

$$G_m P_c E\left\{\sum_{j=1}^{J}\sum_{k=0}^{K-1} \beta_{j,j,k}^2 \bullet F_a\left(\phi_{j,k}\right)\right\} \leq G_m P_c F_a\left(\phi_0\right) \sum_{j=1}^{J}\sum_{k=0}^{K-1} \beta_{j,j,k}^2 \tag{5.25}$$

$$= P_c \sum_{j=1}^{J}\sum_{k=0}^{K-1} \beta j, j, k$$

Substituting equation (5.24) and (5.25) into (5.23), we get

$$SINR_{AAA} \geq \frac{P_c}{P_c\left(K-1\right) + P_c \sum_{j=1}^{J}\sum_{k=0}^{K-1} \beta_{j,j,k} + \sigma_n^2} \tag{5.26}$$

In equation (5.26), $SINR_{AAA}$ is the SINR of the system using smart antenna. Its right hand side is the same as equation (5.19), which is the SINR of the system using isotropic antenna. It is obviously that the performance of the system using smart antenna is much better than the system using isotropic antenna, when the numbers of users per cell of both systems are same.

5.3 Performance Improvement

In order to facilitate the following analysis, a number of assumptions have to be made:

1. The CDMA system operates in an additive white Gaussian noise (AWGN) channel.

2. Perfect power control is achievable.

3. Spreading factor is N.

4. There are K users uniformly distributed in each cell.

5. The pattern of a beam formed by the array does not vary in the elevation plane.

6. A beam formed by the array can be steered in any direction in the azimuth plane such that the desired mobile is always illuminated by the main beam.

If there is no interference from adjacent cells and an omni directional base station antenna is used, the BER can be approximated by [26]

$$BER = Q\left(\sqrt{\frac{3N}{K-1}}\right) \tag{5.27}$$

where

$$Q(x) = \frac{1}{\sqrt{2\pi}} \int_0^\infty e^{-\frac{y^2}{2}} dy \tag{5.28}$$

On the reverse link, if a beam with a directional gain $G(\varphi)$ is formed in the direction φ of the desired signal from a particular user, the signals from the other $K-1$ users are considered to be interference. The average total interference power σ_I^2 with respect to the signal of this particular mobile is given by

$$\sigma_I^2 = E\left[\sum_{k=1}^{K-1} G(\varphi_k)\,\sigma_k^2\right] \tag{5.29}$$

where φ_k denotes the direction of the k^{th} interfering mobile signal. With perfect power control, the signals from all the mobiles have the same power σ_c^2 . Thus,

$$\sigma_I^2 = \sigma_c^2 E\left[\sum_{k=1}^{K-1} G\left(\varphi_k\right)\right] \tag{5.30}$$

By taking into account the pdf that describes the geographical distribution of the mobiles, σ_I^2 is found to be

$$\sigma_I^2 = \frac{\sigma_c^2 (K-1)}{D} \tag{5.31}$$

where D represents the array antenna's directivity given as

$$D = \frac{2\pi}{\int_0^{2\pi} G(\varphi)\, d\varphi} \tag{5.32}$$

It can be shown that the BER can be approximated by [27]

$$BER = Q\left(\sqrt{3N \times SINR}\right) \tag{5.33}$$

Since $SINR = \frac{\sigma_c^2}{\sigma_I^2}$, the BER is therefore given by

$$BER = Q\left(\sqrt{\frac{3ND}{K-1}}\right) \tag{5.34}$$

It can be observed from equation (5.34) that considerable improvement in terms of BER can be obtained when an antenna array is used.

5.4 Simulation Results

In this section, we will compare SINR improvement and the BER performance of different algorithms under different conditions.

To compare SINR improvement, we will consider three E_b/N_0 cases, $E_b/N_0 = 5$, $E_b/N_0 = 15$ and $E_b/N_0 = 25$. For each E_b/N_0 case, we will also consider two different DOA cases.

To compare BER performance of different algorithms, we will consider two cases, single user system and multi user system, for each algorithm. For each case, we will consider five different channel conditions, AWGN and four types of fading.

The CDMA signals were generated at the transmitter as in equation (2.26). The CDMA signals with like users interference and AWGN were generated as in equation (2.27). And the CDMA signals with like users interference as well as both AWGN and different types of fading were generated as in equation (2.29). The modulation scheme used in the system is the binary phase-shift keying (BPSK). The signals were then passed through the every antenna element and the adaptive antenna array algorithms as in the equation performed in Chapter 4.

To generate the BER for the different adaptive algorithms, we transmit different random bit streams for each user's signal and then feed the output of the beamformer into the matched filter to despread the signal and estimate the transmitted data bit. The estimates of the data bits are compared to the original transmitted data bits and the BER of each user is calculated. The BER averaged over all the users is then calculated and used in the BER performance plot.

In the following simulation cases, we assume perfect power control, so all the signals impinging on the array have the same power unless specified otherwise.

5.4.1 SINR Improvement

5.4.1.1 Evolution of SINR with Blind Algorithm

Figure 5.1 - Figure 5.3 show evolution of SINR with blind adaptive algorithm iterations, DOA of desired user=1 rad.

From Figure 5.1 to Figure 5.3, we can see SINR is developed with the beamforming computation iterations of blind adaptive algorithm. The antenna weights converge at last. The convergence speed depends on both E_b/N_0 and interfering noise in the system.

We also can see, for most of the cases, the improvement of SINR is very slightly after 200 iteration, even though the system does not obtain the convergent state. So, in the rest simulation, we use 200 iterations as the maximum iteration number per bit. Thus, the computational requirement of blind algorithms can be reduced greatly without effecting the system performance.

5.4.1.2 SINR Improvement by Using Adaptive Array

Figure 5.4 - Figure 5.6 show SINR development of multi user CDMA systems with different DOA of desired user (E_b/N_0 =15 dB, with flat slow fading).

From Figure 5.4 to Figure 5.6, we can see the SINR of multi system is greatly developed by using adaptive array, compared with the SINR of normal antenna system. With the number of interfering users per cell increasing, the reduction of SINR can be very slight by using adaptive array.

LS-DRMTCMA uses the constant modulus property of the transmitted signal in addition to the PN sequences of all the users to adapt the weight vectors, it can reduce the interference to a lowest lever when it can generate deeper null in the DOSs of the interference. However, the improvement of the LS-DRMTCMA over the other two algorithms becomes smaller when the interfering users increase. This is because under such situation, it is the interference falling into the main beam of the desired user that dominates the overall interference level. Although the LS-DRMTCMA can form deeper nulls in some DOAs of the interference than Wiener solution and LMS, once there is some interference falling into the main beam, the overall interference levels of these three algorithms become almost the same, and

thus the SINR is very close.

5.4.2 BER Performance Improvement by Array Beamforming by Blind Adaptive Algorithm

Figure 5.7 and Figure 5.8 are BER performance of single user system and multi user system with antenna array beamforming by blind adaptive algorithm, respectively. DOA of desired user=1 rad.The ratio of the coefficients a_{PN}/a_{CM} used in the LS-DRMTCMA is set to 2. In the multi user case, E_b/N_0 =15 dB.

5.4.3 BER Performance Improvement with Array Beamforming by Wiener Solution with Pilot Channel

Figure 5.9 and Figure 5.10 are BER performance of single user system and multi user system with antenna array beamforming by Wiener Solution with Pilot Channel, respectively. DOA of desired user=1 rad.The ratio of the coefficients a_{PN}/a_{CM} used in the LS-DRMTCMA is set to 2. In the multi user case, E_b/N_0 =15 dB.

5.4.4 BER Performance Improvement with Array Beamforming by LMS Algorithm with Training Sequence

Figure 5.11 and Figure 5.12 are BER performance of single user system and multi user system with antenna array beamforming by LMS Algorithm with Training Sequence, respectively. DOA of desired user=1 rad.The ratio of the coefficients a_{PN}/a_{CM} used in the LS-DRMTCMA is set to 2. In the multi user case, E_b/N_0 =15 dB.

5.5 Conclusion

In this chapter, we give the theoretical deviation of the improvement of capacity and BER performance by using adaptive in a CDMA system, firstly. And then, we present the simulation results of different adaptive array algorithms. We compare the SINR and BER performance with adaptive array and without adaptive array in various channel environments (e.g., the AWGN channel, the frequency offset case, and the multipath environment).

From the comparisons of SINR, we can see the SINR of the system with adaptive array is reduced much more slightly with the increase of the number of interfering users.

By comparing Figure 5.7, Figure 5.9, Figure 5.11 and Figure 2.8, and comparing Figure 5.8, Figure 5.10, Figure 5.12 and Figure 2.9(b), it is obviously that the system with adaptive array with every algorithms can outperform the system without adaptive array in all the channel environment, in both single user and multi user cases.

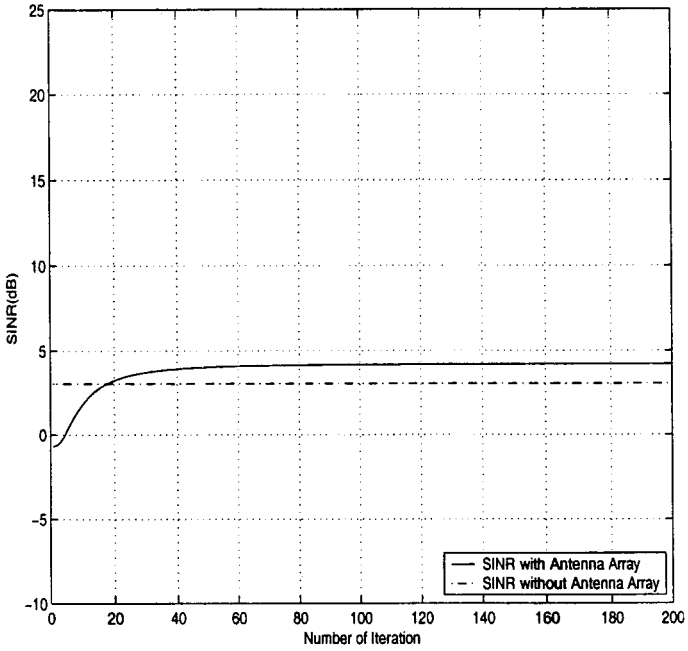

(a) 30 interfering users per cell

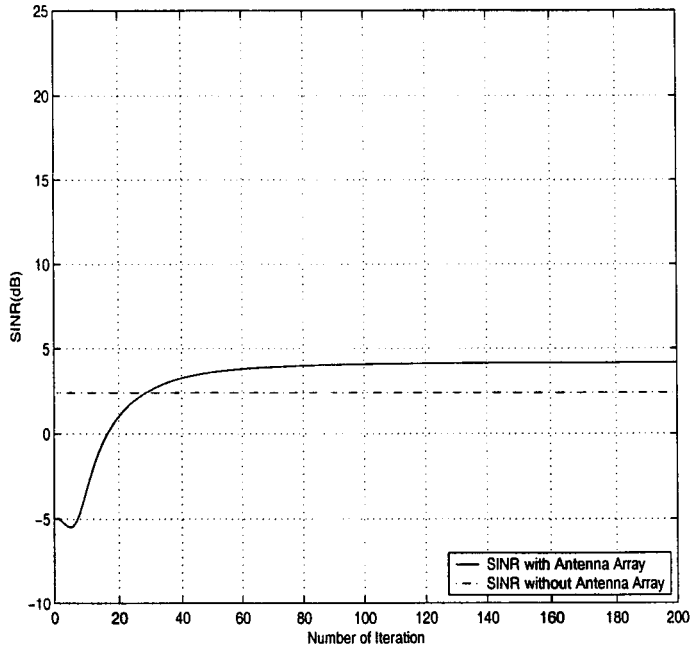

(b) 50 interfering users per cell

Figure 5.1: Evolution of SINR with blind adaptive algorithm iteration, E_b/N_0 =5 dB, with flat slow fading. DOA of desired user=1 rad.The ratio of the coefficients a_{PN}/a_{CM} used in the LS-DRMTCMA is set to 2.

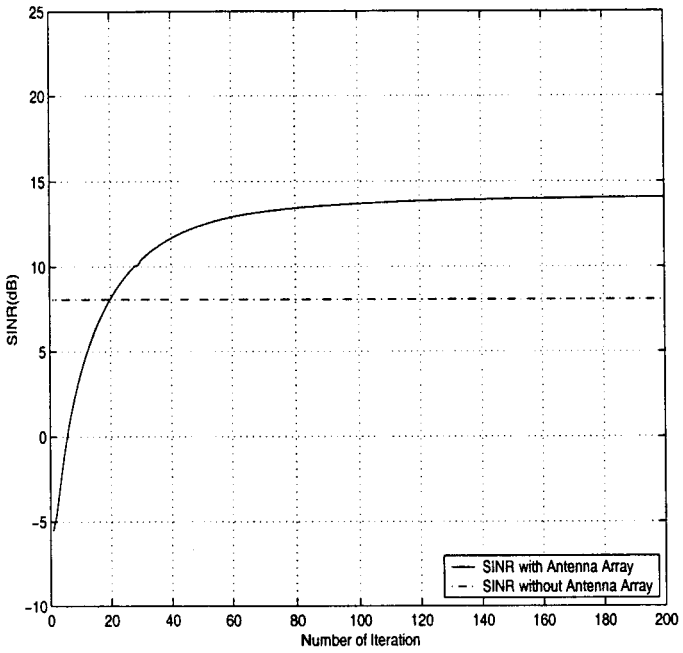

(a) 30 interfering users per cell

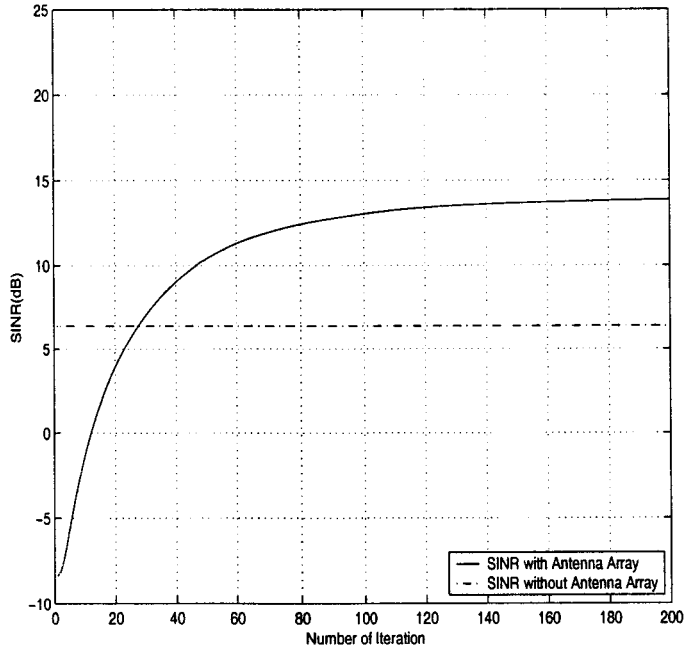

(b) 50 interfering users per cell

Figure 5.2: Evolution of SINR with blind adaptive algorithm iteration, E_b/N_0 =15 dB, with flat slow fading. DOA of desired user=1 rad.The ratio of the coefficients a_{PN}/a_{CM} used in the LS-DRMTCMA is set to 2.

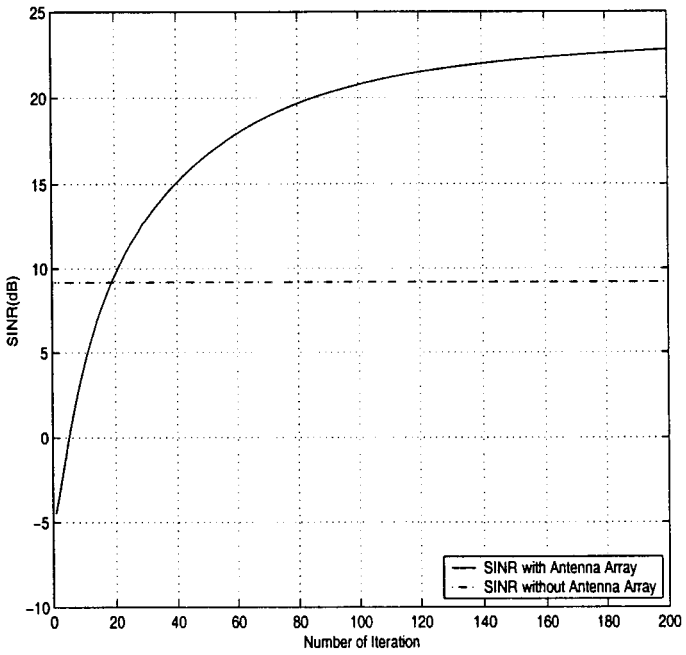

(a) 30 interfering users per cell

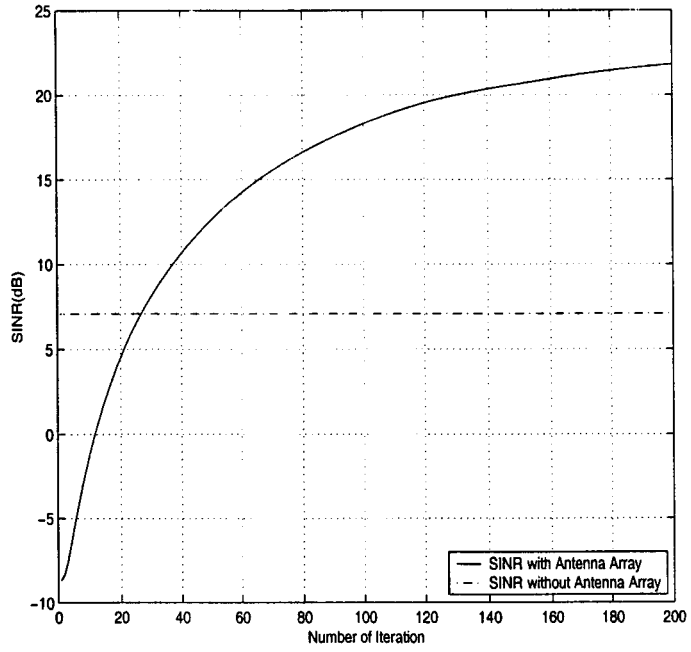

(b) 50 interfering users per cell

Figure 5.3: Evolution of SINR with blind adaptive algorithm iteration, E_b/N_0 =25 dB, with flat slow fading. DOA of desired user=1 rad. The ratio of the coefficients a_{PN}/a_{CM} used in the LS-DRMTCMA is set to 2.

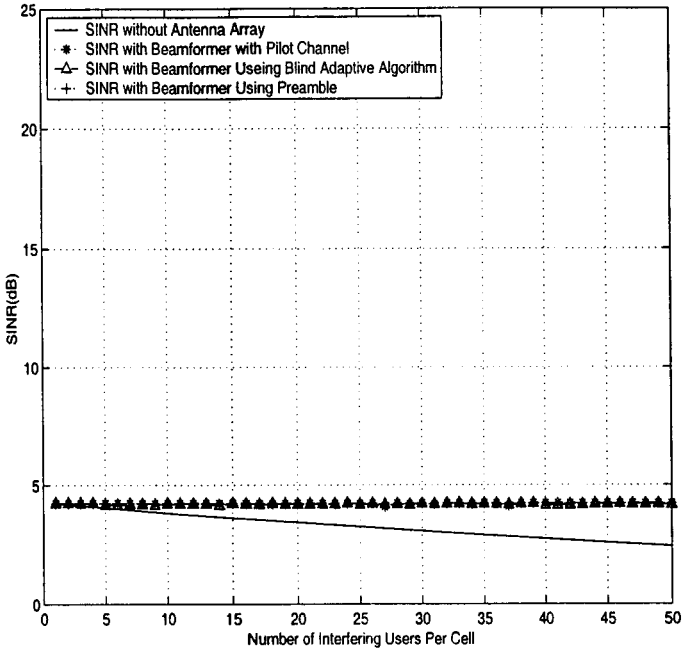

(b) DOA of Desired User is 1 rad

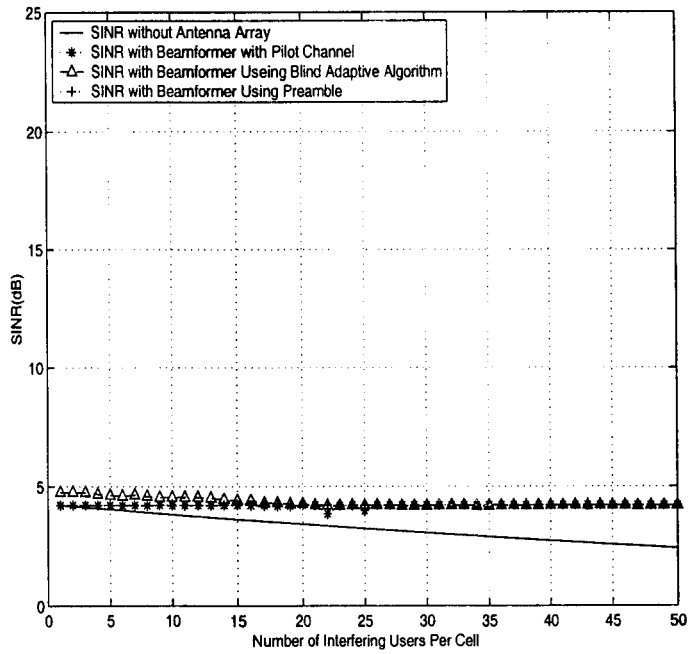

(b) DOA of Desired User is 2.5 rads

Figure 5.4: SINR of multi user CDMA systems (E_b/N_0 = 5 dB, with flat slow fading). DOA of desired user=1 rad. The ratio of the coefficients a_{PN}/a_{CM} used in the LS-DRMTCMA is set to 2.

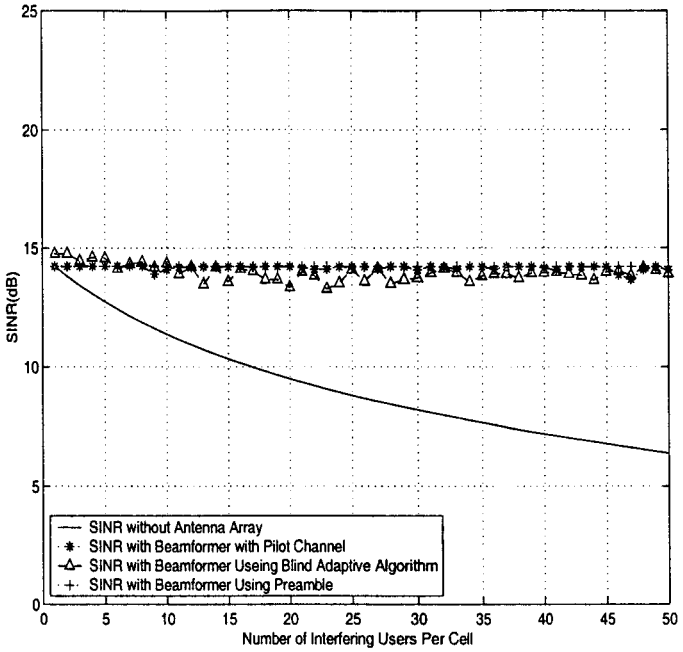

(b) DOA of Desired User is 1 rad

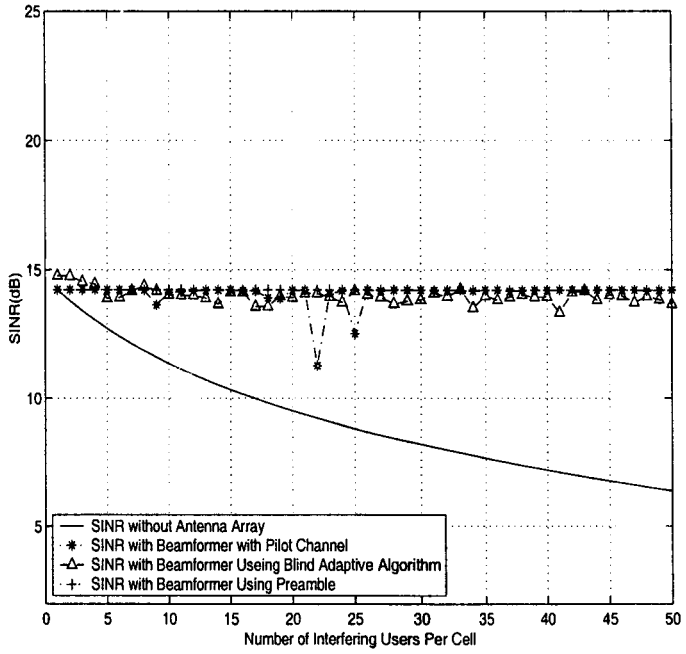

(b) DOA of Desired User is 2.5 rads

Figure 5.5: SINR of multi user CDMA systems (E_b/N_0 =15 dB, with flat slow fading). DOA of desired user=1 rad. The ratio of the coefficients a_{PN}/a_{CM} used in the LS-DRMTCMA is set to 2.

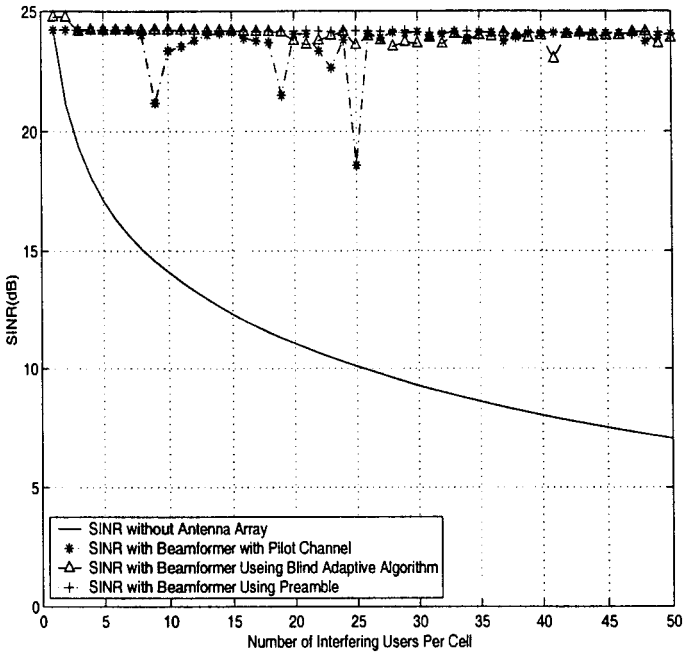

(a) DOA of Desired User is 1 rad.

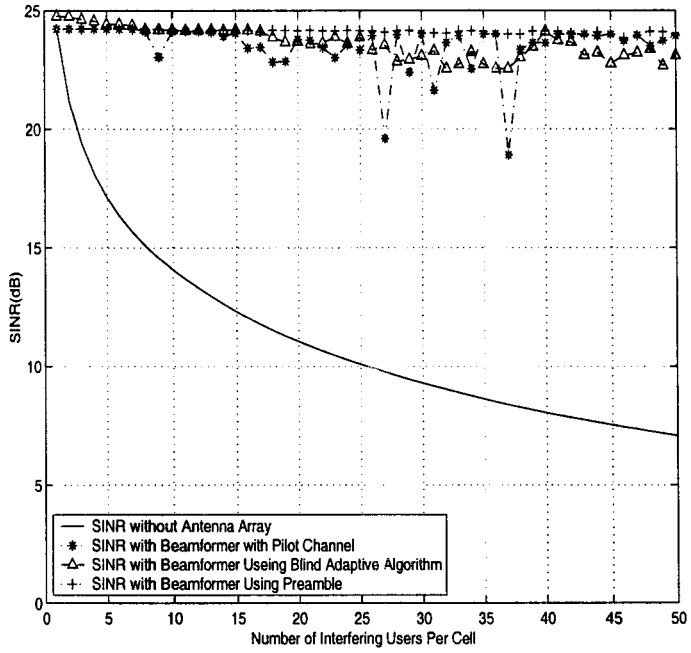

(b) DOA of Desired User is 2.5 rads

Figure 5.6: SINR of multi user CDMA systems (E_b/N_0 =25 dB, with flat slow fading). DOA of desired user=1 rad. The ratio of the coefficients a_{PN}/a_{CM} used in the LS-DRMTCMA is set to 2.

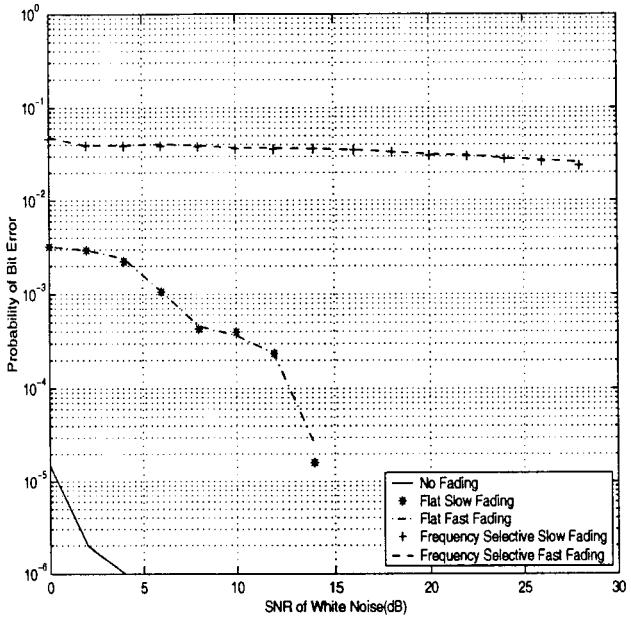

Figure 5.7: BER performance of single user system with antenna array beamforming using blind adaptive algorithm. DOA of desired user=1 rad.The ratio of the coefficients a_{PN}/a_{CM} used in the LS-DRMTCMA is set to 2.

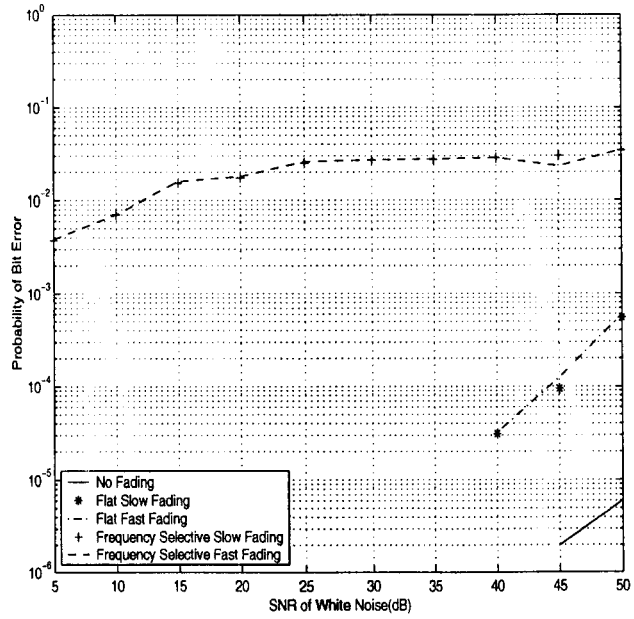

Figure 5.8: BER performance of multi user system with antenna array beamforming by blind adaptive algorithm. E_b/N_0 15 dB. DOA of desired user=1 rad.The ratio of the coefficients a_{PN}/a_{CM} used in the LS-DRMTCMA is set to 2.

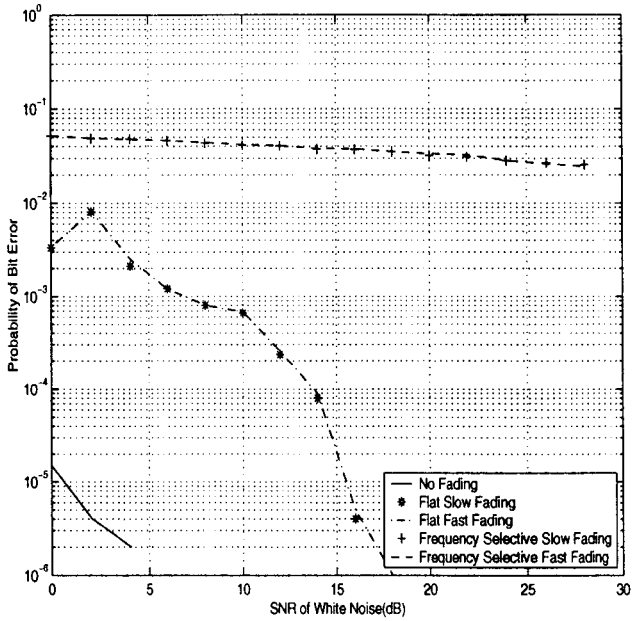

Figure 5.9: BER performance of single user system with antenna array beamforming by Wiener solution with pilot channel on the reverse link of 3G CDMA system. DOA of desired user=1 rad.

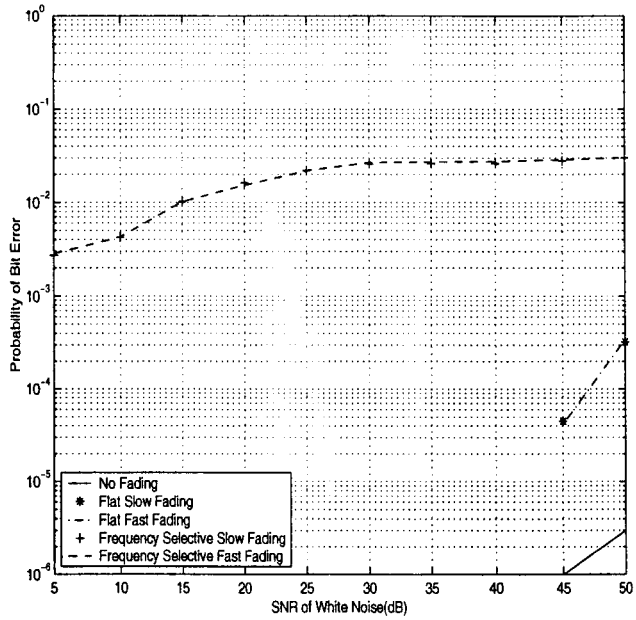

Figure 5.10: BER performance of multi user system with antenna array beamforming by Wiener solution with pilot channel on the reverse link of 3G CDMA system. E_b/N_0 =15 dB. DOA of desired user=1 rad.Wiener Solution with Pilot Channel

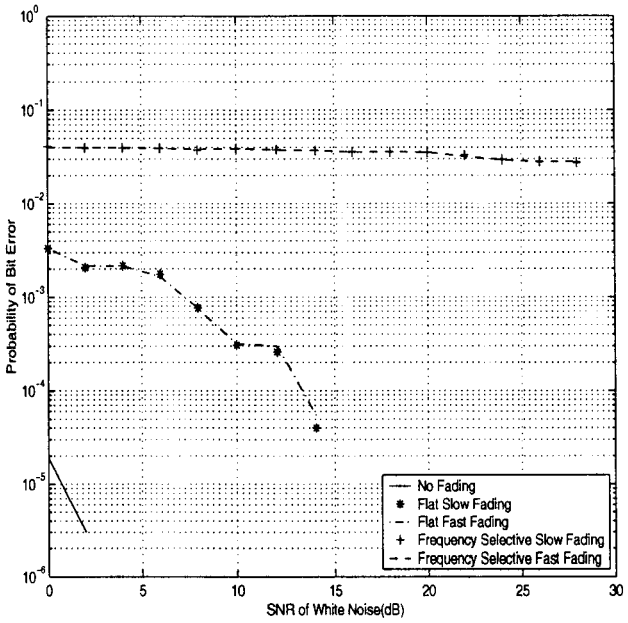

Figure 5.11: BER performance of single user system with antenna array beamforming by LMS algorithm with training sequence. DOA of desired user=1 rad.

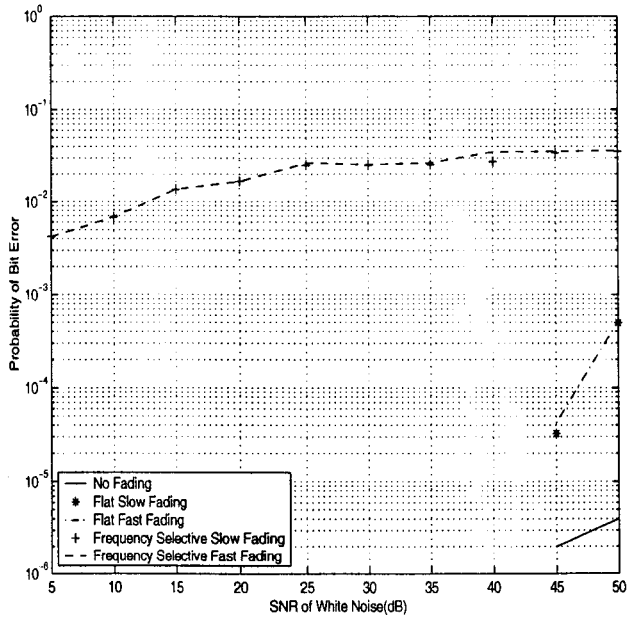

Figure 5.12: BER performance of multi user system with antenna array beamforming by LMS algorithm with training sequence. E_b/N_0 =15 dB. DOA of desired user=1 rad.

Chapter 6

COMPARISON ADAPTIVE BEAMFORMING ALGORITHMS

6.1 Introduction

For one adaptive array, there may exist several adaptive algorithms that could be used to adjust the weight vector. The choice of one algorithm over another is determined by various factor:

- *Rate of convergence.* This is defined as the number of iterations required for the algorithm, in response to stationary input, to converge to the optimum solution. A fast rate of convergence allows the algorithm to adapt rapidly to a stationary environment of unknown statistics.

- *Tracking.* When an adaptive algorithm operates in a non-stationary environment, the algorithm is required to track statistical variations in the environment.

- *Robustness.* In one contest, robustness refers to the ability of the algorithm to operate satisfactorily with ill-conditioned input data. The term robustness is also used in the context of numerical behavior.

- *Computational requirements.* Here the issues of concern include (a) the number of operations (i.e., multiplications, divisions, and additions/subtractions) required to make one complete iteration of the algorithm, (b) the size of memory locations required to store the data and the program, and (c) the investment required to program the algorithm on a computer or a DSP processor.

6.2 Comparison of BER Performance

In this section, we present the BER performance of different algorithms together. To generate the BER for the different adaptive algorithms, we transmit different random bit streams for each user. In the receiver, we use the beamformer adapted by each algorithm to extract each user's signal and then feed the output of the beamformer into correlator to despread the signal and estimate the transmitted data bit. The estimates of the data bits are compared to the original transmitted data bits and BER of each user is calculated. The BER averaged over all the users is then calculated and used in the BER performance plot.

6.2.1 BER Performance of Single User System

Figure 6.1, Figure 6.2, Figure 6.3, Figure 6.4 and Figure 6.5 are comparison of BER performance of single user system in case of AWGN channel, flat slow fading, flat fast fading, frequency selective slow fading and frequency selective fast fading, respectively.

6.2.2 BER Performance of Multi User System

Figure 6.6, Figure 6.7, Figure 6.8, Figure 6.9 and Figure 6.10 are comparison of BER performance of multi user system in case of AWGN channel, flat slow fading, flat fast fading, frequency selective slow fading and frequency selective fast fading, respectively. $E_b/N_0 = 15$ dB.

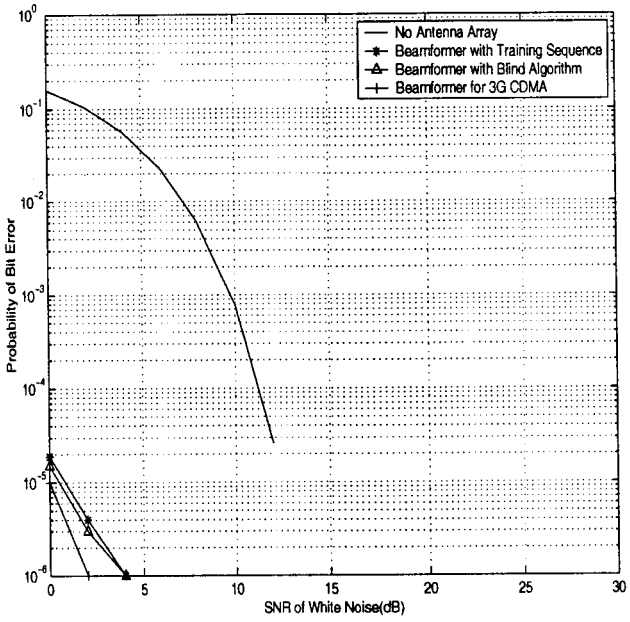

Figure 6.1: Comparison of BER performance of different adaptive algorithms in single user case with white Gaussian noise only. The ratio of the coefficients a_{PN}/a_{CM} used in the LS-DRMTCMA is set to 2.

From Figure 6.1 to Figure 6.10, the BER performance of different algorithm in AWGN channel and multipath fading channels of both single user system and multi user system, wee see that Wiener solution using pilot channel on reverse link of 3G CDMA has the best BER performance . It can outperform LS-DRMTCMA. Because it always has a certain reference signal to assistant beamforming. At the meantime, it can outperform LMS. Because it adjusts weight vectors in every bit.

6.2.3 Mobility Effect on BER Performance

The most difference among three algorithms are:

- LMS algorithm with training sequence adjusts the antenna weights only in the preamble period (the period in which training sequence is transmitted). But during the data period (the period in which information data is transmitted), antenna used the same weights got in the nearest preamble period.

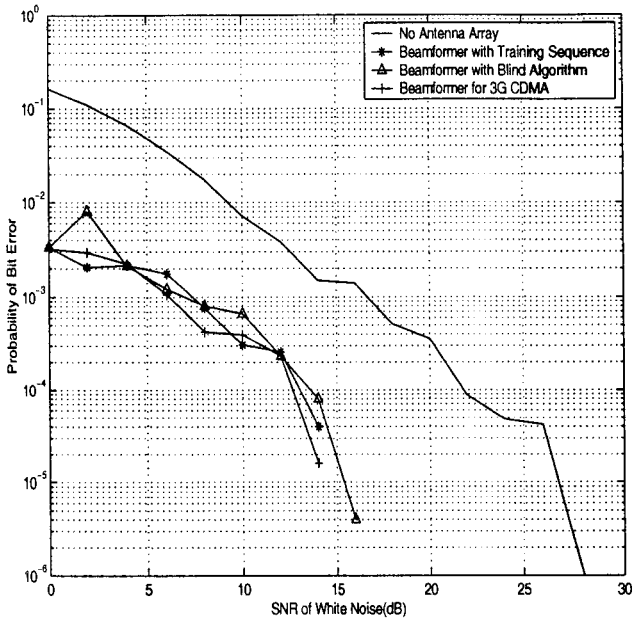

Figure 6.2: Comparison of BER performance of different adaptive algorithms in single user case with flat slow fading and white Gaussian noise. The ratio of the coefficients a_{PN}/a_{CM} used in the LS-DRMTCMA is set to 2.

- Wiener solution with pilot channel on the reverse link of 3G CDMA and blind algorithm adjust the antenna weights all the time.

So, the ability to fit the changing of environment of different algorithms are different.

In this section, in order to know the mobility effect on the BER performance of different algorithms, we simulate the worst case we can have. That is the desired user are moving quickly, $100km/h$, with flat fast fading. The speed of interfering user are uniformly distributed within the range from 0 to $100km/h$, with flat fading. Figure 6.11 is the simulation result in this case.

From Figure 6.11, in the case of subscriber moving, the BER performance of Wiener solution is the best. Because the weight vectors are adjusted bit by bit. It can keep the desired user staying in the main beam.

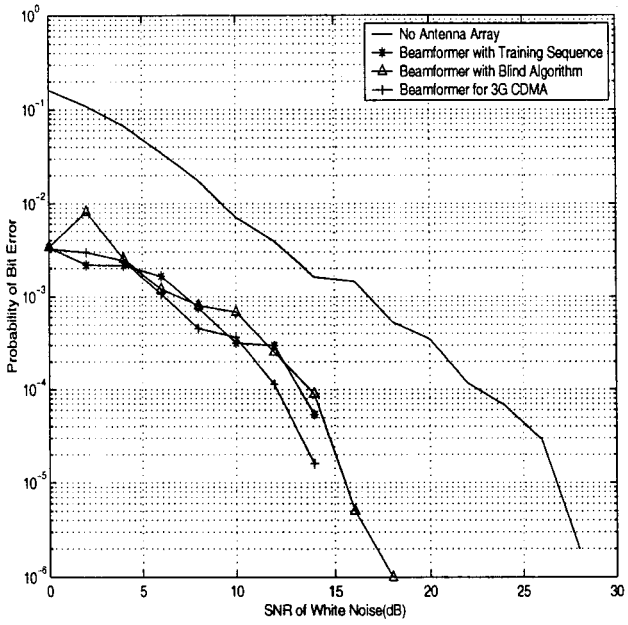

Figure 6.3: Comparison of BER performance of different adaptive algorithms in single user case with flat fast fading and white Gaussian noise. The ratio of the coefficients a_{PN}/a_{CM} used in the LS-DRMTCMA is set to 2.

6.3 Comparison of Computational Requirements

The advantage of Wiener-Hopf equation is it can be solved directly by calculation in every bit. But, in the practice this algorithm has high computatin comlexity because the calculation includes the product of the inverse of the correlation matrix T and the cross-correlation vector P.

The blind algorithm LS-DRMTCMA does not have as much computation as Wiener solution after convergence. But before that, its computational requirement is also very hight. It takes LS-DRMTCMA 50-100 bits to get convergence when there are 50 interfering users per cell.

The LMS algorithm with training sequence does not need a lot of computation, even in the preamble period. There is no need for any computation of inverse matrix.

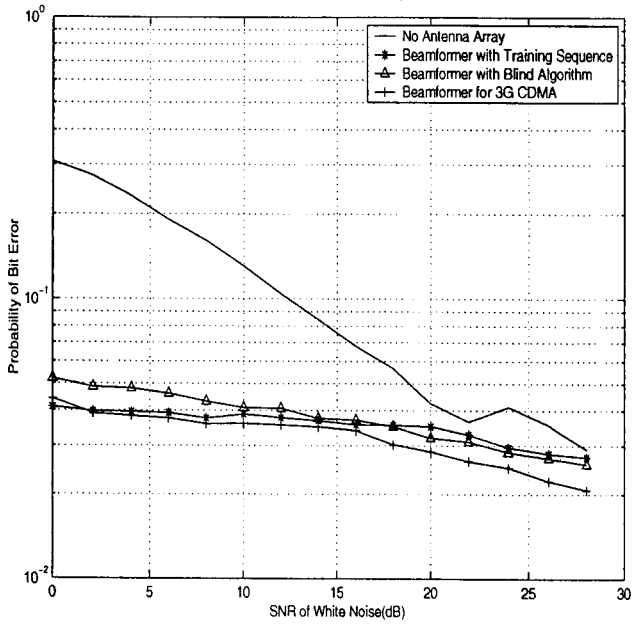

Figure 6.4: Comparison of BER performance of different adaptive algorithms in single user case with frequency selective slow fading and white Gaussian noise. The ratio of the coefficients a_{PN}/a_{CM} used in the LS-DRMTCMA is set to 2.

6.4 Conclusion

In this chapter, we put the simulation results of different adaptive array algorithms under the same condition in a 3G CDMA system together, in order to compare the BER performance of different algorithms in various channel environments (e.g. the AWGN and the multipath environment).

From the comparisons we see that there is a tradeoff between BER performance and cost. Beamforming with Wiener solution using pilot channel on reverse link of 3G CDMA system has the best BER performance and the best ability to fit a quickly changing environment. But it has to finish the most computational work. LMS with training sequence has the least computational requirements. But it can not adjust weight vector during the data period, no matter how much the channel or environment changes.

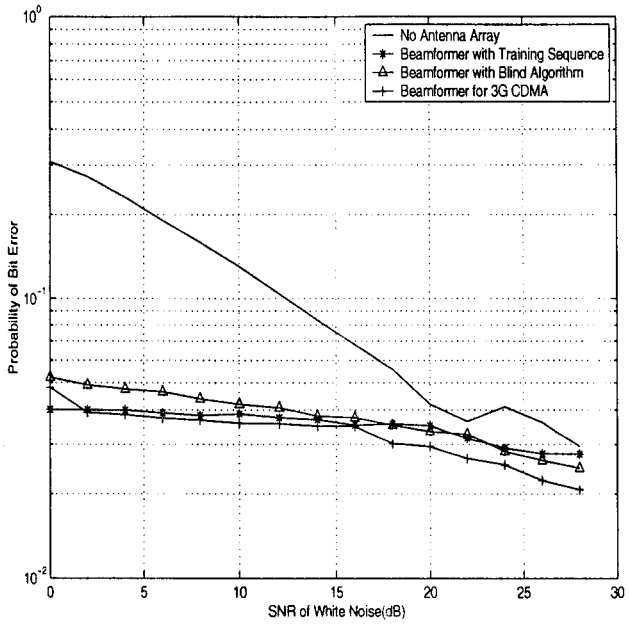

Figure 6.5: Comparison of BER performance of different adaptive algorithms in single user case with frequency selective fast fading and white Gaussian noise. The ratio of the coefficients a_{PN}/a_{CM} used in the LS-DRMTCMA is set to 2.

So which adaptive algorithm we should choose depends on the practical requirements.

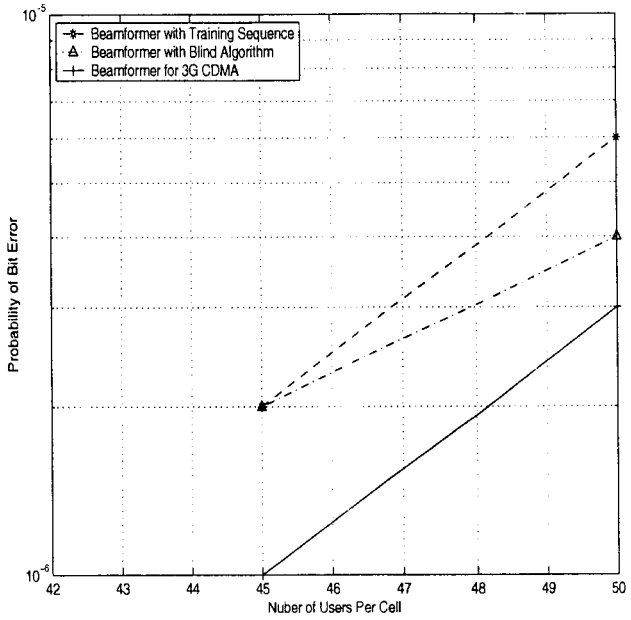

Figure 6.6: Comparison of BER performance of different adaptive algorithms in multi user case with white Gaussian noise. $E_b/N_0 = 15$ dB . The ratio of the coefficients a_{PN}/a_{CM} used in the LS-DRMTCMA is set to 2

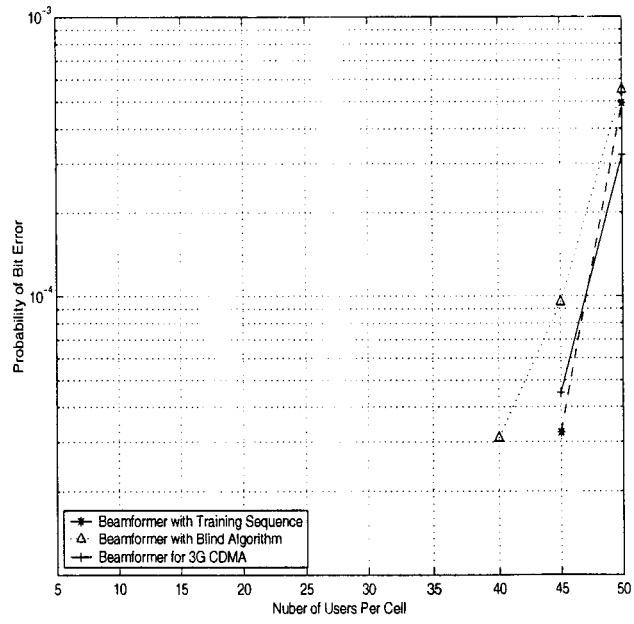

Figure 6.7: Comparison of BER performance of different adaptive algorithms in multi user case with flat slow fading and white Gaussian noise. $E_b/N_0 = 15$ dB. The ratio of the coefficients a_{PN}/a_{CM} used in the LS-DRMTCMA is set to 2.

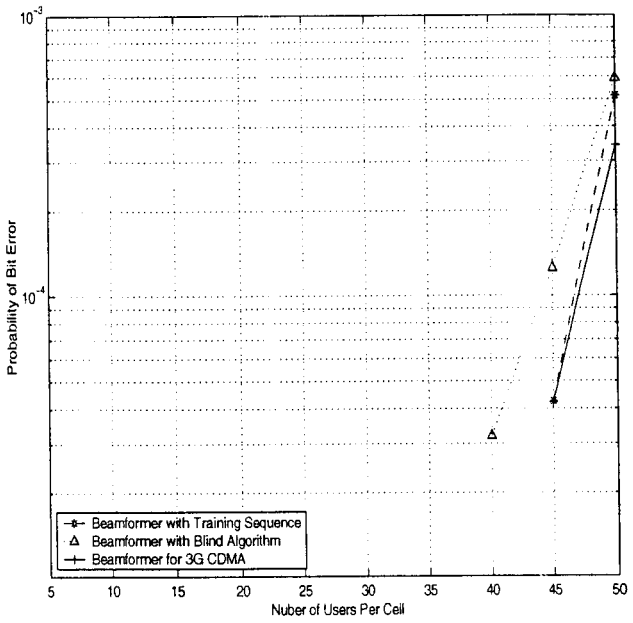

Figure 6.8: Comparison of BER performance of different adaptive algorithms in multi user case with flat fast fading and white Gaussian noise. $E_b/N_0 = 15$ dB. The ratio of the coefficients a_{PN}/a_{CM} used in the LS-DRMTCMA is set to 2.

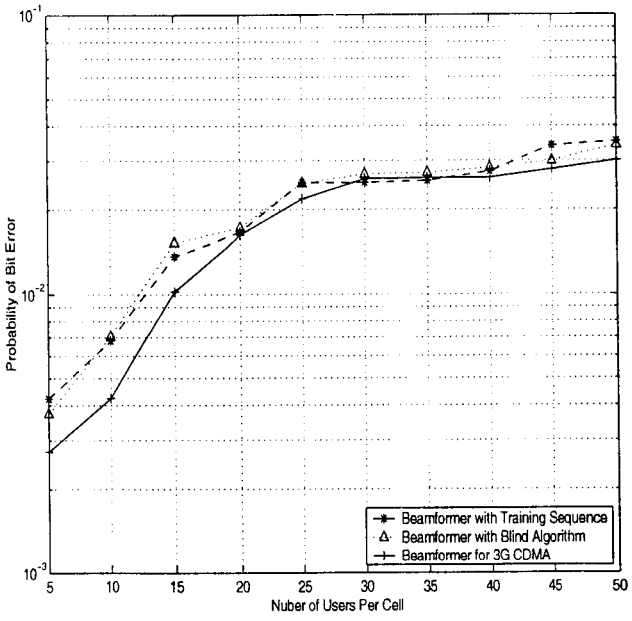

Figure 6.9: Comparison of BER performance of different adaptive algorithms in multi user case with frequency selective slow fading and white Gaussian noise. $E_b/N_0 = 15$ dB. The ratio of the coefficients a_{PN}/a_{CM} used in the LS-DRMTCMA is set to 2.

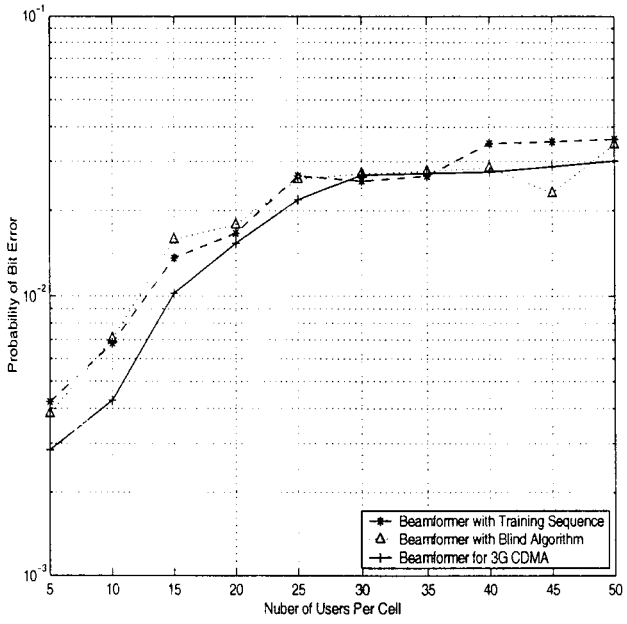

Figure 6.10: Comparison of BER performance of different adaptive algorithms in multi user case with frequency selective fast fading and white Gaussian noise. E_b/N_0 = 15 dB. The ratio of the coefficients a_{PN}/a_{CM} used in the LS-DRMTCMA is set to 2.

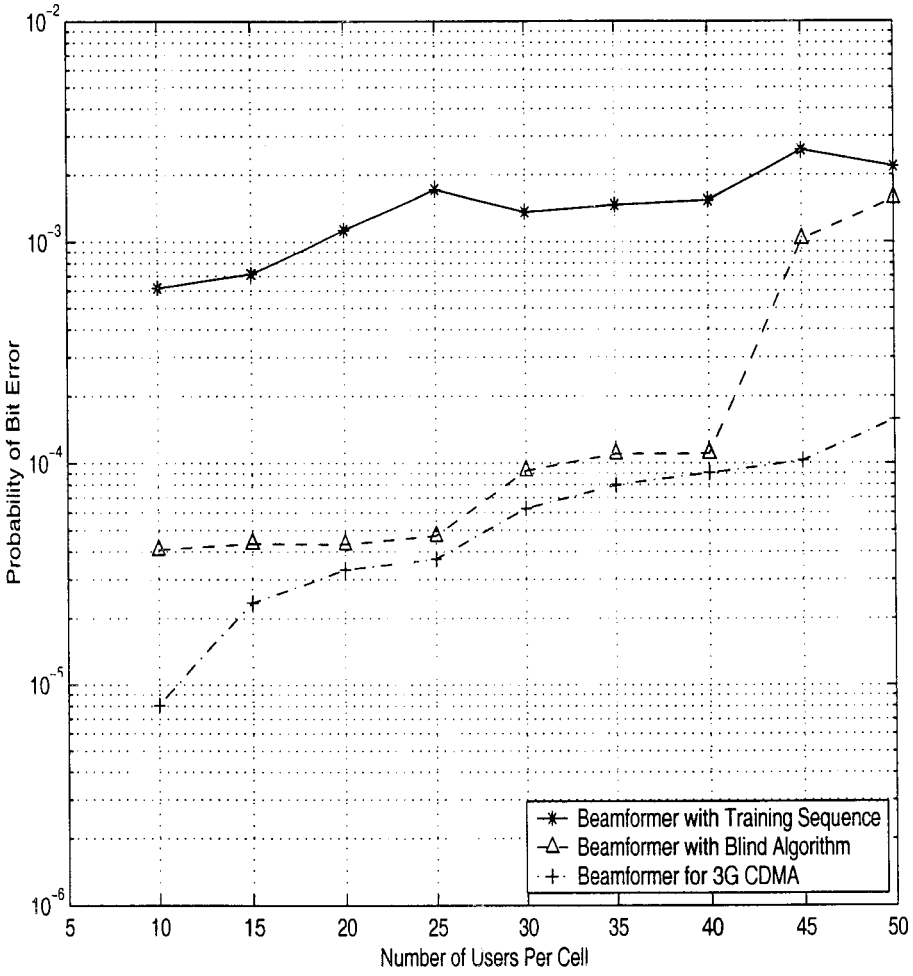

Figure 6.11: Mobility effect on BER performance of different algorithms. Speed of desired user is $100km/h$. Speed of interfering user is uniformly distributed within the range from 0 to $100km/h$. The multipaths of each users are with flat fading. The ratio of the coefficients a_{PN}/a_{CM} used in the LS-DRMTCMA is set to 2. SNR of white Gaussian noise =15.

Chapter 7

CONCLUSION AND FUTURE WORK

7.1 Conclusion

In this thesis, we developed three adaptive algorithms for the beamformer used in a CDMA system. Especially the adaptive beamforming with Wiener solution using pilot channel on the reverse link of 3G CDMA is a very novel algorithm for the coming generation of telecommunication. We provide a detailed derivation of these algorithms and create a C++ simulation testbed to compare the performance of these three algorithms with that of the algorithms presented in the literature. The BER performance of all these algorithms is compared under different conditions (e.g., the AWGN channel, the frequency offset case, and the multipath environment).

First of all, it was shown from the simulation results that both SINR and BER performance are improved significantly by using antenna array of every adaptive algorithm.

Secondly, from the comparison of different adaptive algorithms, it was shown that the algorithm with Wiener solution using pilot channel on the reverse link of 3G CDMA can outperform the other two algorithms in all the test conditions

regardless if the system is single user or multi user. Especially in the case of fast changing environment, the BER performance of array using pilot channel is the best. Blind adaptive algorithm ranks second in this case. The BER performance in the case of stable environment of blind adaptive algorithm and LMS algorithm using training algorithm are proximate. The computational requirement of blind algorithm is much larger than LMS algorithm. But it saves the time of preamble periods.

7.2 Future Work

A number of possibilities exist for future work based on this thesis. These possibilities are outlined below.

- Currently the algorithms are only simulated in the workstation using the C++ code. It will be useful if these algorithms can be implemented in a DSP chip and the 10-element antenna array can be constructed for field trial measurement.

- In this thesis, the performance of all the algorithms is evaluated by using a uniform linear array. In the future, we can use different array geometries, e.g., a circular array, to examine the performance of the algorithms.

- In this simulation, we use the same DOA for all the multipaths of each user. But, actually, different paths through different reflection, diffraction and scattering in the environment come from different directions. In the future simulation about two different multipath angle separation cases, we can investigate the performance of different algorithms under the condition when both multipaths fall into the main beam and the condition with only one multipath fall into the main beam.

- From simulation results, we can see the BER performance of blind algorithm is better than that of LMS algorithm using training sequence. This is because blind algorithm can adjust the weight all the time according to the changing of environment. But its drawback is larger computational requirement. The work we will pursue in the future is semi-blind adaptive algorithm. That is the adaptive algorithm also using training sequence. Blind adaptive algorithm is performed during the data period.

- In the research, we assume a perfect power control for all the users. In the future, we can examine the performance of these algorithms under imperfect power control conditions. It is believed that the algorithms should have the ability to combat the power variation of the signals.

Finally, in this thesis, all the beamforming algorithms are only used in the base station for the reverse link. It will be a challenge to use the weight vectors generated by the algorithms in the reverse link for the beamforming in the forward link, since the reverse link and forward link are always working at different frequencies.

Bibliography

[1] H. Hammuda, J. P. McGeehan and A. Bateman, "Spectral efficiency of cellular land mobile radio systems." in *Proc. 38th IEEE Veh. Technol. Conf.*, Philadelphia, PA, pp. 616-622, June 15-17, 1988.

[2] J. A. Tarallo and G. I. Zysman, "Modulation techniques for digital cellular systems," in *Proc. IEEE Vehicular Technology Conf.*, pp. 245-248, June 15-17, 1988.

[3] J. Uddenfeldt, K. Raith and B. Hedberg, "digital technologies in cellular radio," in *Proc. IEEE Vehicular Technology Conf.*, pp. 516-519, June 15-17, 1988.

[4] F. Lindell, J. Swerup and J. Uddenfeldt, "Digital cellular radio for the future," *The Ericsson Rev.*, no. 3, 1987.

[5] W. C. Y. Lee, "Elements of cellular mobile radio systems," *IEEE Trans. Veh. Technol.*, vol. VT-35, pp. 48-56, May 1986.

[6] P. C. Carlier, "Antennas for cellular phones," *Commun. Int.*, pp. 43-46, Dec. 1987.

[7] S. P. Applebaum, "Adaptive arrays", *IEEE Trans. Antennas Propagat.*, vol. AP-24, pp. 585-598, Sept. 1976.

[8] B. Widrow, P. E. Mantey, L. J. Griffiths. and B. B. Goode, "Adaptive antenna systems," *Proc. IEEE*, vol. 55, pp. 2143-2159, Dec, 1967.

[9] R. T. Compton, "The power inversion adaptive array: Concept and performance," *IEEE Trans. Aerospace Electron. Syst.*, vol. AES-15, pp. 803-814, 1979.

[10] L. Acar and R. T. Compton, "The performance of LMS adaptive array with frequency hopped signals," *IEEE Trans. Aerospace Electron. Syst.*, vol. AES-21, pp. 360-370, May 1985.

[11] K. Bakhru and D. J. Torrieri, "The maximum algorithm for adaptive arrays and frequency-hopping communication," *IEEE Trans. Antennas Propagat.*, vol. AP-32, pp. 919-928, Sept. 1984.

[12] R. T. Compton, R. J. Huff, W. G. Swarner, and A. A. Ksienski, "Adaptive arrays for communicaiton systems: An overview of research at The Ohio State University," *IEEE Trans. Antennas Propagat.*, vol. AP-24, pp. 599-607, 1976.

[13] R. T. Compton, "An adaptive antenna in a spread spectrum communication system," *Proc. IEEE*, vol. 66, pp. 289-298, Mar. 1978.

[14] M. A. Beach, A. J. Copping, D. J. Edwards, and K. W. Yates, "An adaptive antenna for multiple signal sources," in *Proc. IEE Fifth Int. Conf. on Antennas and Propagation*, University of York, 1987.

[15] J. E. Hudson, *Adaptive Array Principles*, IEE Electromagnetic Wave Series No. 11. Strvenage, U.K.: Peter Peregrinus, 1981.

[16] *Dataquest Survey of Worldwide Wireless Subscribers*, Nov. 1999.

[17] T. E. Curtis, "Digital beam forming for sonar system," *IEE Proc. Pt. F*, vol, 127, pp. 257-265, Aug. 1980.

[18] P. Barton, "Digital beamforming for radar," *IEE Proc. Pt. F*, vol, 127, pp. 266-277, Aug, 1980.

[19] M. B. Prusley and D. V. Sarwate, "Performance Evaluation for Phase-Coded Spread-Spectrum Multiple-Access Communication - Part II: Code Sequence Analysis," *IEEE Trans. on Comm.*, Vol. Com-25, No. 8, Aug. 1977.

[20] B. D. Van Veen and K. M. Buckley, "Beamforming: A versatile approach to spatial filtering," *IEEE ASSP Magazine*, pp. 4-24, April 1988.

[21] R. T. Compton, Jr., *Adaptive Antennas, Concept and Performance*, Prentice Hall, Englewood Cliffs, New Jersey, 1988.

[22] B. Widrow, P. E. Mantey, L. J. Griffiths, and B. B. Goode, "Adaptive antenna systems," *Proc. IEEE*, vol. 55, pp. 2143-2159, Dec. 1967.

[23] S. Haykin, *Adaptive Filter Theory*, Prentice Hall, Englewood Cliffs, NJ, 1991.

[24] W. Murray, ed., *Numeral Methods for unconstrained Optimization*, Academic Press, New York, 1972.

[25] J. H. Winters, "Increased data rate for communication systems with adaptive antennas," in *Proc. IEEE Int. Conf. Comm.*, June 1982.

[26] M. B. Pursley, "Performance evaluation for phase-coded spread spectrum multiple access communications with random signature sequences," *IEEE Trans. Comm.*, vol. CON-25, Aug, 1977.

[27] J. C. Liberti and T. S. Rappaport, "Analytical results for capacity improvements in CDMA," *IEEE Trans. Veh. Technol.*, vol. 43, pp. 680-690, Aug. 1994.

[28] J. C. Liberti and T. S. Rappaport, "Reverse channel performance improvement in CDMA cellular communication systems employing adaptive antennas," *IEEE Proc. Globecom*, vol. VI, pp. 42-47, 1993.

[29] A. F. Naguib and A. Paulraj, "Performance of DS/CDMA with M-ary orthogonal modulation cell site antenna arrays," *Proc IEEE ICC*, Seattle (USA), pp. 697-701, June 1995.

[30] B. Suard, A. Naguib, G. xu, and A. Paulraj, "Performance analysis of CDMA mobile communication systems using antenna arrays," *Proc. ICASSP'93*, vol, VI, Minneapolis, MN, pp. 153-156, April 1993.

[31] A. F. Naguib, A. Paularj, and T. Kailath, "Capacity improvement with base-station antenna arrays in cellular CDMA," *Proc. 27th Asilomar Conf. on Signals, systems and Computers*, vol. II, Pacific Grove, GA, pp. 1437-1441, Nov. 1993.

[32] V. Weerackody, "Diversity for the direct-sequence spread spectrum system using multiple transmit antennas," *Proc. ICC'93*, vol. III, Geneva, Switzerland, May 1993.

[33] J. Winters, J. Saltz, and R. Gitlin, "The capacity of wireless communication systems can be substantially increased by the use of antenna diversity," *Proc. Conf. on Information Science and Systems*, vol. II, Princeton, NJ, pp. 853-858, Oct. 1992.

[34] S. Anderson, M. Millnert, M. Viberg, and B. Wahlberg, "An adaptive array for mobile communication systems," *IEEE Trans. Veh. Technol.*, vol. 40, no. 1, pp. 230-236, Feb. 1991.

[35] S. C. Swales, M. A. Beach, D. J. Edwards, and J. P. McGeehan, "The performance enhancement of multibeam adaptive base-station antennas for cellular and mobile radio systems," *IEEE Trans. Veh. Technol.*, vol, 39, pp. 56-57, Feb. 1990.

[36] S. C. Swales, M. A. Beach, D. J. Edwards, "Multi-beam adaptive with base-station antennas for cellular land mobile radio systems," in *Proc. IEEE VTC'89,* San Francisco, CA, 1989, pp. 341-348.

[37] K. S. Gilhousen, I. M. Jacobs, R. Padovani, A. Viterbi, L. A. Weaver, and C. Wheatly, "On the capacity of a cellular CDMA system," IEEE Trans. Veh. Technol., vol. 40, no. 2, pp. 303-312, May 1991.

[38] R. Gooch and J. Lundell, "The CM array: An adaptive beamformer for constant modulus signals," *Proc. IEEE ICASSP*, vol. 4, pp.2523-2526, April 1986.

[39] B. G. Agee, "The least-squares CMA: A new technique for rapid correction of constant modulus signals," *Proc. IEEE ICASSP*, pp. 19.2.1-19.2.4, 1986.

[40] C. S. Beightleer, D. T. Phillips, and D. J. Wilde, *Foundations of Optimizations*, Prentice Hall, Englewood Cliffs, New Jersey, 1979.